AD-A069 712 BOEING VERTOL CO PHILADELPHIA PA F/G 1/3
EVALUATION OF PYLON FOCUSING FOR REDUCED HELICOPTER VIBRATION.(U)
APR 79 R GABEL, D REED DAAJ02-77-C-0034
UNCLASSIFIED D210-11390-1 USARTL-TR-79-6 NL

END
DATE FILMED
7-79
DDC

USARTL-TR-79-6

LEVEL II

AD A069712

EVALUATION OF PYLON FOCUSING FOR REDUCED HELICOPTER VIBRATION

R. Gabel and D. Reed
Boeing Vertol Company
P. O. Box 16858
Philadelphia, Pa. 19142

April 1979

Final Report for Period August 1977 - May 1978

Prepared for

APPLIED TECHNOLOGY LABORATORY
U. S. ARMY RESEARCH AND TECHNOLOGY LABORATORIES (AVRADCOM)
Fort Eustis, Va. 23604

Sec 1473

APPLIED TECHNOLOGY LABORATORY POSITION STATEMENT

Pylon focusing is the kinematic arrangement of transmission mounting structure to minimize fuselage response to vibratory hub loads. Bell Helicopter has had considerable success with this technique for their teetered-rotor helicopters where only vibratory hub shear forces are of concern. This experiment was initiated to investigate pylon focusing for a hingeless rotor system where both hub moments and inplane shear forces are of concern. The premise was that the successful application of pylon focusing could minimize the effects of inplane hub forces and moments, permitting the use of simple, one-dimensional antiresonant devices for vertical isolation.

The results were poor for reasons not fully understood. Two contributing factors have been identified. One is a structural resonance occurring in the 4/rev operating range that may have negated much of the anticipated benefits. The other factor is that the analysis, and hence anticipated results, assumed that the pylon (rotor and transmission) did not translate but merely rotated about its cg (the focal point) when subjected to rotor loads. In actuality the focal point translates, causing the rotor thrust to induce a significant steady and vibratory moment to the pylon.

Results showed that there is no single focal point that will simultaneously "isolate" both inplane forces and pitch/roll moments. An upward focus at the pylon cg appeared to be best. There is no apparent advantage to varying the focal position for different flight regimes.

This contract was conducted under the technical cognizance of Joseph H. McGarvey, Aeronautical Technology Division.

UNCLASSIFIED

SECURITY CLASSIFICATION OF THIS PAGE (When Data Entered)

REPORT DOCUMENTATION PAGE

READ INSTRUCTIONS BEFORE COMPLETING FORM

1. REPORT NUMBER: USARTL-TR-79-6	2. GOVT ACCESSION NO.
3. RECIPIENT'S CATALOG NUMBER	
4. TITLE (and Subtitle): EVALUATION OF PYLON FOCUSING FOR REDUCED HELICOPTER VIBRATION	5. TYPE OF REPORT & PERIOD COVERED: Final Report, Aug 77-May 78
6. PERFORMING ORG. REPORT NUMBER: D210-11390-1	
7. AUTHOR(s): R. Gabel, D. Reed	8. CONTRACT OR GRANT NUMBER(s): DAAJ02-77-C-0034
9. PERFORMING ORGANIZATION NAME AND ADDRESS: Boeing Vertol Company (A Division of The Boeing Company) P.O. Box 16858, Phila., PA 19142	10. PROGRAM ELEMENT, PROJECT, TASK AREA & WORK UNIT NUMBERS: 66209A 1L262209AH76 00 197 EK
11. CONTROLLING OFFICE NAME AND ADDRESS: Applied Technology Laboratory, U.S. Army Research & Technology Laboratories (AVRADCOM) Fort Eustis, VA 23604	12. REPORT DATE: April 1979
	13. NUMBER OF PAGES: 94 (12) 95 p.
14. MONITORING AGENCY NAME & ADDRESS (if different from Controlling Office)	15. SECURITY CLASS. (of this report): Unclassified
	15a. DECLASSIFICATION/DOWNGRADING SCHEDULE

16. DISTRIBUTION STATEMENT (of this Report)

Approved for public release; distribution unlimited.

17. DISTRIBUTION STATEMENT (of the abstract entered in Block 20, if different from Report)

18. SUPPLEMENTARY NOTES

19. KEY WORDS (Continue on reverse side if necessary and identify by block number)

Vibration Reduction
Focal Isolation
Blade Loads
Hub Loads
Helicopter Rotors
Wind Tunnel Tests

20. ABSTRACT (Continue on reverse side if necessary and identify by block number)

A wind tunnel model test program was conducted to investigate the effectiveness of a focused isolation system in reducing the transmission of rotor-induced vibratory loads for a four-bladed hingeless rotor. The model consisted of a four-bladed hingeless rotor and a simulated transmission mounted on a focal isolation system having pitch and roll degrees of freedom. (over)

DD FORM 1 JAN 73 1473 EDITION OF 1 NOV 65 IS OBSOLETE

UNCLASSIFIED

SECURITY CLASSIFICATION OF THIS PAGE (When Data Entered)

403 682

Analytical considerations indicate that there is no single focus which will simultaneously isolate both hub moments and inplane loads. For the four-bladed hingeless rotor with large vibratory hub moments, the optimum focus lies close to the combined rotor/transmission center of gravity. Model test results indicated two configurations with reasonable moment isolation. One was an upward focus near the combined rotor/transmission center of gravity. The second, which had an effective downward focus, produced high lateral and longitudinal loads.

SUMMARY

A test program was conducted on a wind tunnel model consisting of a four-bladed hingeless rotor and a simulated transmission mounted on a focal isolation system having pitch and roll degrees of freedom. The purpose of the program was to investigate the effectiveness of the focused isolation system in reducing transmission of the predominant 4/rev rotor-induced hub vibratory inplane forces and moments.

Based on analytical considerations, there is no single focal point that will simultaneously isolate the inplane loads and pitch/roll moments. For the four-bladed hingeless rotor with large vibratory hub moments, the optimum configuration is an upward focus at the combined rotor and transmission center of gravity. This focus provides isolation of the hub moments and reduces the transmitted moments due to the inplane hub loads without introducing lateral and longitudinal "kick loads" attributable to hub moment.

The dynamic characteristics of the model differed from those of a simple system with only pitch and roll degrees of freedom. Several natural frequencies of the model were present below the desired 4/rev isolation frequency. Despite the less than ideal dynamic characteristics, the wind tunnel test results tend to confirm the analytical findings. Airspeed sweep data at a rotor speed of 1300 rpm showed good moment isolation for two configurations. One configuration was an upward focus near the combined rotor/transmission center of gravity. The second configuration, which had an effective downward focus, produced high lateral and longitudinal balance "kick loads" due to the hub moments.

Blade flap bending moments of the significant 3rd, 4th, and 5th harmonics and chord bending moments at the 3rd and 5th harmonics were generally similar for all the model configurations. Consequently, the induced 4/rev rotor hub loads at the input of the isolation system were not significantly altered by the presence of the isolator.

TABLE OF CONTENTS

LIST OF ILLUSTRATIONS

LIST OF TABLES

INTRODUCTION

The forward flight operating envelope of a helicopter rotor blade creates vibratory airloads containing all harmonics of the rotor rotational frequency. These harmonics of the airloading are summed within the rotor. Assuming all blades are identical, some harmonics cancel, while others add and are transferred to the fixed system of the fuselage. These are felt as vibratory forces and moments at the blade passage frequency (number of blades times rotor speed) and its integer multiples. Barring unusual circumstances, it is well known that the predominant loads are at the blade passage frequency.

One method of dealing with these vibratory loads is to confine them to the rotor system by isolating the fuselage from the rotor. This involves a soft mounting of the rotor transmission to obtain dynamic decoupling of the rotor system so that selected vibratory loads are not transmitted to the fixed system. If the isolator consists simply of very soft springs, rotor lift and drive torque would create excessive static deflections. Similarly, the static moments commonly induced for maneuvering would also create excessive angular deflections. Consequently, the isolator springs in some axes must be statically stiff while remaining dynamically soft. While this isolator characteristic may be obtained in a variety of ways, it introduces an unwanted complication of the system.

The system is greatly simplified if one or more of its duties can be eliminated. For example, in a teetering rotor system there is no requirement to handle either vibratory or steady hub moments. Since vibratory yaw moments (drive system torques) are not generally of concern, the only disturbing forces are the horizontal (inplane) and vertical hub forces. In the case of the horizontal forces, the dynamic decoupling required can be provided by a soft, focalized mounting of the transmission so that the rotor and transmission are free to pitch and roll. The vertical position of the pivot or focal point is selected to obtain optimum isolation of the horizontal forces. Static deflections in pitch and roll are negligible since the teetering rotor generates no steady moments. Therefore, the mounting may be soft both statically and dynamically. Thus, for a teetering rotor, a simple focused isolation system isolates all the significant vibratory forces except the vertical. This arrangement is the time-proven configuration used on the Bell teetering rotor system.

The present investigation was aimed principally at the four-bladed hingeless rotor configuration typified by the MBB BO-105 and the Boeing Vertol Model 179. For this configuration the most significant disturbing forces are typically the

vibratory hub moments at the blade passage frequency. In addition, steady control and trim moments are carried by the rotor shaft. The essentials of moment isolation can be satisfied most simply by a focalized transmission mounting structure that does not provide isolation of vibratory vertical forces. Even greater simplification is possible if isolation of the vibratory drive system torques are also omitted. Angular deflections due to quasi-steady hub moments in maneuvers are the principal complicating factor. While these deflections and their limit values are functions of the particular installation, examination of a typical situation indicates that statically stiff isolators are required.

A model test program was conducted using a four-bladed, 10-foot-diameter, hingeless rotor model. That portion of the model equivalent to the rotor transmission was supported on a focused isolation system having variable geometry. To avoid the model complexity associated with statically stiffened isolators, cyclic trim was adjusted to maintain steady angular deflections within prescribed limits. The principal objectives of the program were to:

1. Experimentally investigate the efficacy of pylon focusing to minimize the transmission of rotor-induced vibratory inplane hub forces, pitching moments, and rolling moments.

2. Determine how the residual rotor-induced vibratory vertical forces and shaft torques vary with flight conditions.

The scope of the testing was limited to that necessary to answer the following specific questions:

1. Can inplane loads, as well as pitch and roll moments, be confined to the dynamic system by adjusting the focal point vertically?

2. How well will one focal point serve all flight regimes?

3. Will a focal point that is different for lateral motion than for longitudinal motion better serve all flight regimes?

4. If different focal points are needed for various flight regimes, what trades are involved?

5. What is the magnitude of the residual vertical forces?

DESCRIPTION OF MODEL AND TEST STAND

MODEL

A schematic illustrating the details of the focal isolatior system and other important aspects of the model is presented in Figure 1. A photograph of the assembled model is shown in Figure 2. The isolated upper body consisting of the rotor, rotor shaft, bearing housing, swashplate slider and controls is attached to a baseplate by four focusing links and an anti-torque bellows. Bending and moment stiffness of the anti-torque bellows is controlled by the material and thickness of the replaceable diaphragm plates. The focusing links, fitted with ball-type rod ends, establish a virtual pitch/roll pivot located at the point where the link centerlines intersect. A relatively soft pitch and roll restraint is provided by the shear and moment stiffness of the antitorque bellows.

Adjustment of the vertical position of the pitch/roll pivot or focal point is accomplished by changing the angle of the focusing links. A series of predrilled holes in the lugs that receive the upper end of the link provide for six focus points above the mounting plane (baseplate) and six points below the mounting plane. (NOTE: Upper focus No. 1 was not usable due to physical interference.) To permit testing in a semirigid condition, lockbars with a moment-carrying capability at both the upper and lower attachments are installed in lieu of the focus links. The purpose of the lockbars was to provide baseline data in an unisolated condition.

The baseplate of the model is mounted on the five-component balance of the Dynamic Rotor Test Stand (DRTS). Power to the model is provided by the DRTS through a drive shaft equipped with Bendix three-element diaphragm couplings. These couplings have a low moment stiffness to prevent the drive shaft from contributing significantly to the pitch/roll restraint of the model.

In order to prevent excessive angular deflection of the drive shaft couplings, the model was equipped with pitch/roll limit stops, which are visible in Figure 2. The limit stops consisted of links with a clearance dimension at the upper attachment, which are installed in parallel with the focus links. Pitch/roll motion transducers were also installed with the output displayed at the operator's station. This permitted the operator to maintain the model in a centered attitude.

Model Properties

Significant dimensional and physical properties of the model are summarized in Figure 3. The model weight and inertia are measured values and the baseplate properties are calculated. Indicated stiffness values for the balance were obtained from a static deflection test. The bellows stiffness (.030-inch-thick steel plates) is an adjusted value based on test data from a unit with alternate (.020-inch aluminum) diaphragm plates. For convenience, the combined bellows shear and moment stiffness effects have been reduced to an equivalent shear stiffness acting at the top of the bellows.

Blade Properties

The rotor used on the model was a four-bladed, 10-foot-diameter, soft inplane, hingeless rotor. Blade properties were Mach scaled to an early version of the blades for the Boeing Vertol Model 179. The blade natural frequency spectrum as a function of rotor speed is presented in Figure 4. Placement of the blade frequencies relative to the scaled operating speed of 1386 RPM is typical with the exception of the second chord and third flap frequencies. These frequencies are closer to 5/rev at the scaled operating speed than is normally desired.

TEST STAND

Figure 5 illustrates the essential details of the DRTS and the installation in the wind tunnel. As indicated in the sketch, the major components of the test stand are:

- The model.
- The DRTS, containing the drive motor.
- A short cannon fitting.
- The Gilmore strut, which is cantilevered from the tunnel floor structure.

From the indicated weights, it is obvious that the test stand is quite massive relative to the model. The slender structure of the test stand results in a DRTS lateral/roll frequency below 2 Hz, and the structure, together with the torsion bar suspension in the vertical plane, produces a vertical mode at approximately the same frequency. Even with the torsion bar suspension, however, the DRTS pitch mode is located at 8 Hz. By comparison, the desired frequency of the model on the focal isolation system is in the range of 30 Hz. Due to its large mass and low frequency, the test stand therefore behaves as a seismic mass or ground insofar as the model is concerned. A photograph showing the model and DRTS installed in the wind tunnel test section is presented in Figure 6.

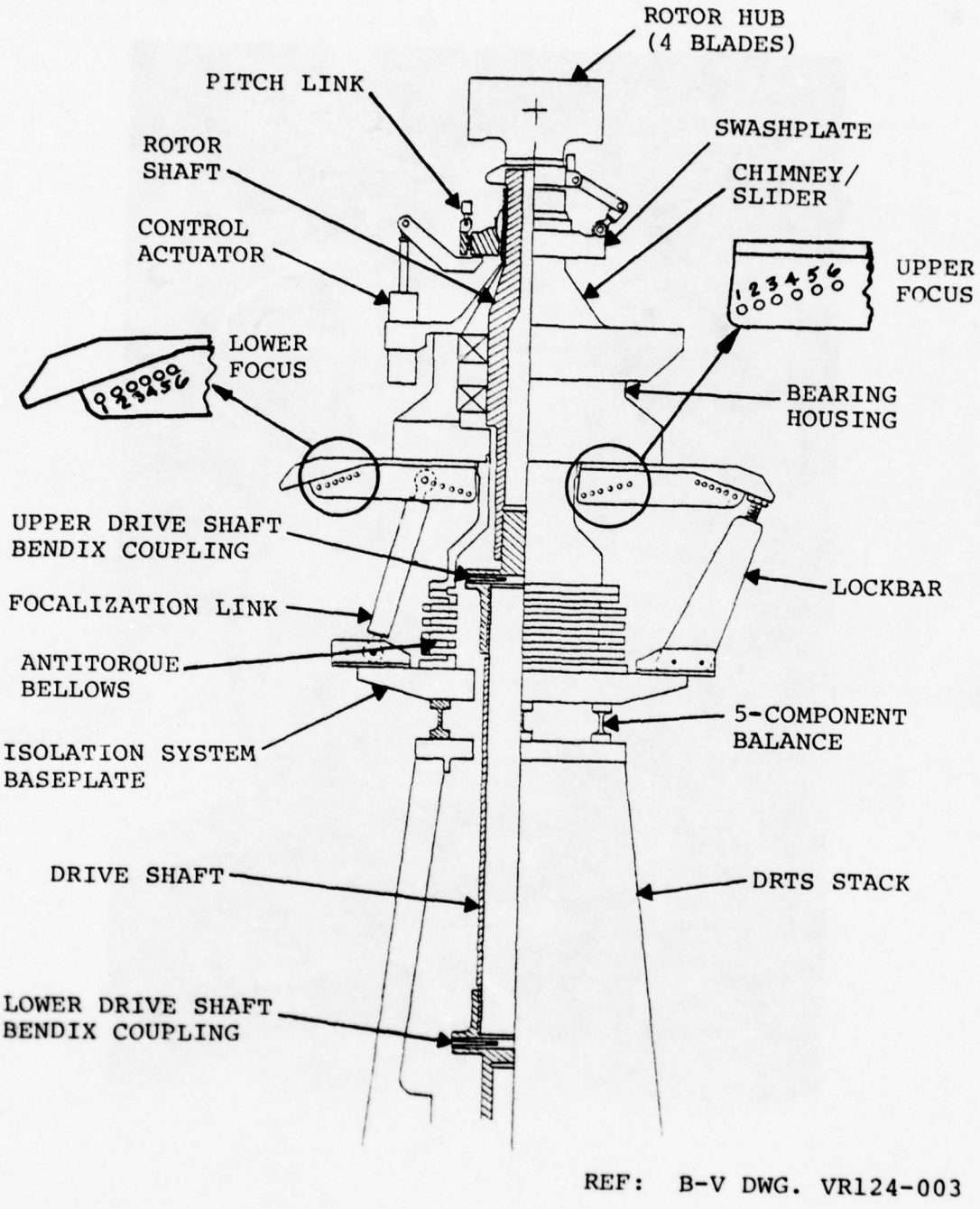

Figure 1. Model Schematic

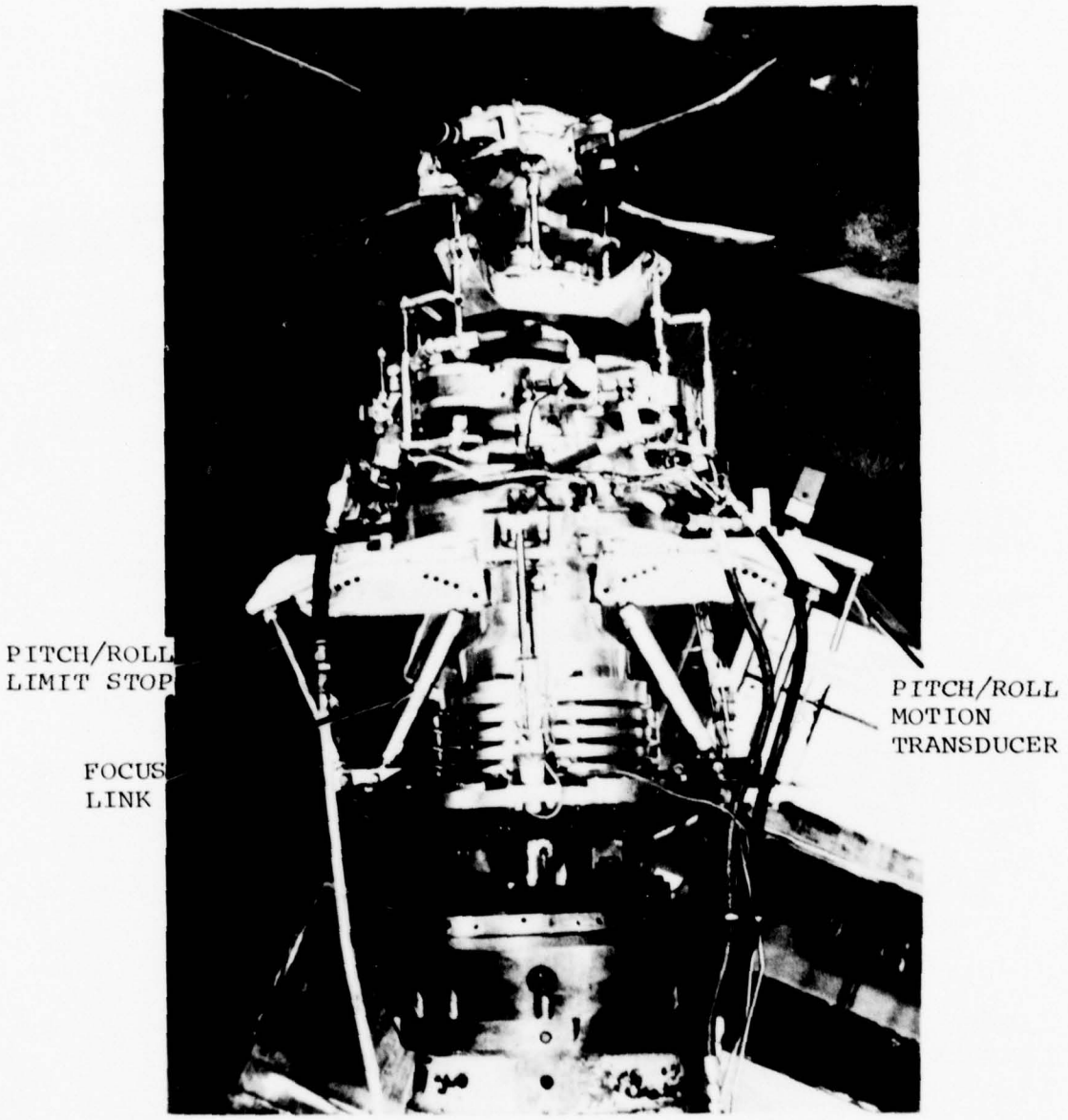

Figure 2. Side View - Focused Isolation Model

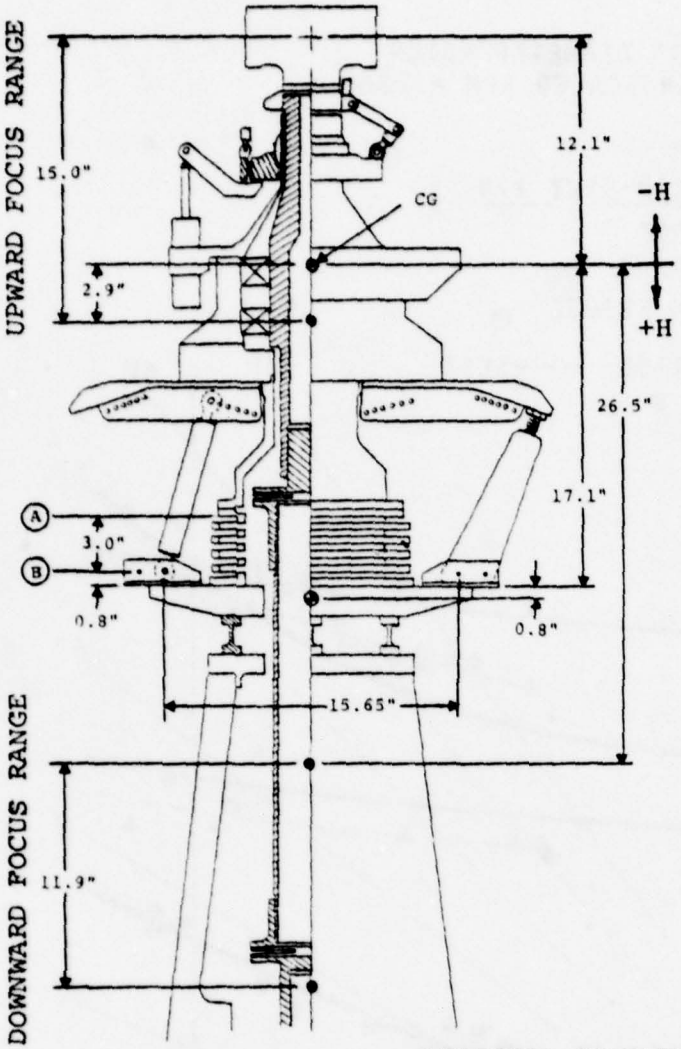

UPWARD FOCUS

NO.	H (in.)
1	+2.9
2	+1.1
3	-0.8
4	-3.65
5	-7.2
6	-12.1

DOWNWARD FOCUS

NO.	H (in.)
1	+26.5
2	+27.9
3	+29.5
4	+31.8
5	+34.5
6	+38.4

PHYSICAL PROPERTIES

Model Weight = 205 Lb
Model Inertia = 25.4 Lb-In.-Sec^2
Baseplate Weight = 77.6 Lb
Baseplate Inertia = 3.81 Lb-In.-Sec^2
Blade Weight = 1.86 Lb Each (7.44 Lb Total)
Balance Moment Stiffness @ (B) = 31.71 x 10^6 In.-Lb/Rad
Balance Shear Stiffness @ (B) = .76 x 10^6 Lb/In.
Equivalent Bellows Shear Stiffness @ (A) = .032 x 10^6 Lb/In.
(Assumes No Moment Restraint) (.030 Stl Plate)
Coupling Moment Stiffness = 18343 In.-Lb/Rad

Figure 3. Model Properties

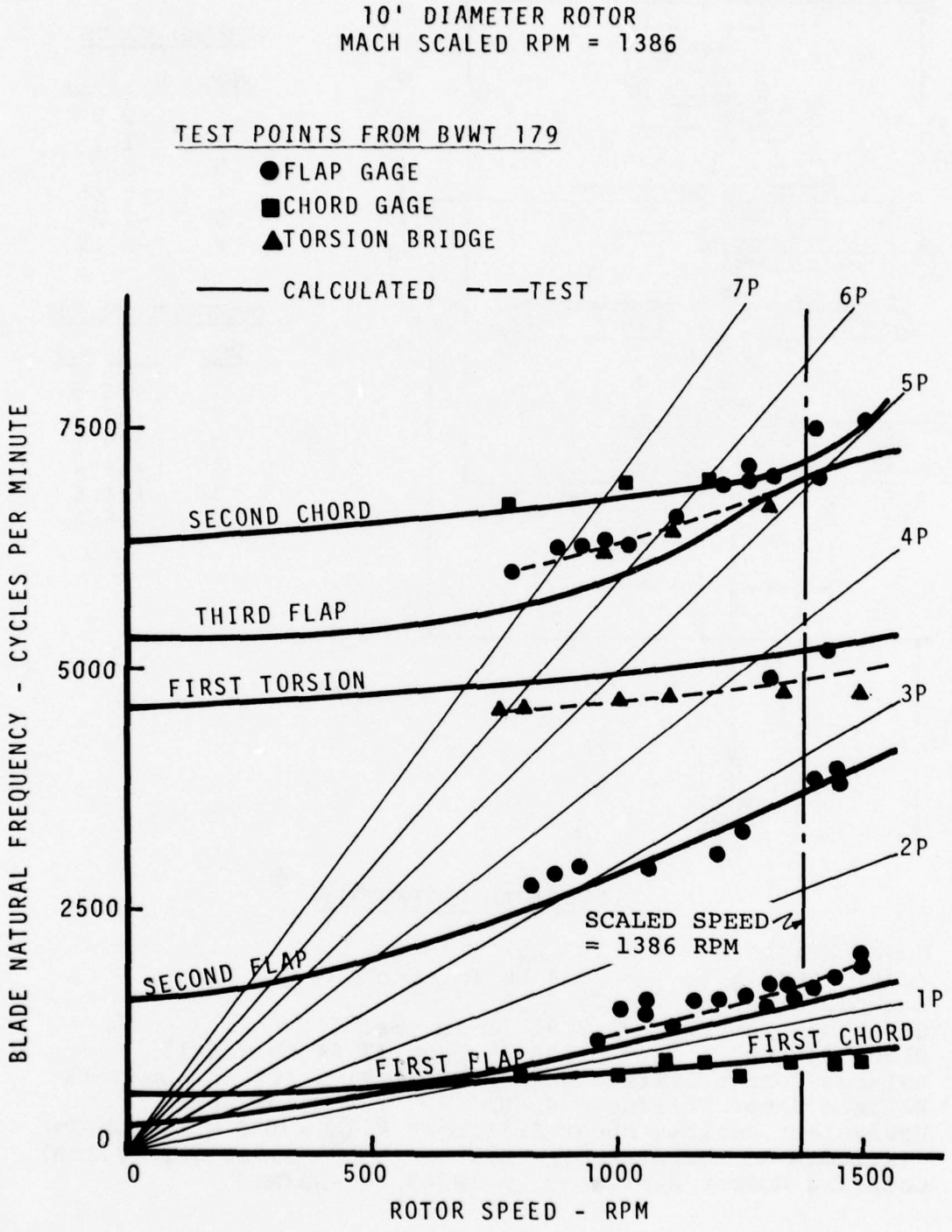

Figure 4. Rotor Blade Natural Frequency Spectrum

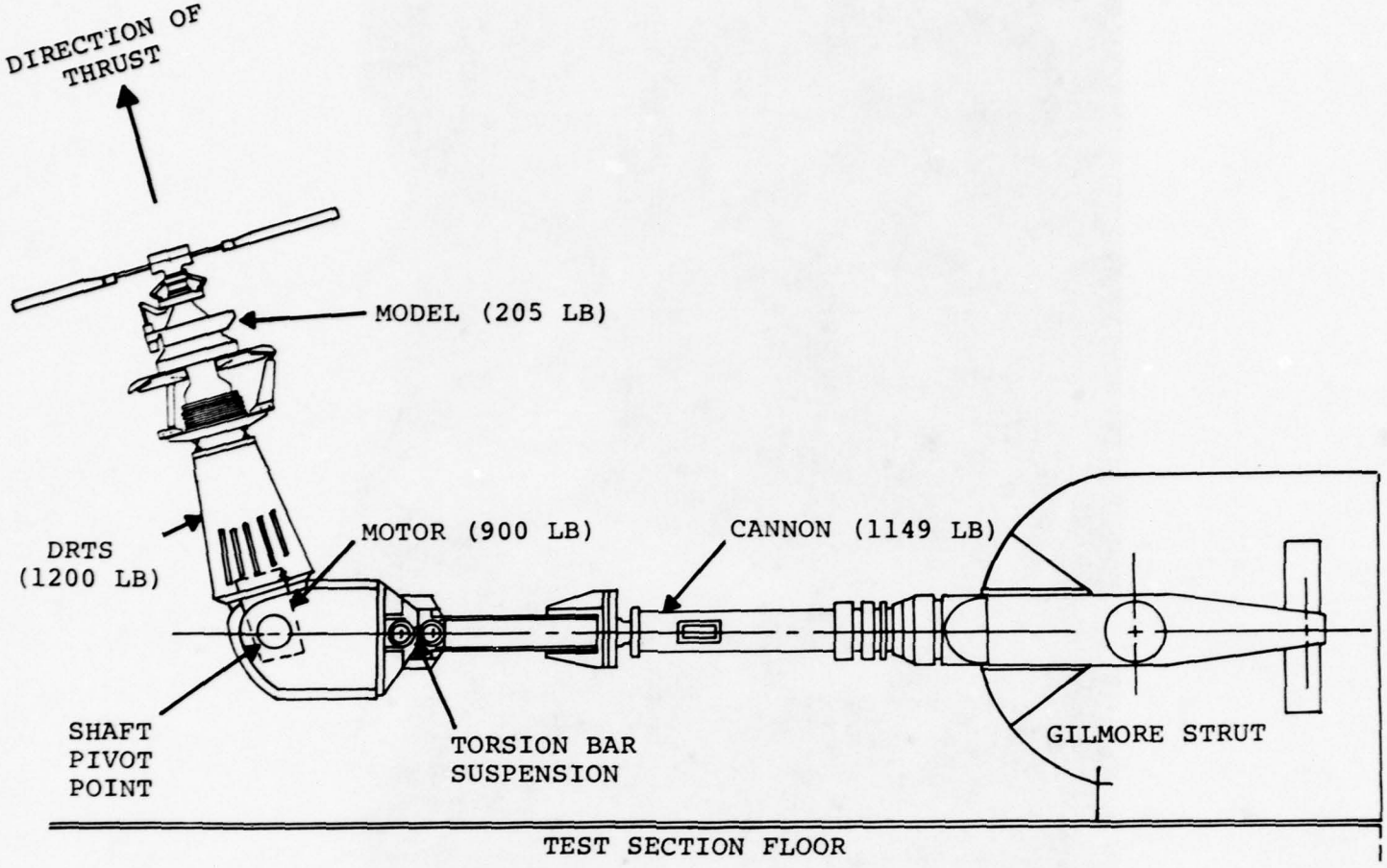

Figure 5. Test Stand Schematic

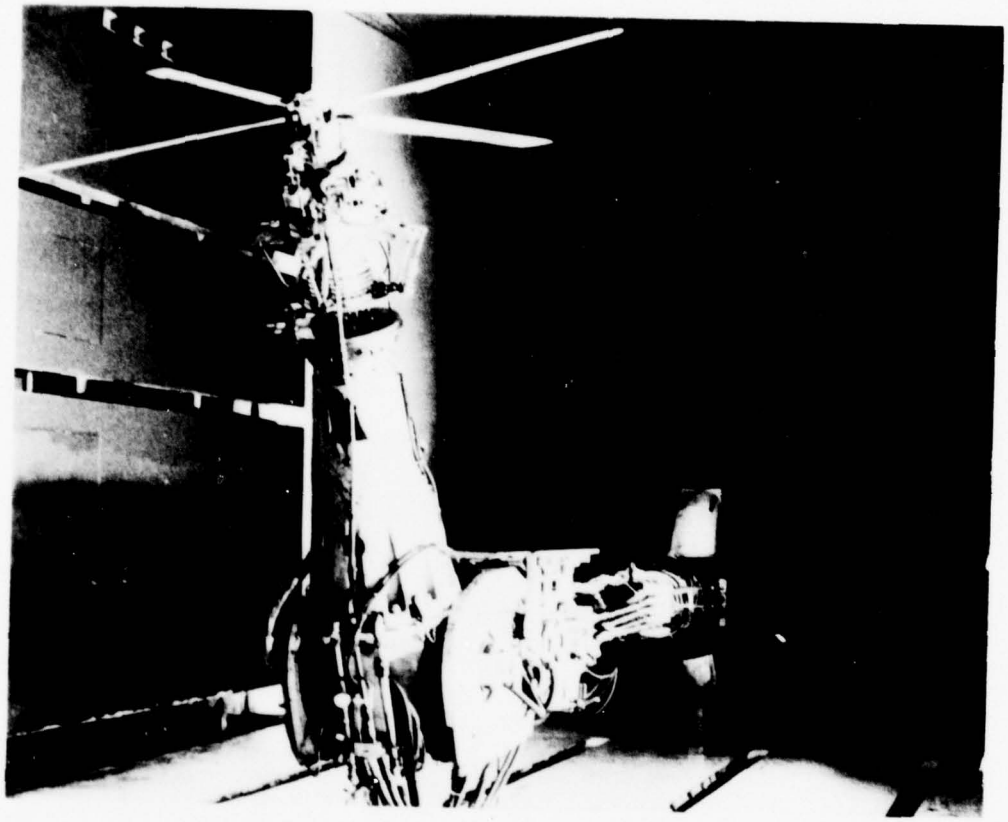

Figure 6. Wind Tunnel Installation

ANALYTICAL INVESTIGATION

EFFECT OF FOCUS POSITION

A brief study using the stick model of Figure 7 was conducted in order to obtain an improved understanding of the focused isolation concept. The simplified model considers only the pitch degree of freedom about the focus point and calculates the loads at the balance due to loads at the hub. Note that the balance loads correspond to the loads transferred to the airframe in an aircraft installation. A development of the equations for the analytical model is given in Appendix A.

Results of the analytical study are summarized in nondimensional form in Figure 8, upward focus, and in Figure 9, downward focus. In each figure, the first plot shows the balance shear load resulting from an inplane hub force. The second and third plots illustrate the balance shear load due to hub moment and the balance moment due to an inplane hub force, respectively. The final plot presents the balance moment due to hub moment. A number of significant facts are evident from the plots. A tabular summary of Figures 8 and 9, shown in Table 1, facilitates comprehension of the following discussion.

Upward Focus

Examination of Figure 8 showing analytical results with an upward focus reveals the following salient features:

- The balance shear load (KF_B/M_H) due to a hub moment is greater than the rigidly mounted condition for all focus conditions except the c.g. focus ($H = 0$). This force is the so-called "kick load", which is an inertial load resulting from translation of the c.g. mass.

- For a condition where only the hub moment need be considered, a c.g. focus ($H = 0$) is beneficial. The "kick load" (KF_B/M_H) due to hub moment is zero and the balance moment (M_B/M_H) due to hub moment is minimal if the natural frequency is sufficiently below the exciting frequency.

- For the case where only the inplane hub force is important, the optimum configuration involves a natural frequency and focus combination, which gives the best compromise between the anti-resonant or null load frequencies of the shear (F_B/F_H) and moment loads (M_B/KF_H) due to the

inplane hub force. One such point exists at a frequency ratio of approximately 2.25 and H = 2.9 inches.

- There is no single focus point that will simultaneously isolate both the applied hub force and moment. When both the hub moment and force are appreciable, the only feasible focus is close to the c.g. (H = 0) with a low natural frequency; otherwise the "kick load" (KF_B/M_H) becomes objectionable. This arrangement isolates the hub moment and reduces the balance moment (M_B/KF_H) due to the inplane hub forces; however, there is no reduction in the balance shear force (F_B/F_H) due to the inplane hub force.

Downward Focus

Figure 9 shows the analytical results at the upper and lower limits of the downward focus range. Previous upward focus results for a c.g. focus (H = 0) are shown for reference. The following observations pertain:

- Complete isolation of the hub moment is not possible with a downward focus. A reduction in the balance moment (M_B/M_H) which is comparable with the best upward focus (H = 0) is possible; however, the "kick load" (KF_B/M_H) due to hub moment is always greater than the upward focus H=0 case.

- For the condition where only the inplane hub force need be considered, a low balance shear force (F_B/F_H) and moment (M_B/KF_H) due to the inplane hub force are obtained with a high frequency ratio. Unless the natural frequency is extremely low (frequency ratio much greater than three), the balance shear force (F_B/F_H) is larger than that possible with the best upward focus.

- Since the "kick load" (KF_B/M_H) due to hub moment is always present, there can be no simultaneous isolation of both hub moments and forces. When both hub moments and forces are present, the possibility of a system with an overall beneficial effect is dependent on the magnitude of the hub moment. If the hub moment is relatively large, the resulting "kick load" (KF_B/M_H) offsets any benefits due to the reduction of the other loads.

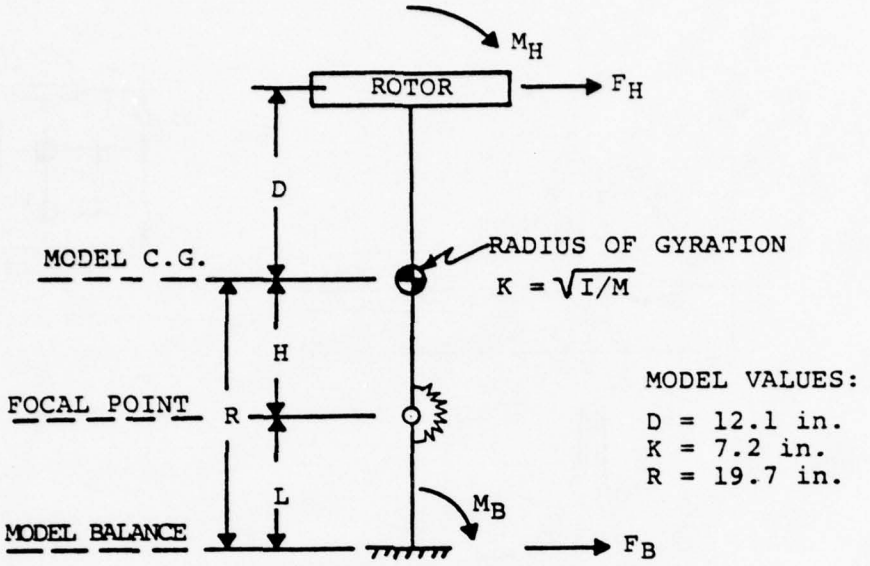

LOADS REFERRED TO BALANCE

- BALANCE FORCE DUE TO HUB FORCE

$$\frac{F_B}{F_H} = 1 + \frac{(H/K)(H/K + D/K)\beta^2}{(1 + H^2/K^2)(1-\beta^2)}$$

- BALANCE FORCE DUE TO HUB MOMENT

$$\frac{K F_B}{M_H} = \frac{(H/K)\beta^2}{(1 + H^2/K^2)(1-\beta^2)}$$

- BALANCE MOMENT DUE TO HUB FORCE

$$\frac{M_B}{K F_H} = \frac{(H/K+D/K)}{(1-\beta^2)} + (L/K) + \frac{(L/K)(H/K)(H/K+D/K)\beta^2}{(1+H^2/K^2)(1-\beta^2)}$$

- BALANCE MOMENT DUE TO HUB MOMENT

$$\frac{M_B}{M_H} = \frac{1}{(1 - \beta^2)} + \frac{(L/K)(H/K)\beta^2}{(1+H^2/K^2)(1 - \beta^2)}$$

WHERE: $L/K = R/K - H/K$

β = EXCITING FREQ/NATURAL FREQ

Figure 7. Simplified Analytical Model

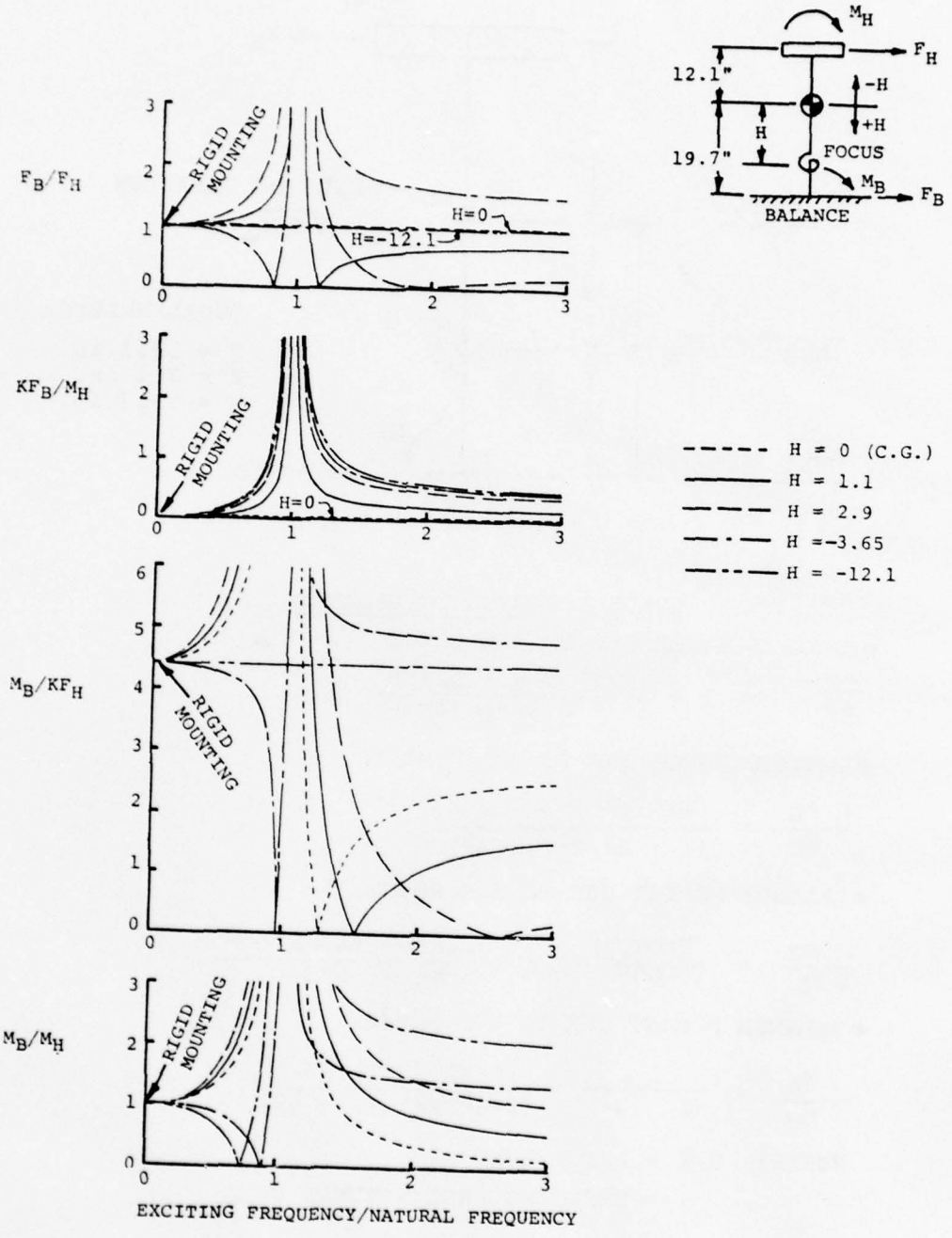

Figure 8. Analytical Results - Upward Focus

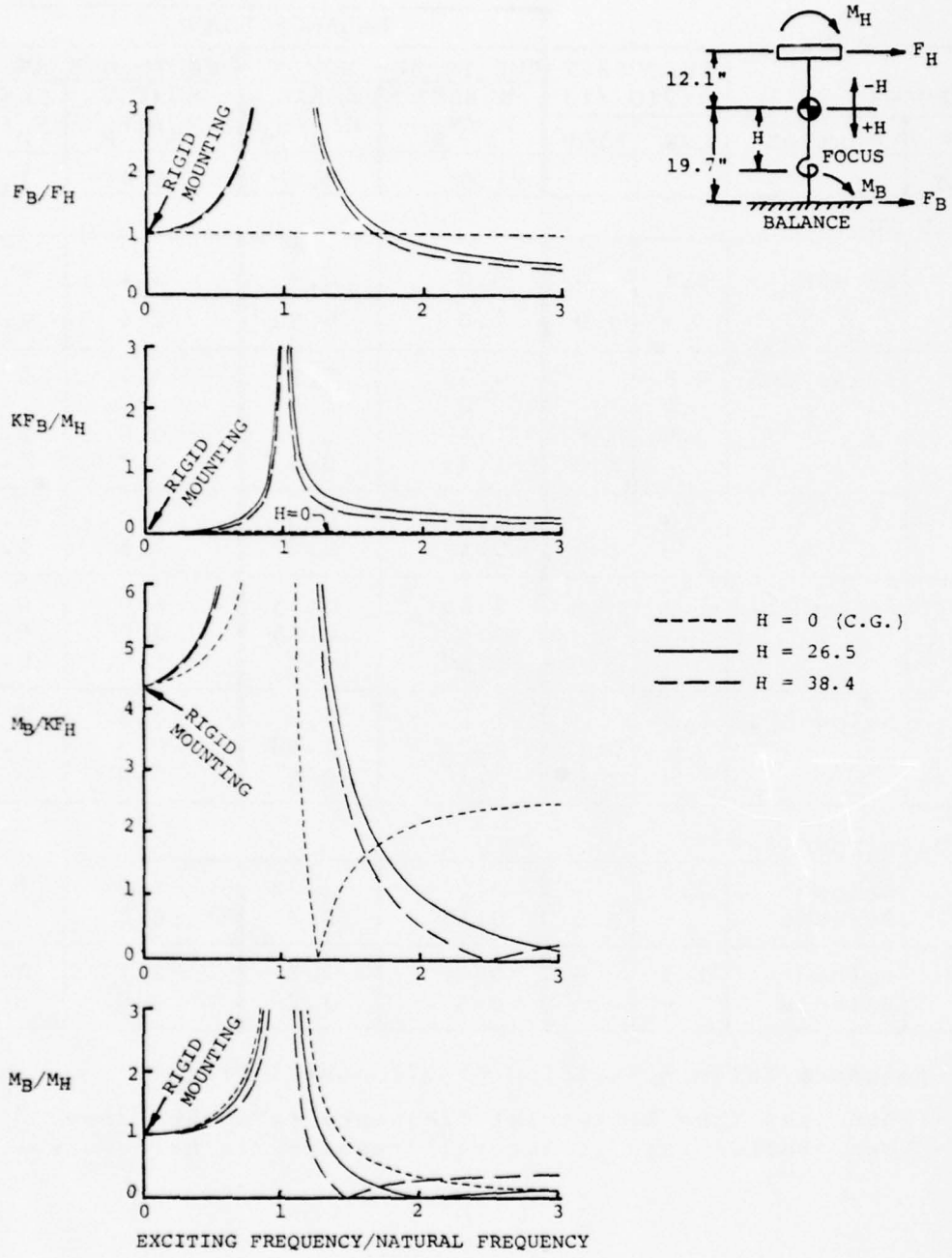

Figure 9. Analytical Results - Downward Focus

TABLE 1. ANALYTICAL SUMMARY

FOCUS		FREQUENCY RATIO (1)		BALANCE LOAD			
				DUE TO HUB MOMENT		DUE TO HUB SHEAR	
H (in.)	LOCATION	LOW	HIGH	MOMENT M_B/M_H	SHEAR KF_B/M_H	MOMENT M_B/KF_H	SHEAR F_B/F_H
RIGID				1.0	0.0	4.4	1.0
UPWARD FOCUS							
-12.1	At Hub	0.7	-	0.0	0.5	4.4	1.0
		-	3.0	2.0	0.53	4.4	1.0
-3.65	Below Hub	0.8		0.35	0.9	3.6	0.0
		0.9	-	0.0	1.5		
		0.95	-	1.5	3.0	0.0	2.7
		-	3.0	1.35	0.5	4.8	1.5
0.0	At C.G.	1.3	-	1.55	0.0	0.0	1.0
		-	3.0	0.13	0.0	2.5	1.0
1.1	Below C.G.	1.2	-	3.85	0.55	6.0	0.0
		1.5	-	1.4	0.25	0.0	0.6
		-	3.0	0.5	0.2	1.6	0.75
2.9	Below C.G.	1.9	-	1.55	0.5	0.8	0.0
		-	2.25	1.24	0.48	0.3	0.08
		-	2.6	1.1	0.4	0.0	0.15
DOWNWARD FOCUS							
26.5	Below	2.05	-	0.0	0.33	0.9	0.8
	Balance	-	3.0	0.15	0.3	0.2	0.55
38.4	Below	1.5	-	0.0	0.3	2.7	1.4
	Balance	-	2.5	0.4	0.2	0.0	0.5

(1) Frequency Ratio = Exciting Freq./Natural Freq.

- When less than 1, natural frequency is above 4/rev.
- When greater than 1, natural frequency is below 4/rev.

EXPERIMENTAL PROGRAM

SHAKE TEST

Prior to wind tunnel testing, a shake test program was conducted to investigate the model dynamic properties. The rotor hub was removed and replaced by a dummy hub that duplicated the hub and blade static mass. Hub excitation was provided by a small electrodynamic shaker and responses were measured with a number of fixed system accelerometers and a probe. In addition to accelerometer data, dynamic loads at the model balance were also obtained.

Initially, several diaphragm thickness configurations for the antitorque bellows were evaluated to define the final model configuration. The object of this evaluation was to select a bellows configuration having a satisfactory placement of the pitch/roll frequency relative to the operating speed. When this was accomplished, natural frequencies and modes were determined for a range of focus conditions. Frequency response characteristics were defined in most cases for hub longitudinal and combined vertical/pitch (offset vertical) excitations. A summary of the test configurations is presented in Table 2.

TABLE 2. SHAKE TEST CONFIGURATION SUMMARY

FOCUS POSITION (IN.)	DIAPHRAGM PLATES (IN.)	EXCITATION		
		LONGITUDINAL	VERTICAL/ PITCH	LATERAL
H = 1.1	.020 Alum.	x	x	x
H = 1.1	.030 Stl.	x	x	x
H = -12.1	.030 Stl.	x	x	x
H = 26.5	.030 Stl.	x	x	
Lockbars	.030 Stl.	x	x	

WIND TUNNEL TESTS

A wind tunnel test program was conducted to:

1. Experimentally investigate the efficacy of pylon focusing to minimize the transmission of rotor-induced vibratory inplane hub forces and pitching and rolling moments; and,

2. Determine how the residual rotor-induced vibratory vertical forces and shaft torques vary with flight condition.

Test Procedure

The model and test stand were installed in the test section of the Boeing Vertol wind tunnel. Track and balance runs and a general check of the model and instrumentation were performed prior to testing. The test program consisted of rotor speed and airspeed sweeps for a range of focus conditions. Rotor speed sweeps were conducted at an advance ratio $\mu = 0.3$ over the range from 1000 to 1400 RPM. Airspeed sweeps were performed primarily at 1175 and 1300 RPM for advance ratios from $\mu = 0.1$ to $\mu = 0.4$. The choice of rotor speeds was based on a preliminary evaluation of test data from initial testing.

Because of the very low natural frequencies associated with the downward focus positions, testing was limited to the lockbar and upward focus conditions. Model configurations and test conditions are summarized in Table 3.

TABLE 3. WIND TUNNEL TEST CONFIGURATION SUMMARY

Focus Position		RPM Sweep	Airspeed Sweep		
Pitch	Roll	$\mu = .3$	1175 RPM	1300 RPM	1386 RPM
H = 1.1" (Near C.G. Focus)	H = 1.1"	x	x	x	-
H =-3.65" (Above C.G. Focus)	H = -3.65"	x	x	x	-
H =-12.1" (Hub Focus)	H = -12.1"	x	x	-	x
H =-12.1" (Mixed Pitch/Roll Focus)	H = 1.1"	x	x	x	-
Lockbars (Effective Downward Focus)	Lockbars	x	x	x	-
Lockbars and Dummy Balance		x	x	x	x

In general the model was flown in a manner representative of ideal full-scale operation; i.e., shaft angle and cyclic trim were adjusted to obtain near-zero steady hub moments. Concessions were made where necessary to avoid blade endurance limits and to maintain the steady angular deflection of the model on the isolation system within prescribed limits.

Model Instrumentation

Instrumentation was installed to measure the following rotating system parameters:

- Blade root flap and chord bending, and root torsion at 11 percent blade radius.
- Pitch link loads on two adjacent arms.
- Drive shaft torsion.

Fixed system instrumentation consisted of the following:

- Five-component balance to measure longitudinal, lateral, and vertical forces and pitch and roll moments.
- Seven accelerometers installed as shown in Figure 10.

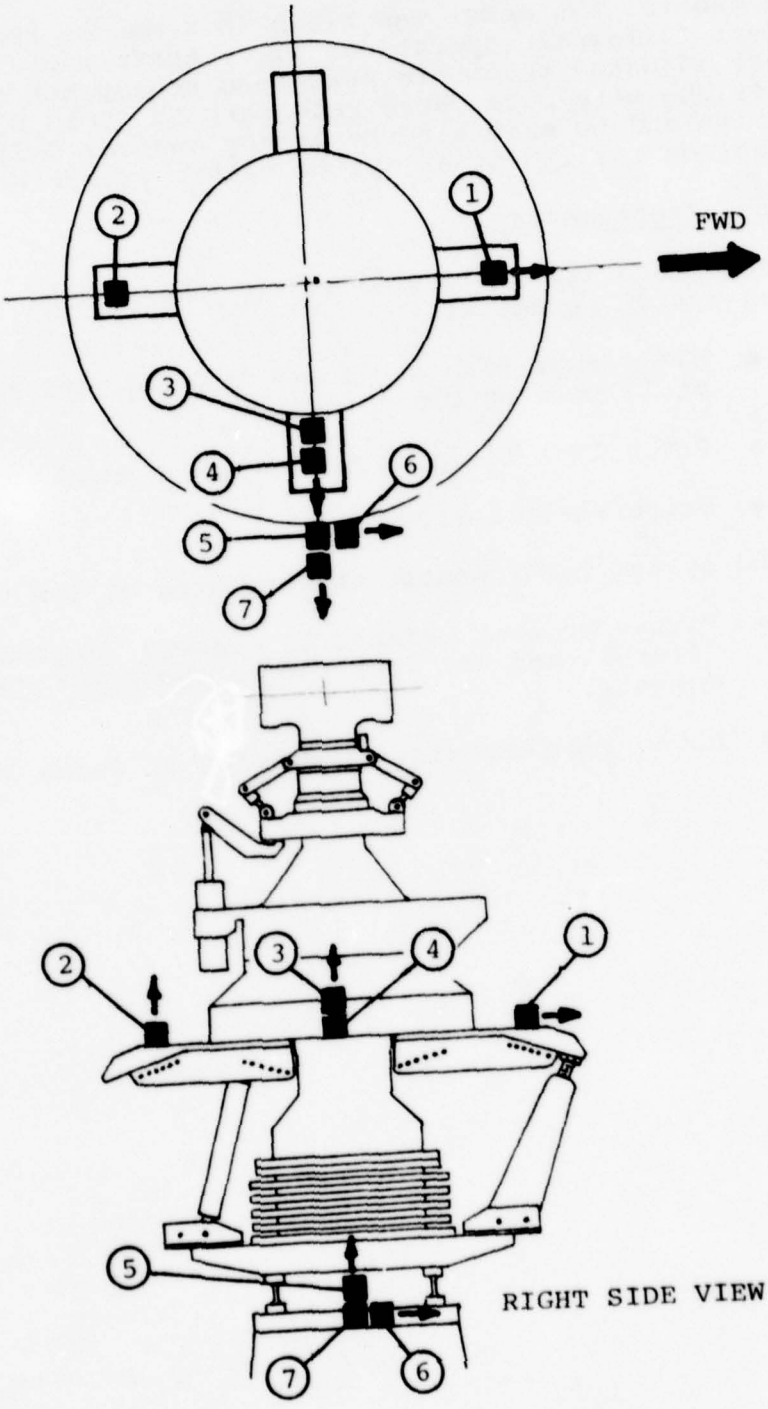

Figure 10. Accelerometer Locations

TEST RESULTS

SHAKE TEST

A brief evaluation was conducted with .020-inch-thick aluminum diaphragm plates installed in the antitorque bellows. The pitch natural frequency of this configuration for an upward focus with H = 1.1 inches was 1140 RPM compared to the scaled rotor speed of 1386 RPM. This arrangement was considered unacceptable principally because it would severely limit the test operating speed range. In addition, it was not felt to be representative of a practical full scale design. Available .030-inch-thick steel diaphragm plates were installed in the bellows, which resulted in a more acceptable placement of the pitch frequency at 1800 RPM. The remainder of the testing was therefore performed with the stiffer plates.

Frequency Response - Upward Focus

Balance frequency response data for upward focus positions H = 1.1 inches (1.1 inches below c.g.) and H = -12.1 inches (focus at hub) and with the lockbars installed are summarized in the comparison plots of Figures 11 through 14. Where available, the plots show the balance responses for longitudinal, lateral, and combined vertical/pitch hub excitation. Hub input forces referred to the balance are shown to indicate the degree of amplification or attenuation obtained.

The longitudinal and moment balance responses to hub longitudinal excitation, Figure 11, and to hub vertical/pitch excitation, Figure 12, display a number of significant features. Both focus positions and the lockbar configuration show a major response centered in the range from 30 to 35 Hz, and it is immediately evident that the lockbar configuration is not rigid. While less evident with the lockbars, all of the configurations tend toward a double peak in the 30 to 35 Hz range. Examination of mode shape data indicates that the lower peak is principally a rotor shaft pitching motion (associated with bearing clearance and low bearing stiffness at light loads) and the higher peak is a pitch mode of the model. A second major resonance for both of the upper focus positions is also present below the scaled 4/rev frequency. The lockbar configuration indicates a similar, but less pronounced resonance. This second resonance point is most evident with vertical/pitch excitation (Figure 12). For the focus at H = 1.1 inches and the lockbar configuration, the resonance is centered at 65 Hz, while for the focus at H = -12.1 inches the frequency drops to 50 Hz. Due to the presence of the second resonant frequency, the dynamic characteristics in the area of 4/rev will differ from those of the simple focused system with a single natural frequency.

Vertical balance response data for a combined vertical/pitch hub excitation is illustrated in Figure 13. No significant response to the natural frequencies below 4/rev is evident. However, load amplification is indicated in the 4/rev region due to a response peak in the region of 150 Hz.

A comparison of balance responses for longitudinal and lateral hub excitations is presented in Figure 14. While there are differences in detail, the lateral responses show the same two major resonance points. Since the model is essentially symmetric, the variations in peak frequencies and levels are due to differences in the longitudinal and lateral dynamics of the test stand.

Frequency Response - Downward Focus

Response characteristics for a downward focus at H = 26.5 inches with hub longitudinal excitation are presented in Figure 15. This configuration was considered impractical because of the extremely low first mode frequency of 12.3 Hz (.53/rev at scaled operating speed). As a minimum, significant modification of the antitorque bellows would be required to raise the frequency of this mode to an acceptable value.

Mode Shapes

The basic concept of the focal isolation system requires that the pitch/roll motions of the model be executed about a real or virtual pivot referred to as the focal point. At the natural frequency of the isolation system, therefore, the node point of the natural mode shape corresponds to the focal point. Mode shapes at the natural frequencies, depicting the longitudinal/pitch motions of the model, were obtained from accelerometer data. Natural frequencies were defined as the frequencies at which the phase of the major responses lagged the input force by 90 degrees. The corresponding natural mode shapes were then plotted using the components of the acceleration at 90 degrees and 270 degrees.

Mode shapes for the upward focus at H = 1.1 inches are illustrated in Figure 16. The lower mode at 32.2 Hz is clearly the model pitch mode as previously indicated. Ideally the node point should be at the focus; however, the mode shape shows that the node is slightly below the focal point. The second mode at 64.4 Hz displays a coupled longitudinal/pitch motion with a node somewhat above the hub; consequently, the effective focus of this mode is near the hub. In addition to a large longitudinal motion of the link focus point, significant pitch motion across the model balance is also evident. As discussed previously, the presence of this

second resonant frequency below 4/rev is undesirable, since it alters the isolation characteristics in the 4/rev region. This is particularly true in view of the character of the mode shape, which shows an effective focus at the hub rather than at the desired focal point. In addition to increased pitch/roll stiffness of the balance, it is also evident from the mode shape that the inplane stiffness of the focus links would have to be increased by a significant factor to place this mode above 4/rev. Alternately, the model weight would have to be drastically reduced. Neither of these was possible with the existing model. An increase in stiffness inevitably leads to a weight increase. Conversely, a significant reduction in the weight is possible only if the stiffness and strength requirements are relaxed. These arguments suggest the use of a Froude rather than a Mach-scaled model.

Figure 17 shows the modes for the upward focus with H = -12.1 inches, which is the hub focus. Both modes display appreciable pitch motion across the model balance, and large relative motion of the rotor shaft is apparent. The lower mode at 33.2 Hz is basically a pitch mode with a node near the balance. The second mode at 48.8 Hz is the longitudinal/pitch mode with a node above the hub. In this case, therefore, the lower mode is the unwanted mode since the effective focus is far below the desired focal point. The effective focus of the second mode is above the desired focal point at the hub. Examination of the mode shape at 33.2 Hz shows that the low frequency pitch motion of the model is due principally to the pitch deflection across the model balance indicating that the pitch/roll stiffness of the balance causes this mode. Of course, the balance cannot be too stiff or it would be unable to measure any loads.

The first mode at 30 Hz with the lockbars installed, Figure 18, is seen to be a pitch mode with a low effective focal point. Some pitch motion about the c.g. is evident, but the principal motion in the mode is due to the pitch deflection of the balance. This confirms the previous observation that the balance pitch/roll stiffenss is low, or alternately, the model weight is large. The presence of a balance mode at this frequency is undesirable. The balance stiffness contribution in the mode offsets the effect of the focus links, making it difficult to force a node at the desired focal point.

Analytical Correlation

The analytical model assumes that the pitch motion takes place about the focal point while the test mode shapes show, in general, that this is not the case. This situation makes it difficult to correlate the test and analytical results. For the upward focus at H = 1.1 inches, Figure 16 indicates that

at least the first mode (32.5 Hz) has a pitch motion with a node reasonably close to the focal point. A comparison of the shake test balance loads for this configuration and the appropriate analytical values is shown in Figures 19 and 20.

With hub longitudinal excitation, Figure 19, results for the longitudinal balance show reasonably good agreement. Results for the pitch balance do not compare as favorably, particularly in the region above 70 Hz. This is due to the presence of the second natural frequency at 64.6 Hz. Results for hub pitch excitation, Figure 20, clearly indicate the effect of the second natural frequency. Except for the peak due to the presence of this higher frequency mode, the test results show the same trend as the analysis.

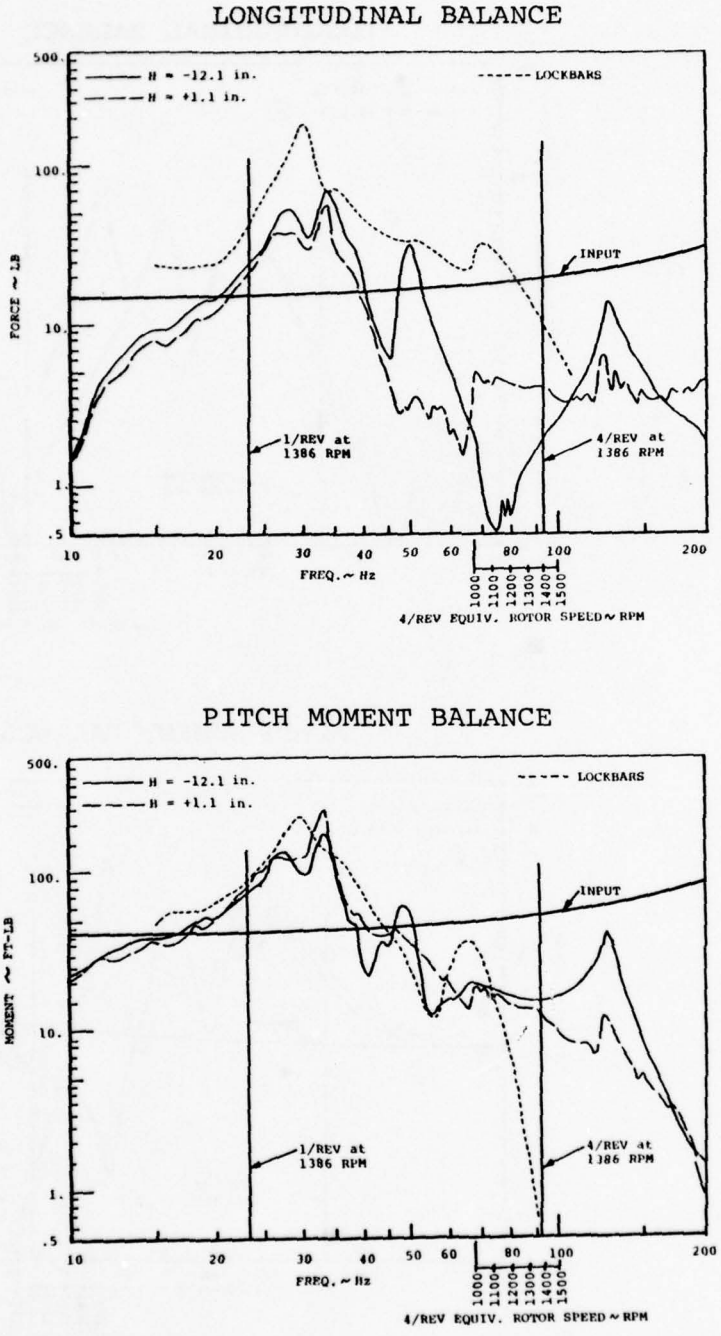

Figure 11. Upward Focus Force and Moment Balance Response - Hub Longitudinal Excitation

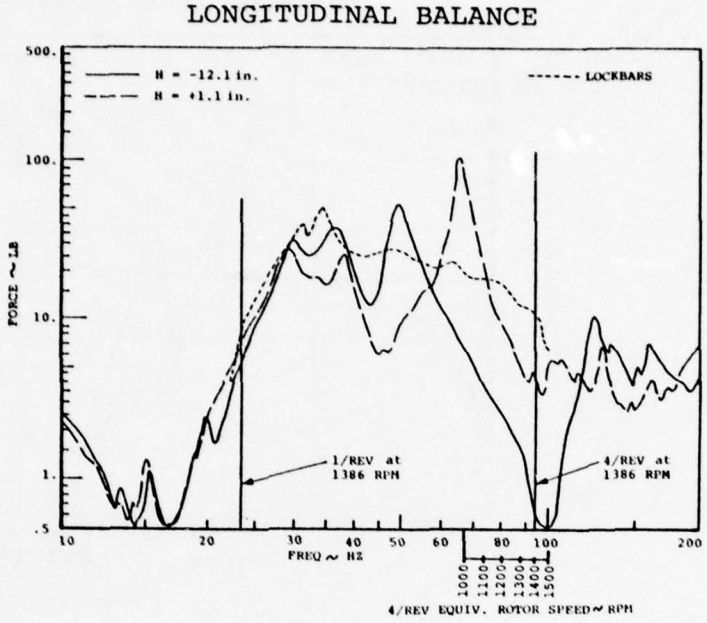

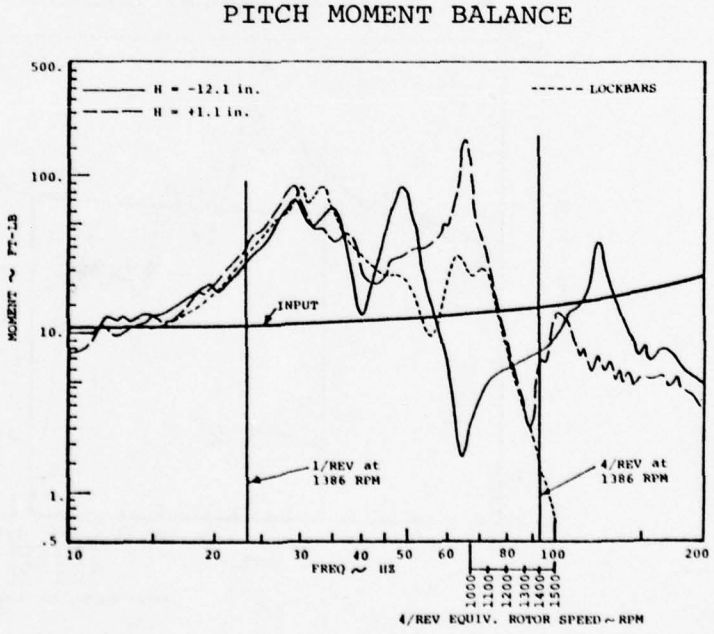

Figure 12. Upward Focus Force and Moment Balance Response - Hub Vertical/Pitch Excitation

VERTICAL BALANCE

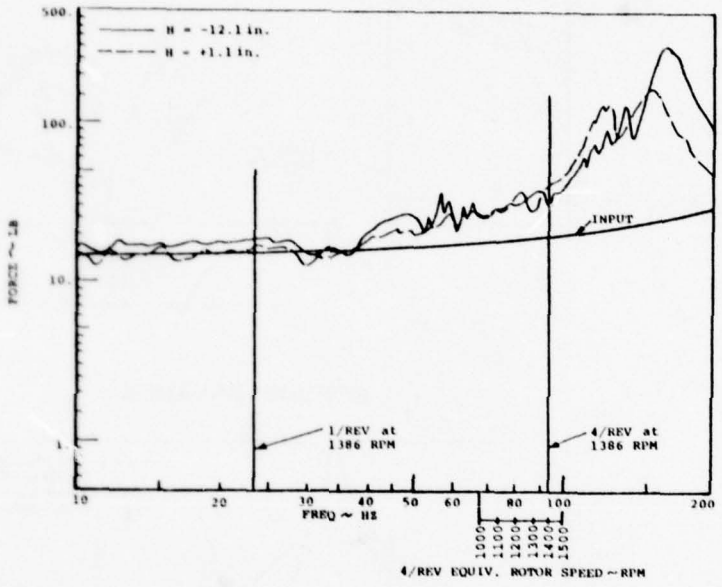

Figure 13. Upward Focus Vertical Balance Response - Hub Vertical/Pitch Excitation

HORIZONTAL BALANCE

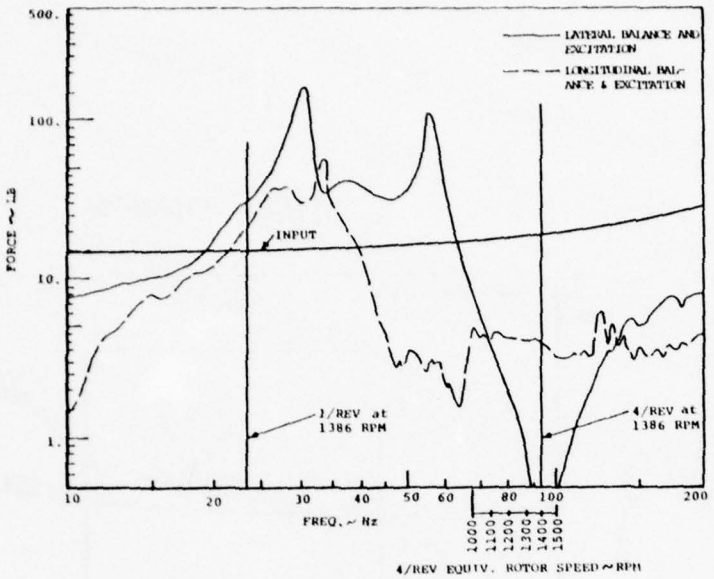

MOMENT BALANCE

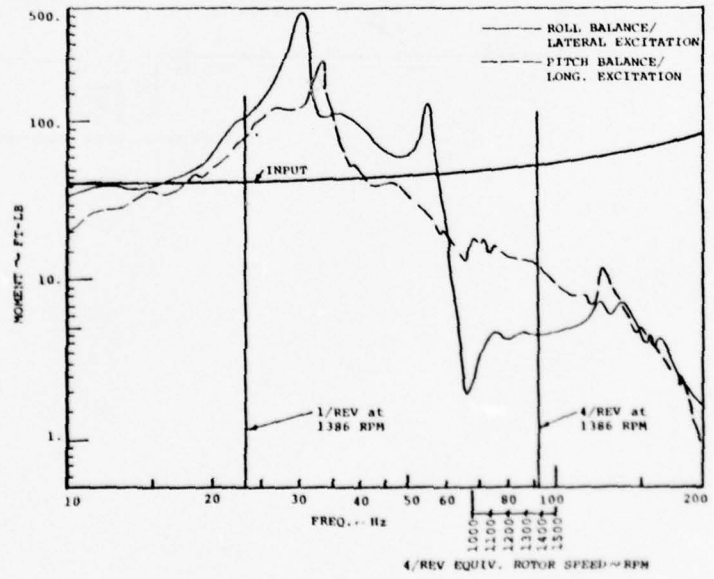

Figure 14. Focus at H = 1.1 in., Response Comparison for Hub Longitudinal and Lateral Excitation

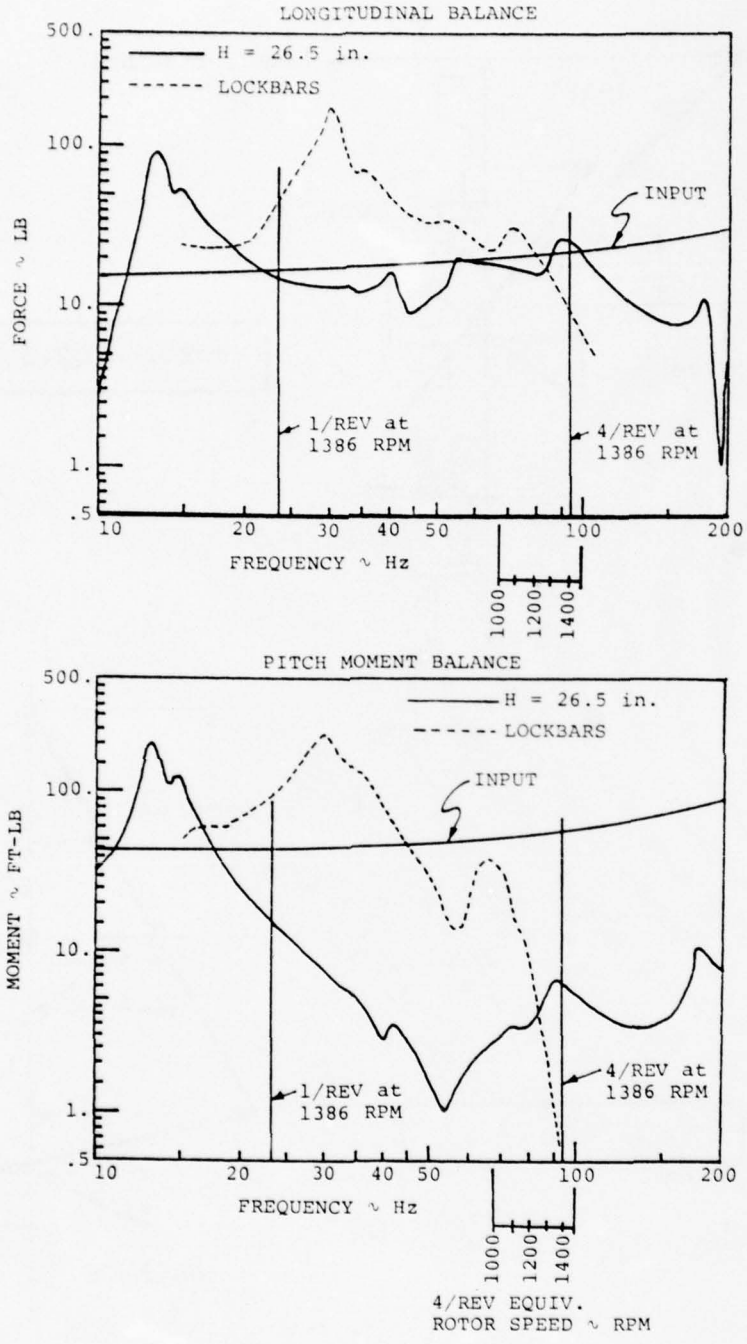

Figure 15. Downward Focus Force and Moment Balance Response - Hub Longitudinal Excitation

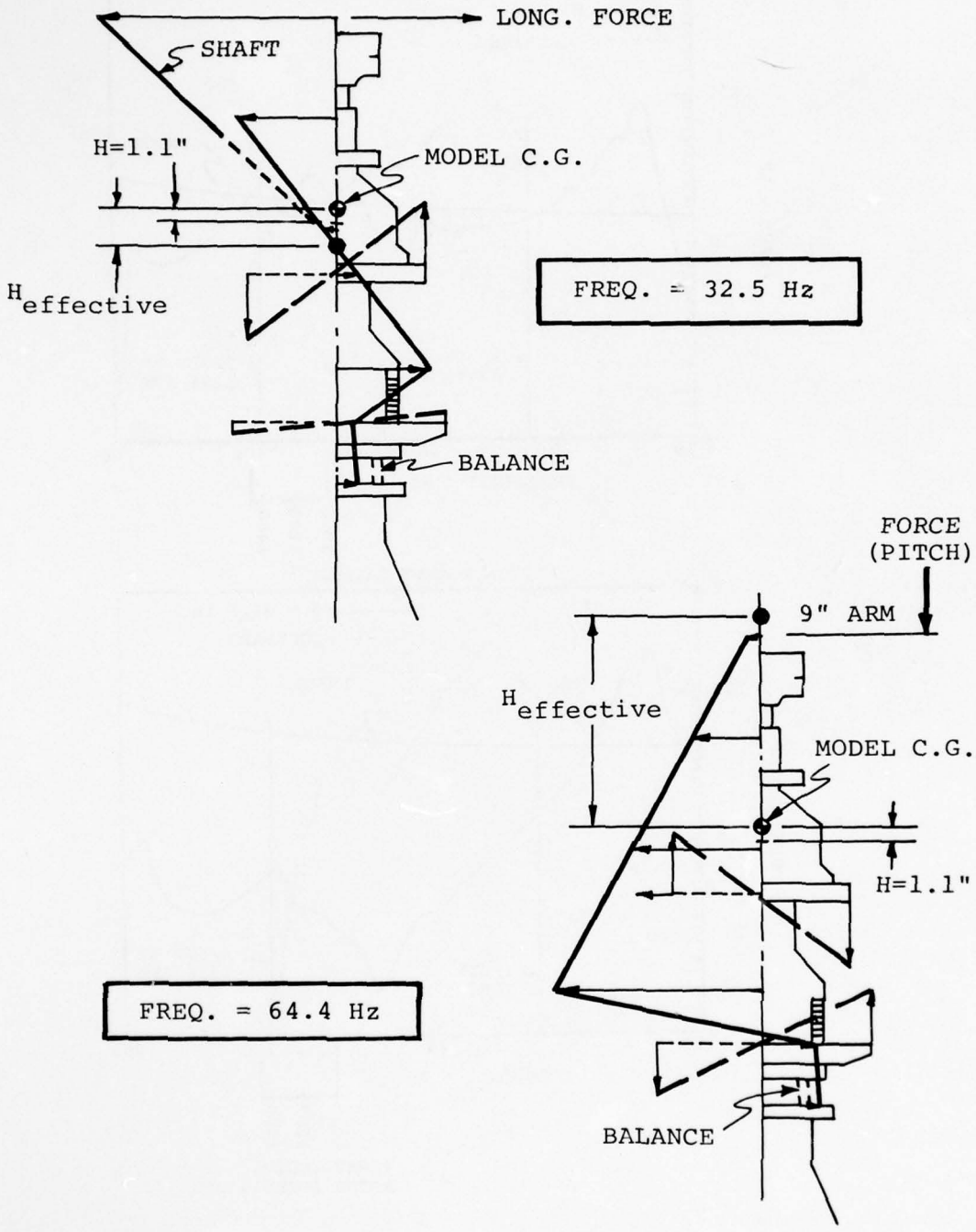

Figure 16. Longitudinal/Pitch Modes - Focus at H = 1.1 in.

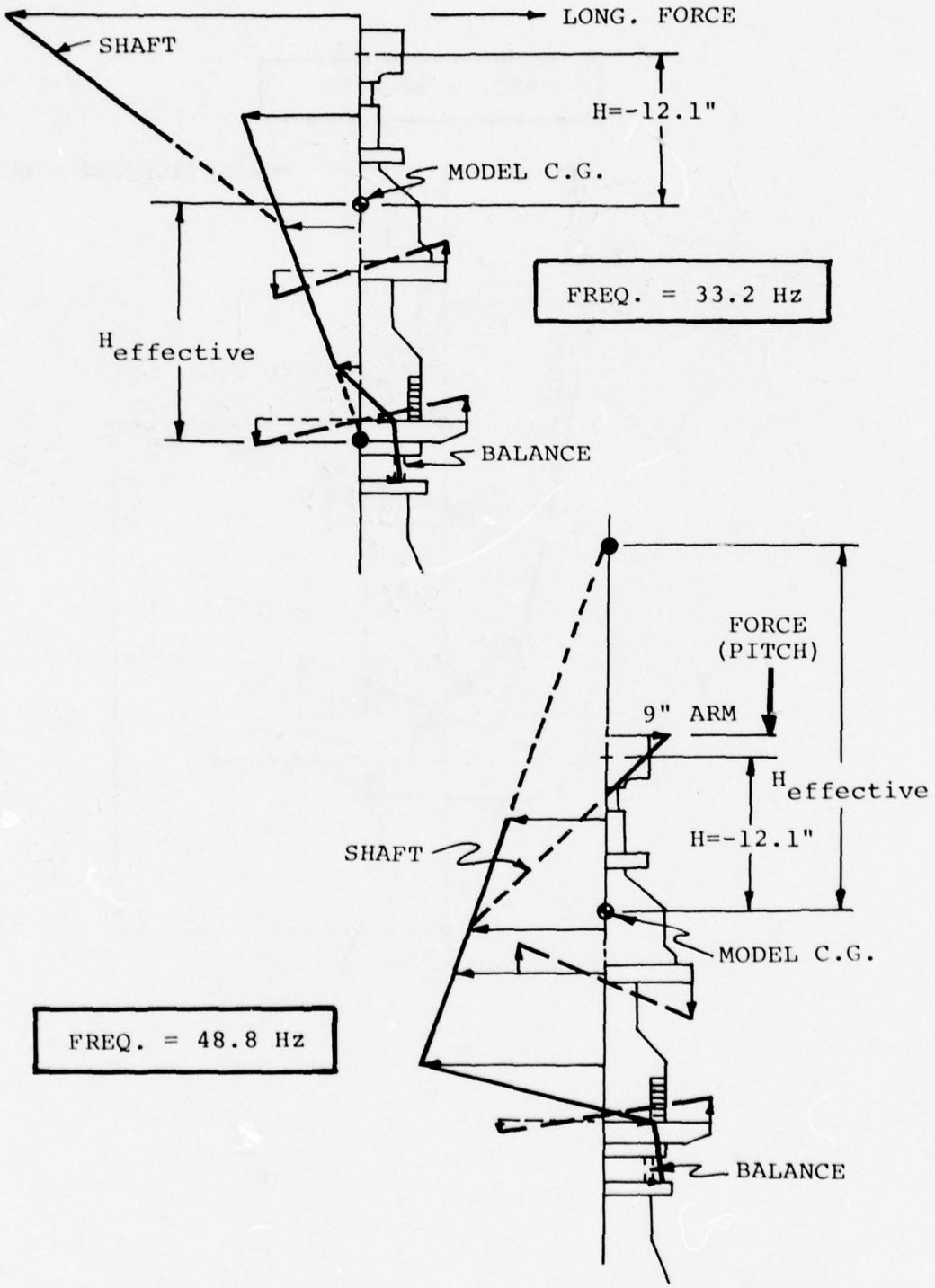

Figure 17. Longitudinal/Pitch Modes - Focus at H = -12.1 in.

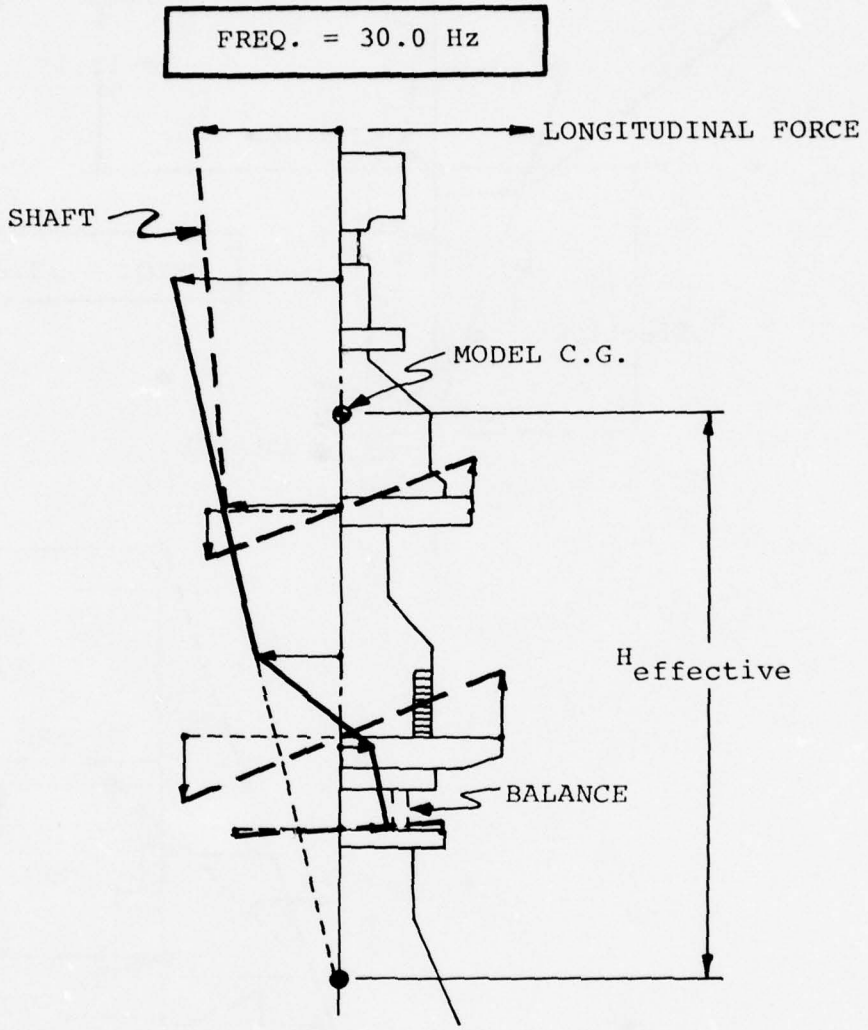

Figure 18. Longitudinal/Pitch Mode - Lockbars Installed

LONGITUDINAL BALANCE

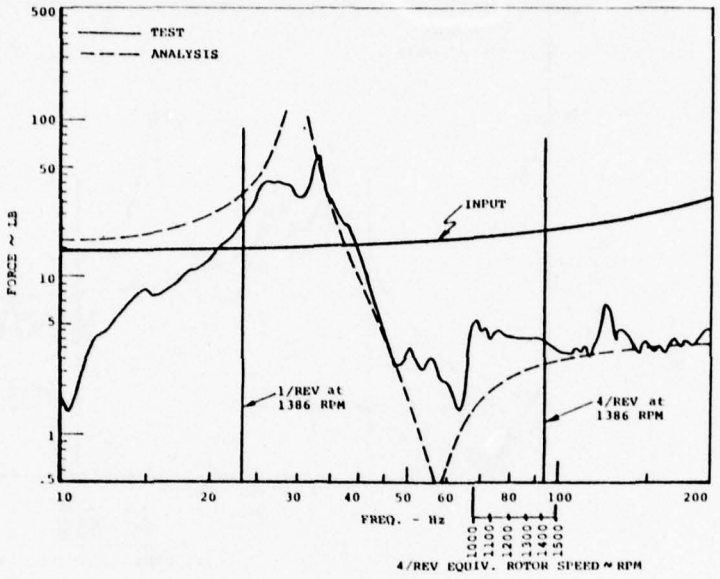

PITCH MOMENT BALANCE

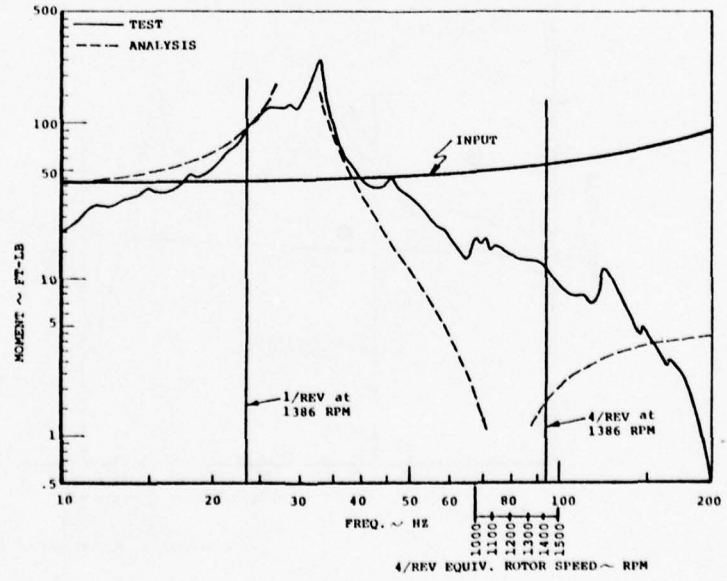

Figure 19. Focus at H = 1.1 in., Comparison of Test and Analysis - Hub Longitudinal Excitation

LONGITUDINAL BALANCE

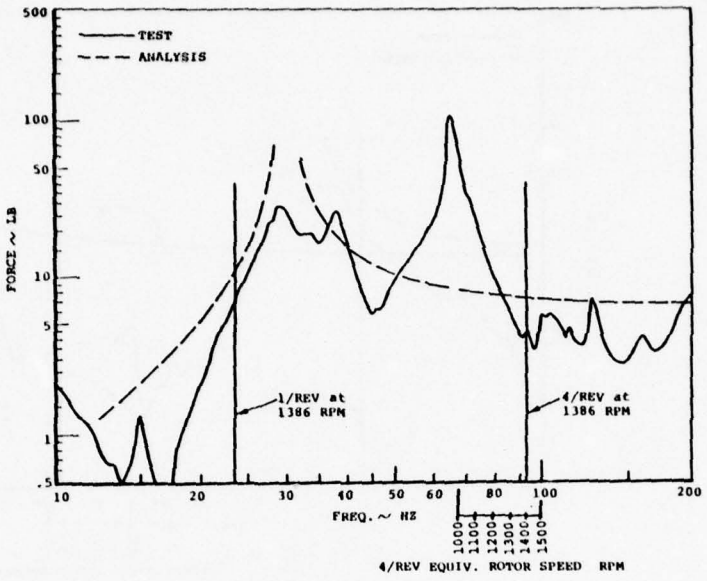

PITCH MOMENT BALANCE

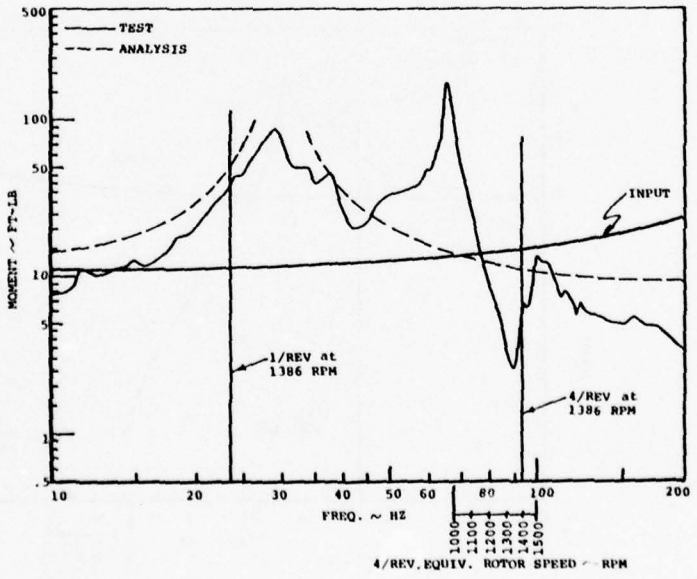

Figure 20. Focus at H = 1.1 in., Comparison of Test and Analysis - Hub Pitch Excitation

WIND TUNNEL TEST

Test results are divided into two groups. The first examines the influence of the isolation system on blade and hub loads, and the second deals with the effectiveness of the isolation system in reducing the rotor loads transmitted to the model balance. Harmonically analyzed balance and blade data are presented in the form of rotor speed sweeps at constant airspeed (advance ratio μ = .3) and airspeed sweeps at constant rotor speeds of 1175 and 1300 RPM. In addition, the predominant 4/rev fixed-system loads of the four-bladed model rotor are presented for the various focal conditions and compared with balance loads. Fixed-system vertical, pitch, and roll hub loads were computed from blade bending data using the method of Appendix B.

The test configuration with the lockbars was intended as a rigid reference configuration that would provide unisolated baseline data. The shake test, however, indicates that this configuration has a relatively low frequency mode (30 Hz) on the model balance. Consequently, the configuration cannot provide the unisolated baseline data desired.

Blade and Hub Loads

With the four-bladed model rotor, the predominant 4/rev fixed system loads arise from 3rd, 4th, and 5th harmonic blade flap bending moments and the 3rd and 5th harmonic chord bending moments. Blade flap and chord bending moment results for the rotor speed sweeps are summarized in Figures 21 and 22, which show a comparison of the harmonic responses for the various focal conditions including the lockbar configuration. Figure 23 presents a comparison of 4/rev fixed system loads (vertical, pitch and roll) computed from the blade bending data. The 3/rev flap moment with lockbars, Figure 21, appears near constant with rotor speed, while the focused configurations show an increase in the moment with increasing rotor speed. The remaining flap bending harmonics of Figure 21 and the chord bending moments, Figure 22, display a generally similar trend for all the test configurations. The computed fixed system hub loads of Figure 23 show little significant difference for the various configurations. Hub moments for the lockbar configuration, in particular the pitch moment, are relatively constant with rotor speed due to a similar characteristic previously noted in the 3/rev flap moment.

Blade bending moment airspeed sweep results are summarized in Figures 24 and 25 for 1175 RPM, and in Figures 26 and 27 for 1300 RPM. Fixed system hub loads for 1175 and 1300 RPM are presented in Figures 28 and 29 respectively. The most signi-

ficant variations in the blade moments occur in the 3/rev flap bending moments, Figures 24 and 26, at the maximum advance ratio. At the maximum advance ratio the loads are more sensitive to trim conditions, and it is surmised that the observed load variations are due in large measure to minor variations in trim. In this regard it is noted that there were several operators, each of whom flew the model in a slightly different manner. The computed fixed system hub loads, Figures 28 and 29, show similar trends for all the configurations. While the greatest variation still tends to occur at the high-speed point, it appears less significant than that observed in the blade loads.

A blade load comparison for the lockbar configuration with a live balance and a dummy balance is presented in Figures 30 through 35. The configuration with the dummy balance was the most rigid possible, whereas the configuration with the live balance was relatively soft, having a pitch natural frequency of 30 Hz (1800 RPM) due to balance flexibility. Blade flap and chord moments from the rotor speed sweep, Figures 30 and 31, are reasonably similar with the exception of the 3/rev chord moment. The 3/rev chord moment with the dummy balance, Figure 31, displays a peak in the mid-speed range while the results with the live balance are nearly constant over the rotor speed range. Airspeed sweep results at 1175 RPM are summarized in Figures 32 and 33. Again, both configurations show similar results except for the 3/rev chord moment, Figure 33, where the dummy balance shows an unexplained peak in the middle of the airspeed range. Finally, the airspeed sweep data at 1300 RPM, Figures 34 and 35, display highly comparable loads for both configurations at all the harmonics.

Balance Loads - Rotor Speed Sweeps

The predominant 4/rev balance loads as a function of rotor speed are compared in Figures 36 and 37 for the various focal configurations. Comparisons of balance and computed hub loads are presented in Figures 38 through 42.

Referring to Figure 36, the lowest vertical loads (not an isolated direction) occur in the vicinity of 1300 RPM with the lockbar configuration and a focus at H = -12.1 inches. The best configurations for minimum lateral and longitudinal loads are the focus at H = 3.65 inches and the mixed focus with H = 1.1 inches in the lateral axis and H = -12.1 inches in the longitudinal axis. Near-minimum lateral and longitudinal loads occur simultaneously at 1300 RPM for both these configurations. The highest overall levels in both the lateral and longitudinal directions are obtained with the lockbar configuration.

Examination of Figure 37 indicates that the best configurations for minimum pitch and roll moment are the lockbar configuration and the focus at H = 1.1 inches. Low levels are obtained with either of these configurations at speeds above 1200 RPM. At speeds approaching 1400 RPM the focus at H = 1.1 inches is slightly superior to the lockbar configuration. It is also observed that reasonably low pitch and roll moments occur simultaneously at 1300 RPM for H = -3.65 inches, which was one of the two best arrangements for the lateral and longitudinal loads. In this regard, it is noted that the best choices for the pitch and roll moments (in particular the lockbar configuration) are poor choices for lateral and longitudinal force isolation.

In the absence of a rigid reference configuration or measured inplane hub loads, it is not possible to assess the relative benefit of the configurations that produce the minimum lateral and longitudinal loads. Measured vertical, pitch, and roll hub loads are, however, available. A comparison of these loads with the balance loads gives an indication of the relative effectiveness of the various test configurations. Such a comparison, however, is not necessarily an indication of true isolation efficiency since an unknown portion of the measured moment balance loads are due to inplane hub forces.

Comparison of the balance and hub loads for H = 1.1 inches and the lockbars, Figures 38 and 39 respectively, generally confirm the previous observations. On the plots, isolation regions are shown by the cross-hatched areas where the hub load is greater than the balance force. With the focus at H = 1.1 inches, the pitch moment indicates isolation above 1200 RPM while the roll moment is isolating over the entire speed range. In both cases, the effectiveness increases at speeds above 1200 RPM. The lockbar configuration shows similar results for the roll moment, but no apparent isolation of the pitch moment. Comparison of the hub pitch moments for H = 1.1 inches and the lockbars indicates that the apparent lack of pitch isolation with the lockbars is due to a lower hub load rather than to a higher balance load. Above 1150 RPM it is also noted that both configurations display substantial isolation of the vertical hub load. This result was unanticipated and appears to be in conflict with the shake test results of Figure 13 which, for H = 1.1 inches at least, show amplification of the vertical load. A probable explanation lies in the fact that the shake test data was not processed through the wind tunnel data system; consequently, the shake test results are not corrected for vertical/pitch interaction.

The balance and hub load comparison for the mixed focus (H = 1.1 inches lateral and H = -12.1 inches longitudinal) is shown in Figure 40. This configuration, considered as a possible choice for isolating both the inplane loads and moments, displays reasonable isolation of roll moments at speeds above 1300 RPM; however, isolation of the pitch moment is minimal. Comparisons for the remaining test configurations, H = 3.65 inches and H = -12.1 inches, Figures 41 and 42 respectively, exhibit a small degree of roll isolation in the range of 1300 RPM and no isolation in pitch.

Balance Loads - Airspeed Sweeps

Rotor speeds of 1175 and 1300 RPM for the airspeed sweep testing were selected early in the program based on a preliminary evaluation of rotor speed sweep data from the first two model configurations.

Airspeed sweep results at 1175 RPM are presented in Figures 43 through 49. Figure 43, showing the inplane balance loads, indicates the best compromise for lateral and longitudinal loads is the mixed focus (H = 1.1 inches lateral and H = -12.1 inches longitudinal). The moment balance loads, Figure 44, show that the locked configuration is best in both the pitch and roll directions. For the pitch and roll moments the relative effectiveness is illustrated by the balance and hub load comparisons of Figures 45 through 49. The focus at H = 1.1 inches, Figure 45, displays some roll moment isolation over most of the airspeed range while the pitch moment shows none. Results for the lockbar configuration, which had the lowest moment balance loads, are presented in Figure 46. Significant roll moment isolation is evident over the full speed range; however, the pitch moment has meaningful isolation only at the maximum advance ratio. For the mixed focus (H = 1.1 inches lateral and -12.1 inches longitudinal), the results of Figure 47 exhibit roll moment isolation at low speed, but little effective isolation of the pitch moment. The remaining configurations, Figures 48 and 49, display little isolation in either pitch or roll. While isolation was not intended, it is noted that all of the test configurations, except the lockbar configuration of Figure 46, show substantial vertical isolation over most of the airspeed range.

Airspeed sweep results illustrating the balance loads at a rotor speed of 1300 RPM are summarized in Figures 50 and 51. For the lateral and longitudinal balance loads, Figure 50, the mixed focus configuration (H = 1.1 inches lateral and -12.1 inches longitudinal) appears to be the best compromise. The lockbar configuration is favored for the pitch and moment balances, Figure 51, with the focus at H = 1.1 inches as a

second choice. In contrast, the lockbar configuration is the worst possible choice for both of the inplane balance loads, while the focus at H = 1.1 inches is an excellent choice for lateral, but a poor choice for longitudinal force isolation.

Recalling from the shake test that the lockbar configuration had an effective focus below the balance, an interesting observation presents itself. Referring to the analytical results of Figure 9, it is noted that the downward focus has low moments, and "kick loads" (KF_B/M_H, due to hub moment) that tend to increase as the focus is moved up. On this basis, low balance moments and high longitudinal and lateral balance forces would be anticipated. As indicated previously, the test results of Figures 50 and 51 show this to be the case.

Comparisons of the balance and hub loads at 1300 RPM for H = 1.1 inches and the lockbar configuration, Figures 52 and 53, confirm the preceding observations relative to the pitch and roll moments. With the focus at H = 1.1 inches, Figure 52, substantial isolation is indicated over most of the airspeed range. Due principally to somewhat lower measured hub loads, the pitch moment results for the lockbar configuration, Figure 53, display less effective isolation. On the other hand, improved effective roll moment isolation is evident with the lockbars. This improvement results from a small variation in the hub load and significantly lower balance loads compared to the focus at H = 1.1 inches. With regard to vertical loads, the focus at H = 1.1 inches displays lower balance loads and a consistently higher degree of isolation due to a lower balance force.

The mixed focus (H = 1.1 inches lateral and H = -12.1 inches longitudinal) hub and balance load comparisons are presented in Figure 54. Relatively low effective roll isolation is evident and the pitch moment isolation is poor. Results for the remaining configurations, shown in Figures 55 and 56, indicate little or no isolation of the pitch and roll moments. On the contrary, significant amplification of the pitch moments is present over most of the speed range.

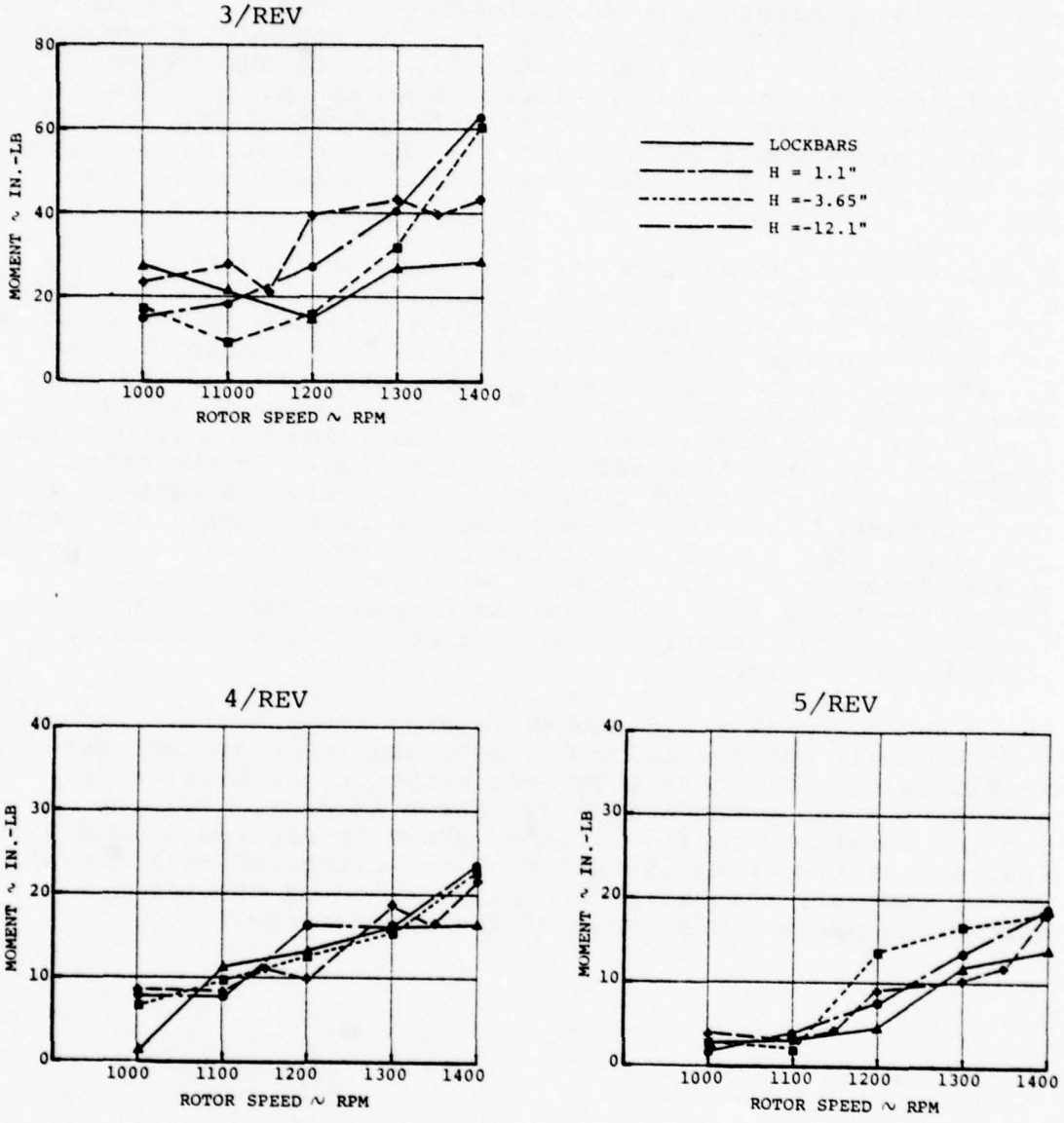

Figure 21. RPM Sweep at μ = .3, Blade Flap Moments at 11% Radius

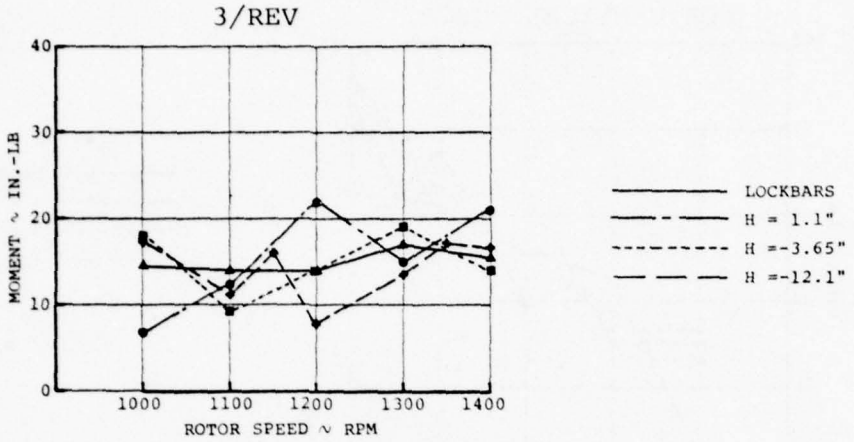

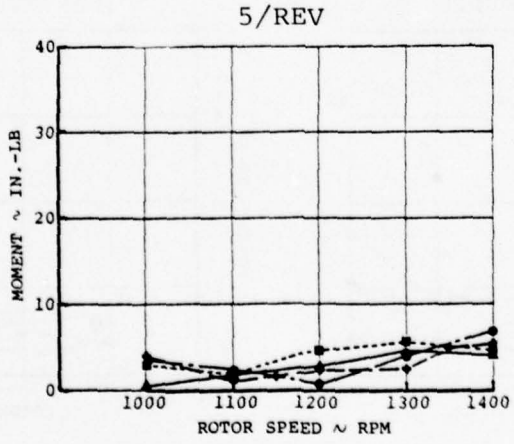

Figure 22. RPM Sweep at $\mu = .3$, Blade Chord Moments at 11% Radius

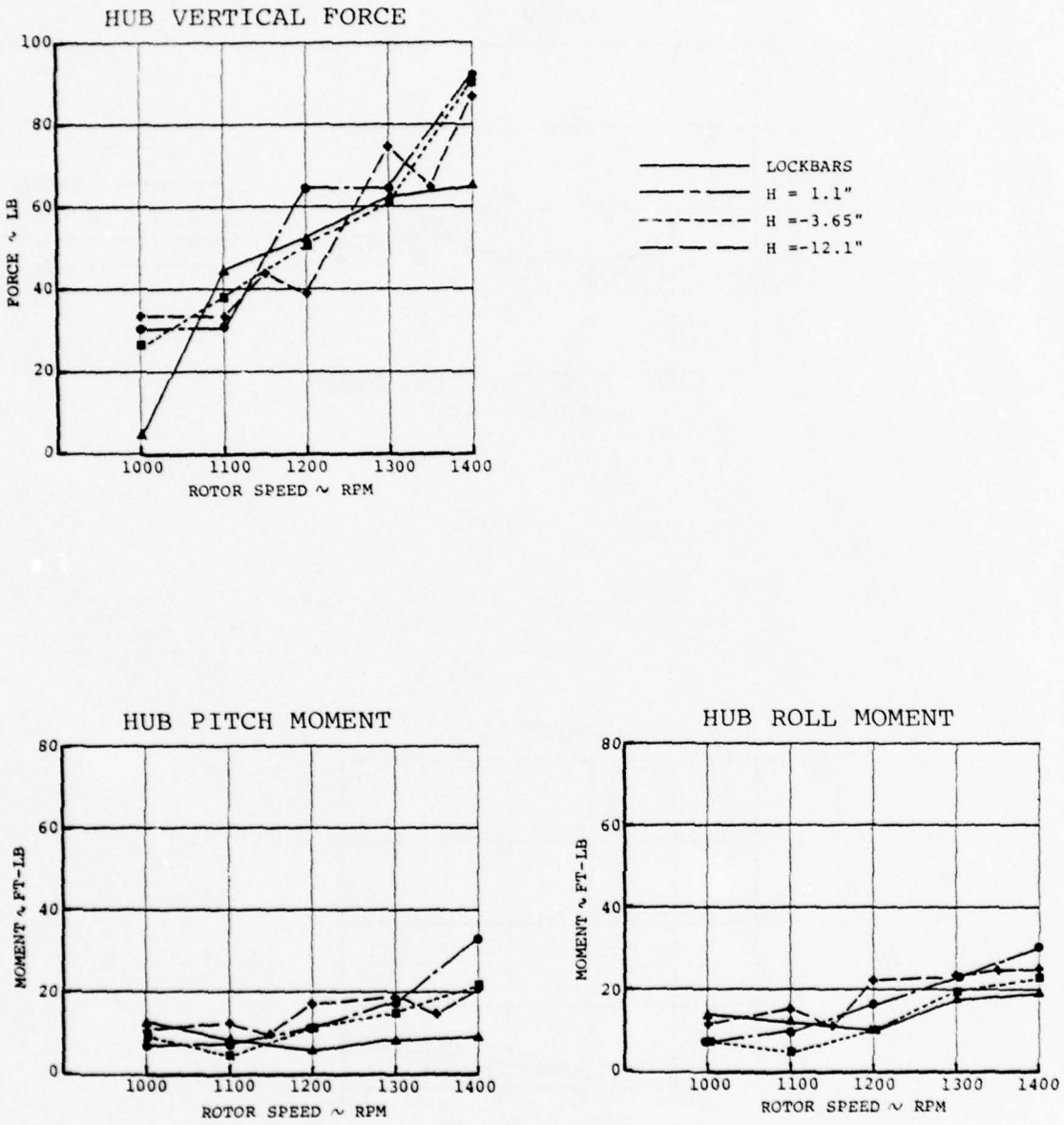

Figure 23. RPM Sweep at $\mu \approx .3$, 4/Rev Fixed System Hub Loads

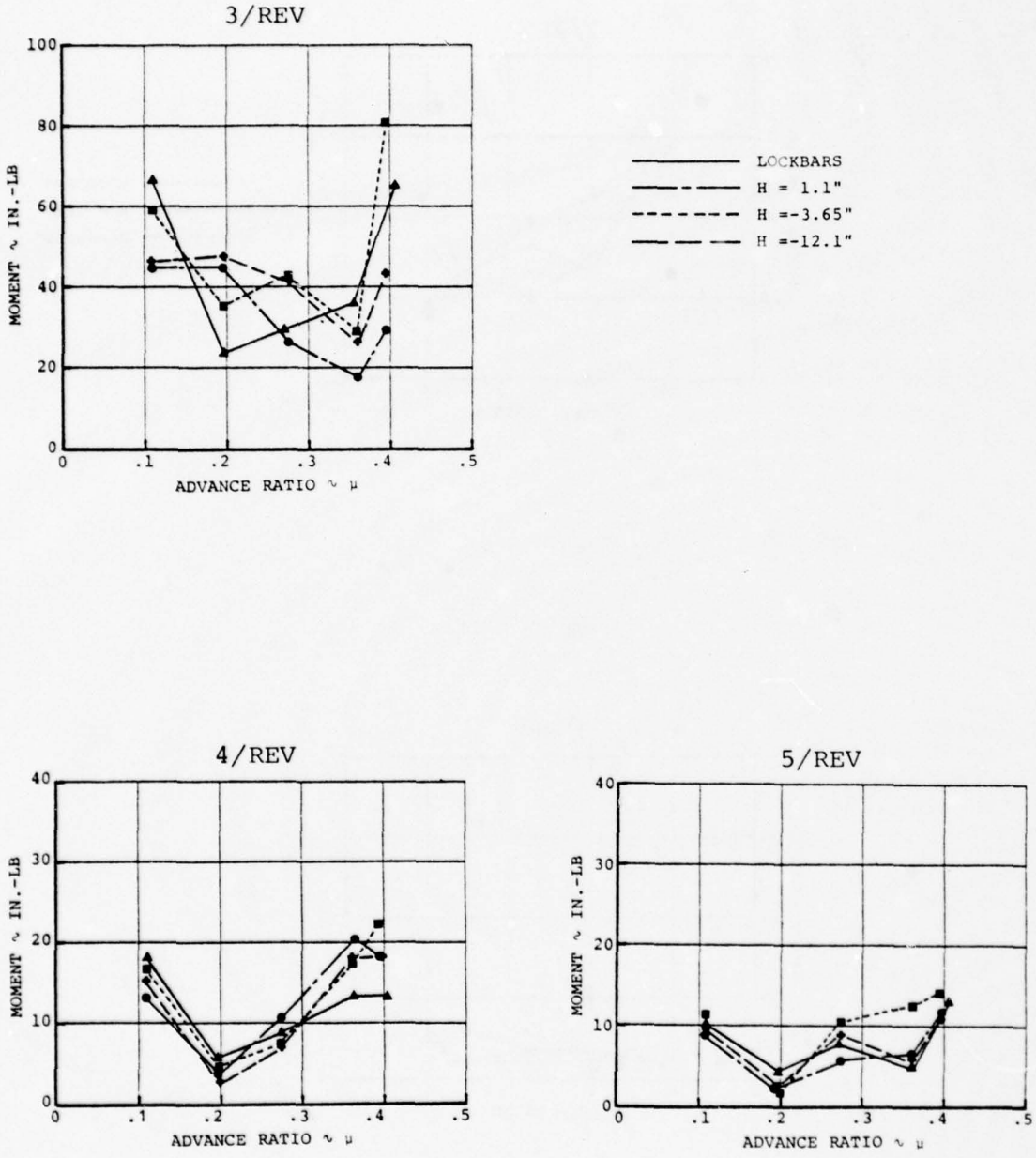

Figure 24. Airspeed Sweep at 1175 RPM, Blade Flap Moments at 11% Radius

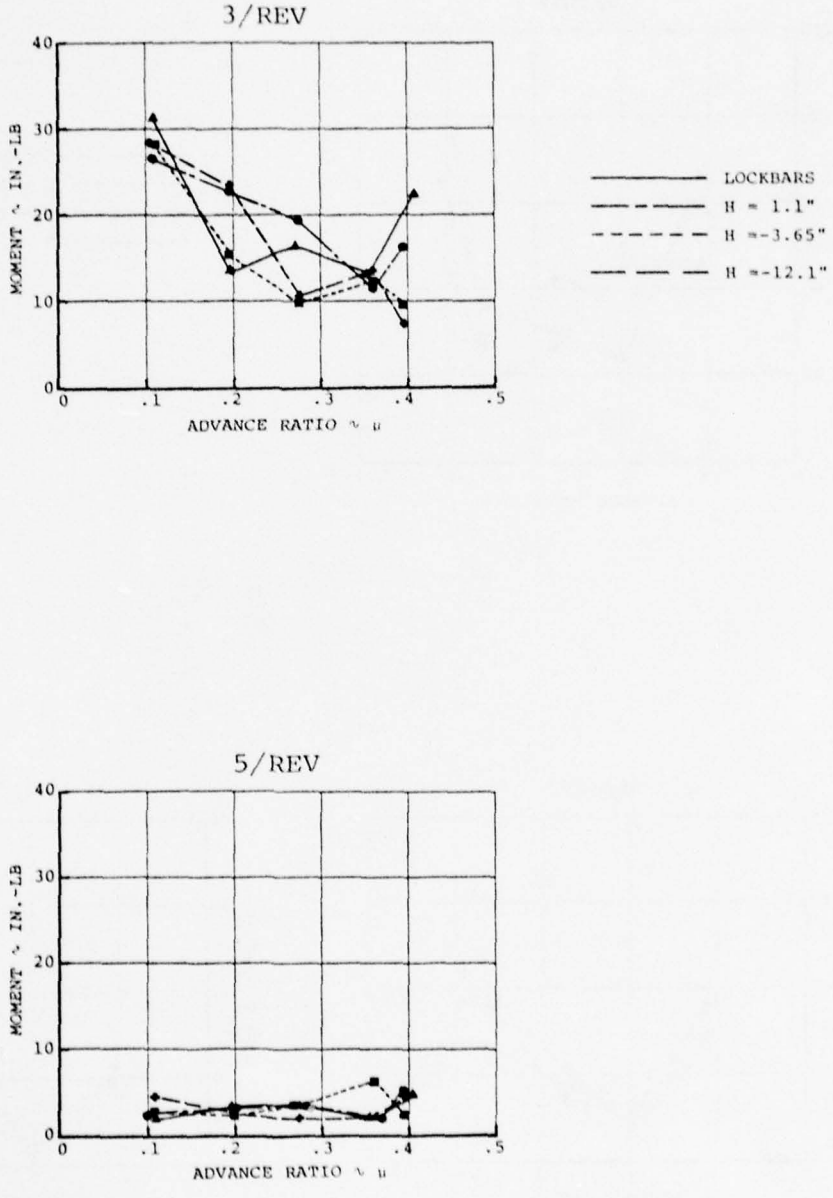

Figure 25. Airspeed Sweep at 1175 RPM, Blade Chord Moments at 11% Radius

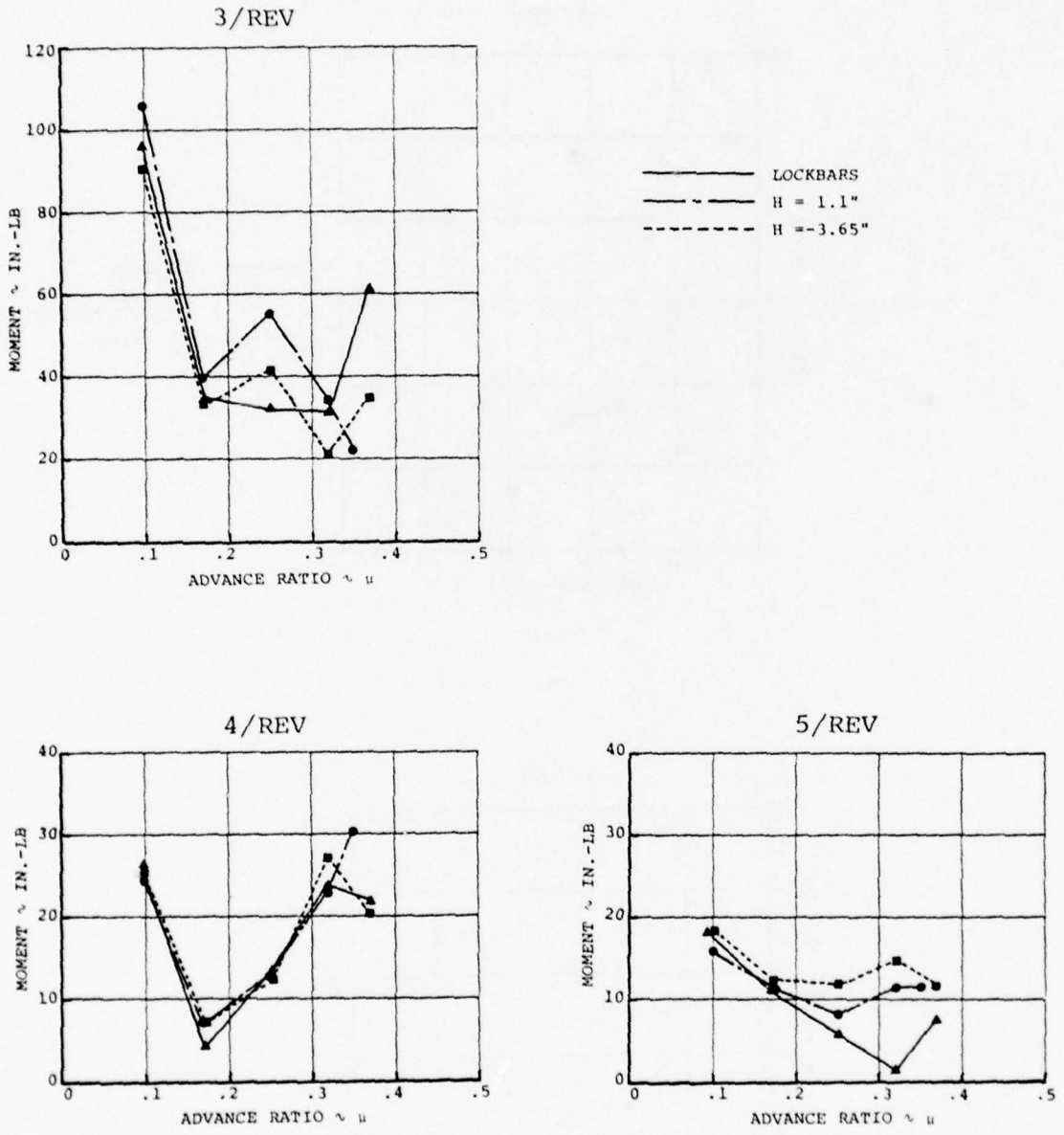

Figure 26. Airspeed Sweep at 1300 RPM, Blade Flap Moments at 11% Radius

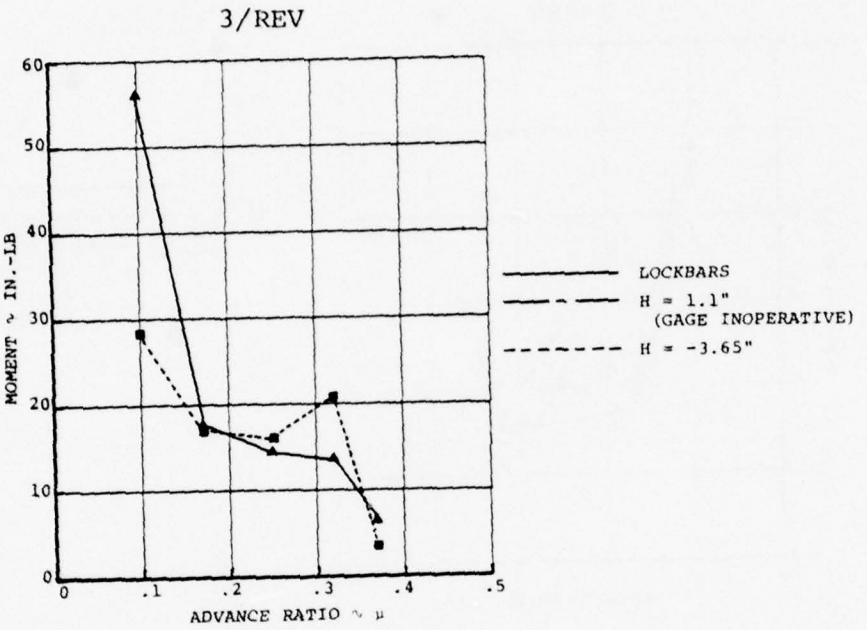

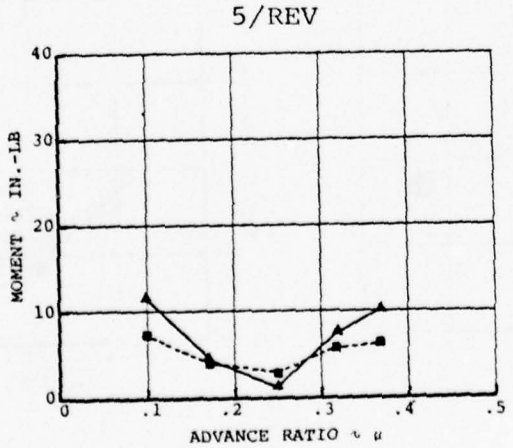

Figure 27. Airspeed Sweep at 1300 RPM, Blade Chord Moments at 11% Radius

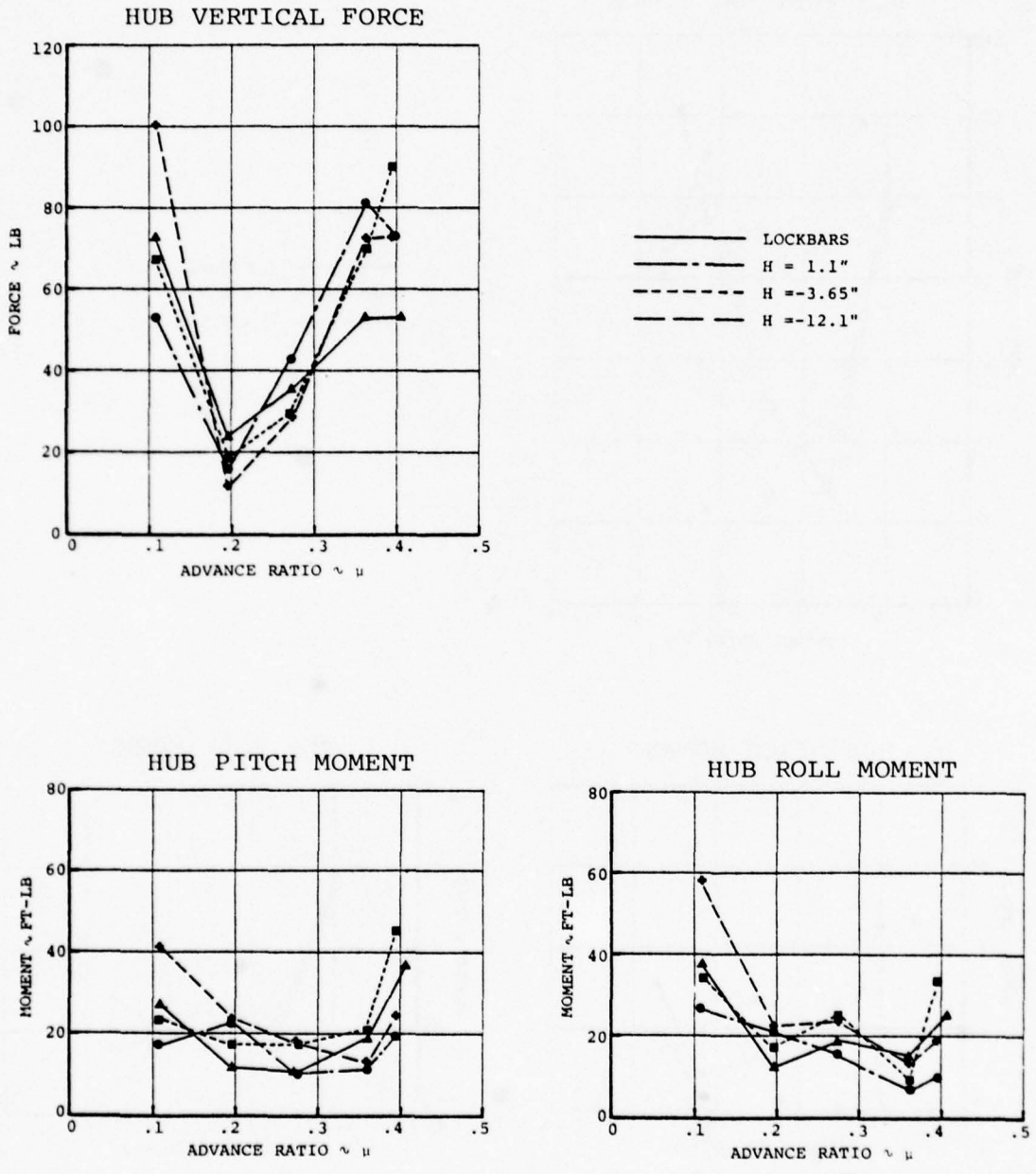

Figure 28. Airspeed Sweep at 1175 RPM, 4/Rev Fixed System Hub Loads

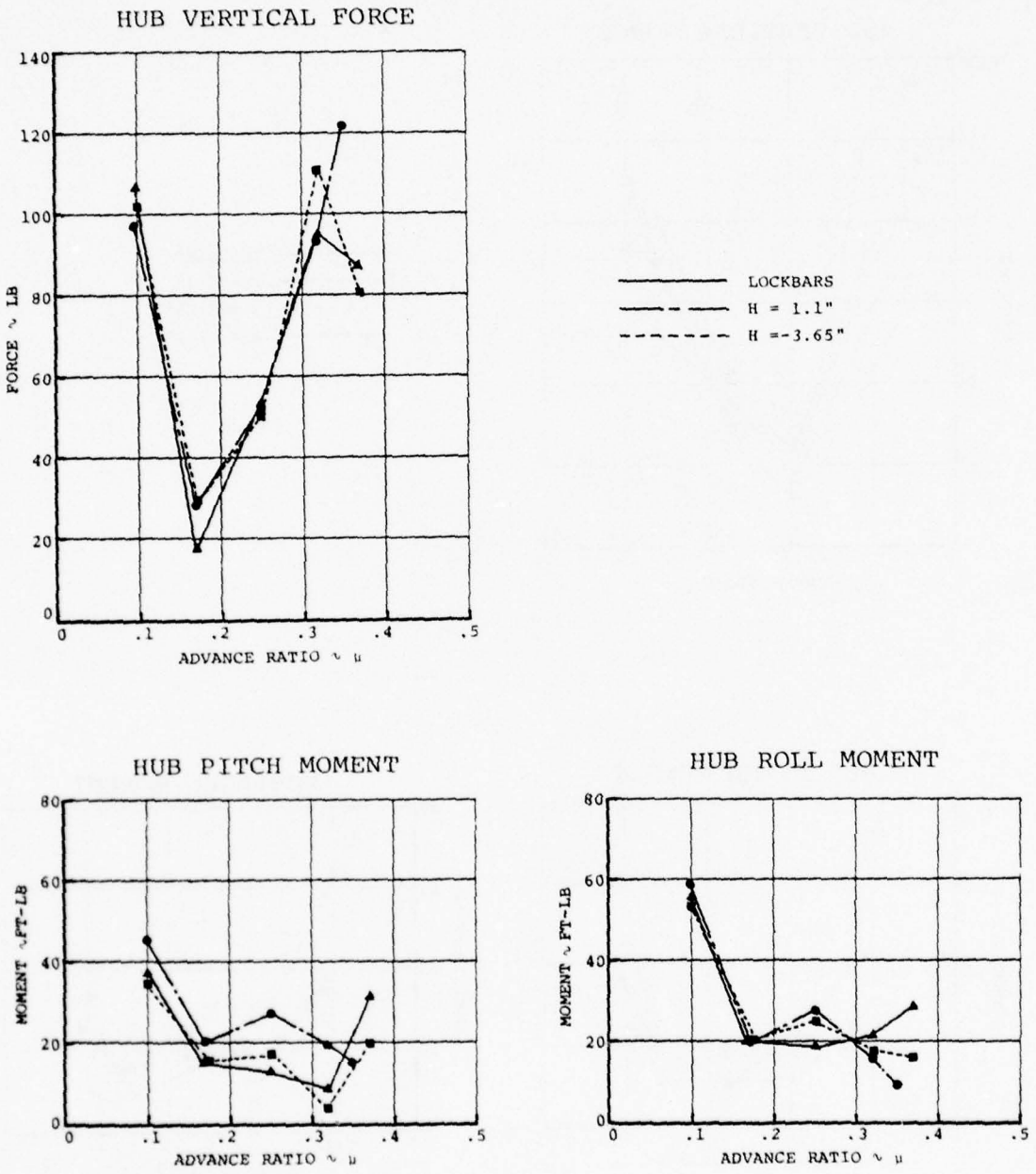

Figure 29. Airspeed Sweep at 1300 RPM, 4/Rev Fixed System Hub Loads

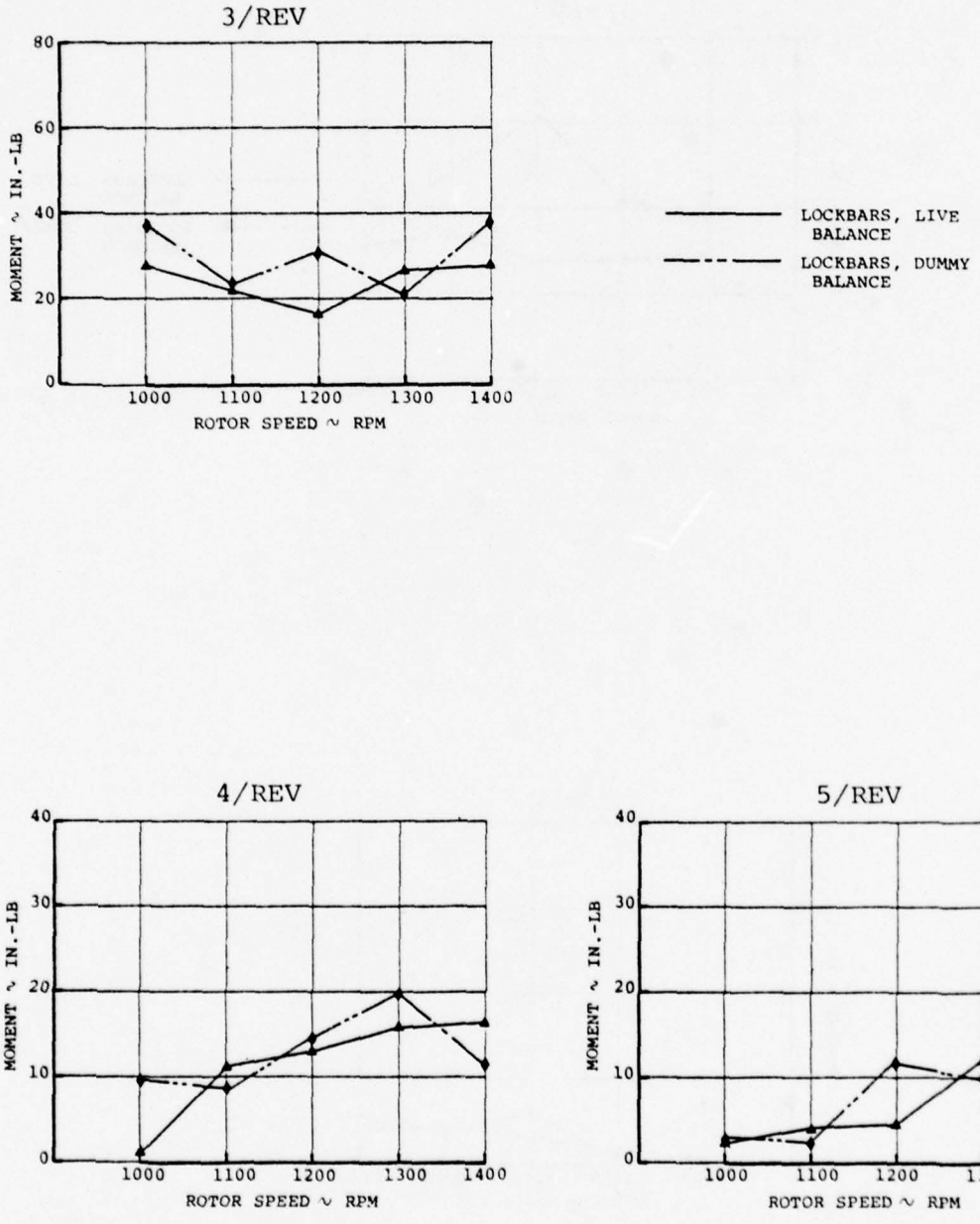

Figure 30. RPM Sweep at μ = .3, Live vs Dummy Balance, Blade Flap Moments at 11% Radius

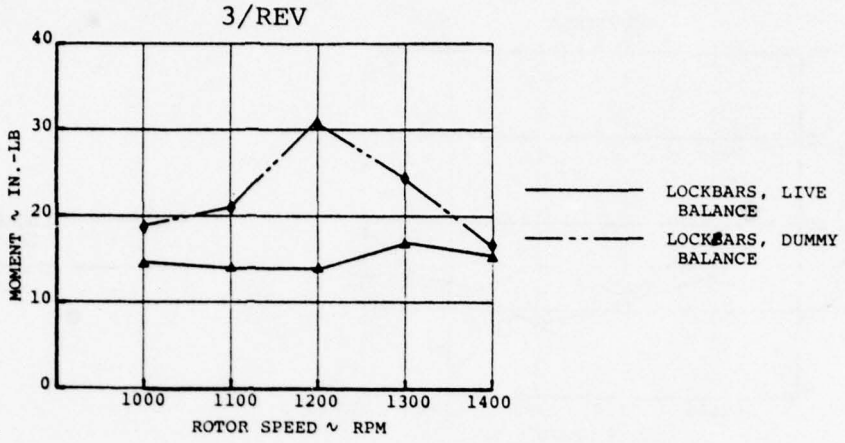

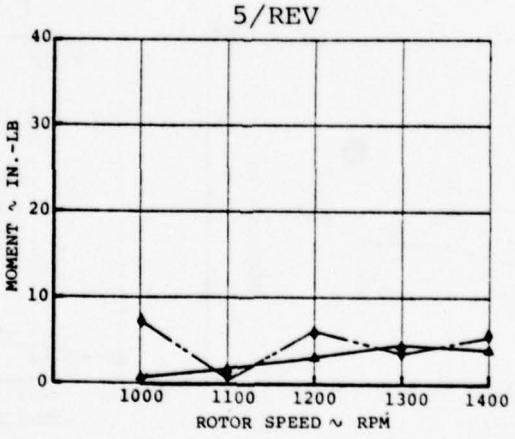

Figure 31. RPM Sweep at μ = .3, Live Vs Dummy Balance, Blade Chord Moments at 11% Radius

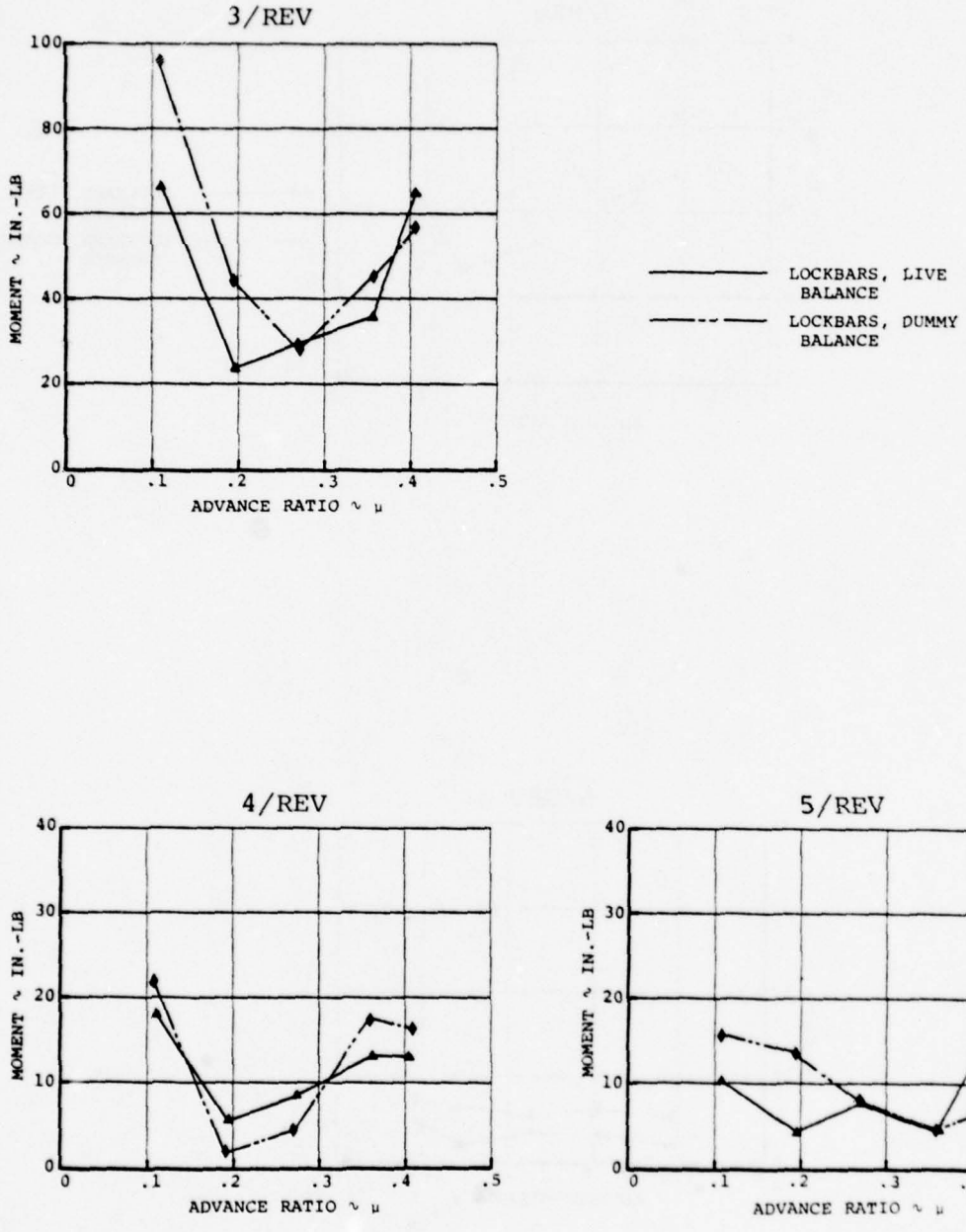

Figure 32. Airspeed Sweep at 1175 RPM, Live vs Dummy Balance, Blade Flap Moments at 11% Radius

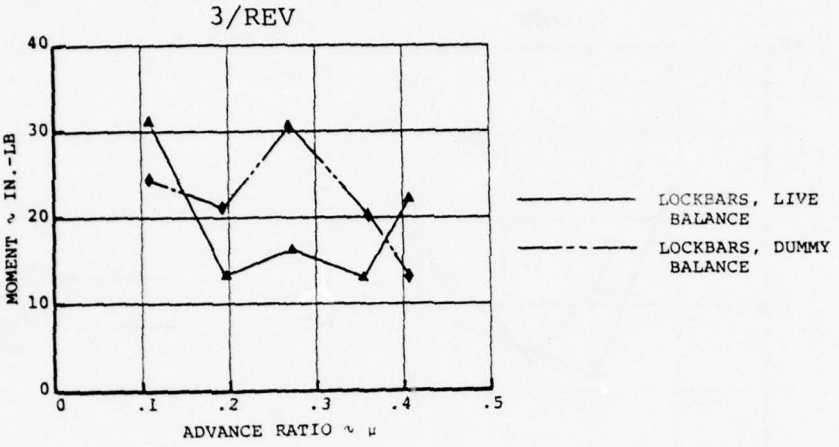

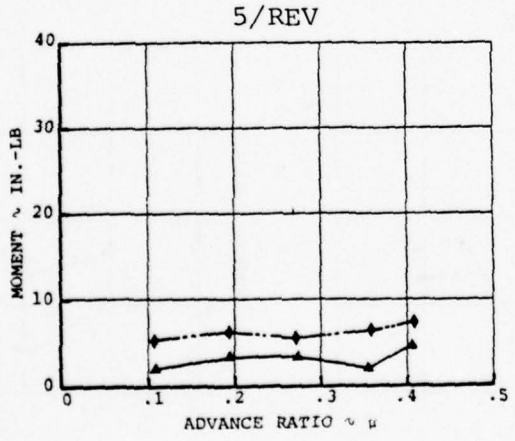

Figure 33. Airspeed Sweep at 1175 RPM, Live vs Dummy Balance, Blade Chord Moments at 11% Radius

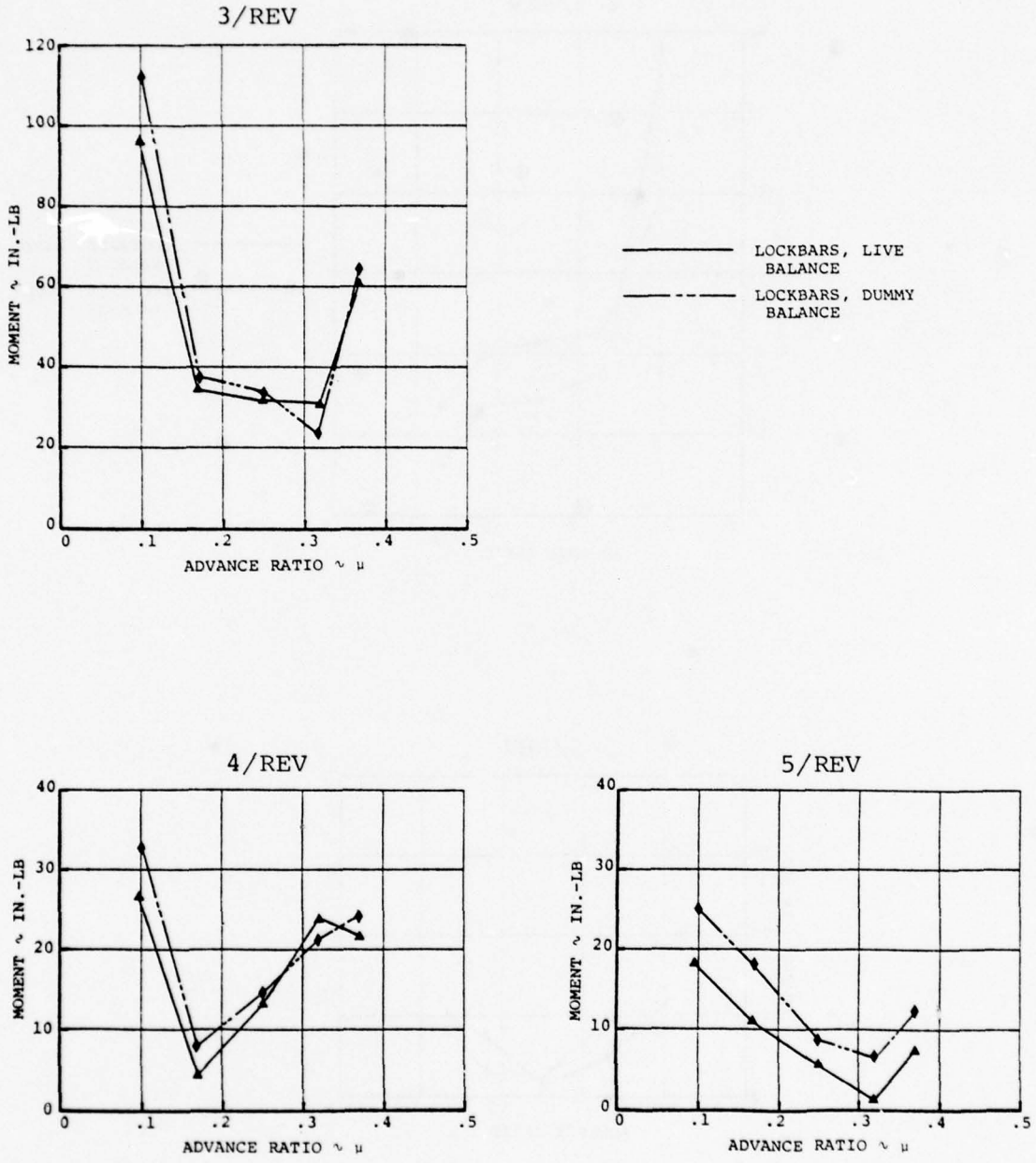

Figure 34. Airspeed Sweep at 1300 RPM, Live vs Dummy Balance, Blade Flap Moments at 11% Radius

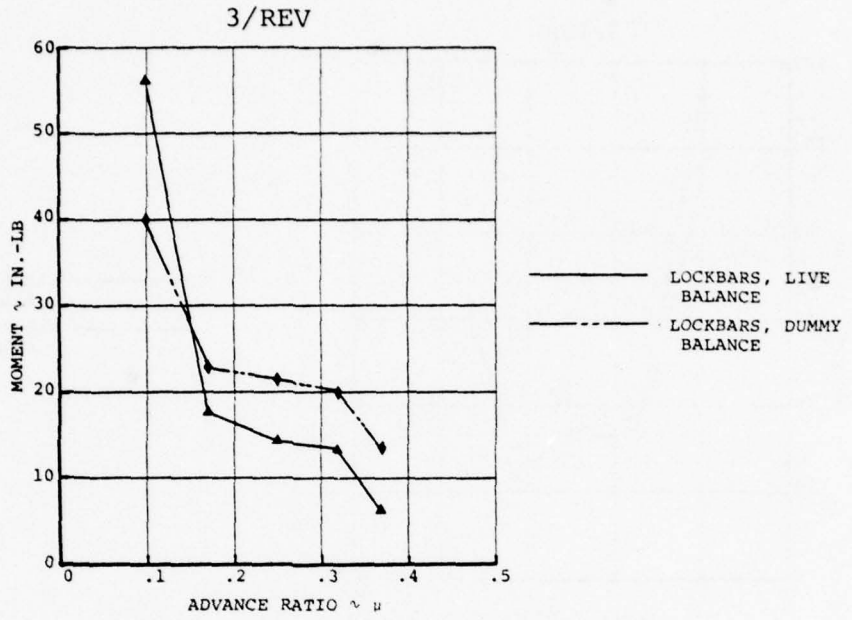

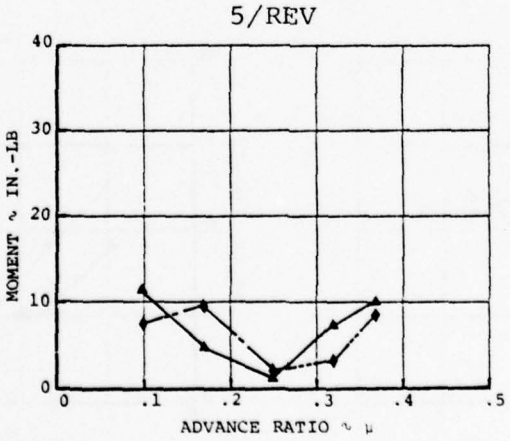

Figure 35. Airspeed Sweep at 1300 RPM, Live vs Dummy Balance, Blade Chord Moments at 11% Radius

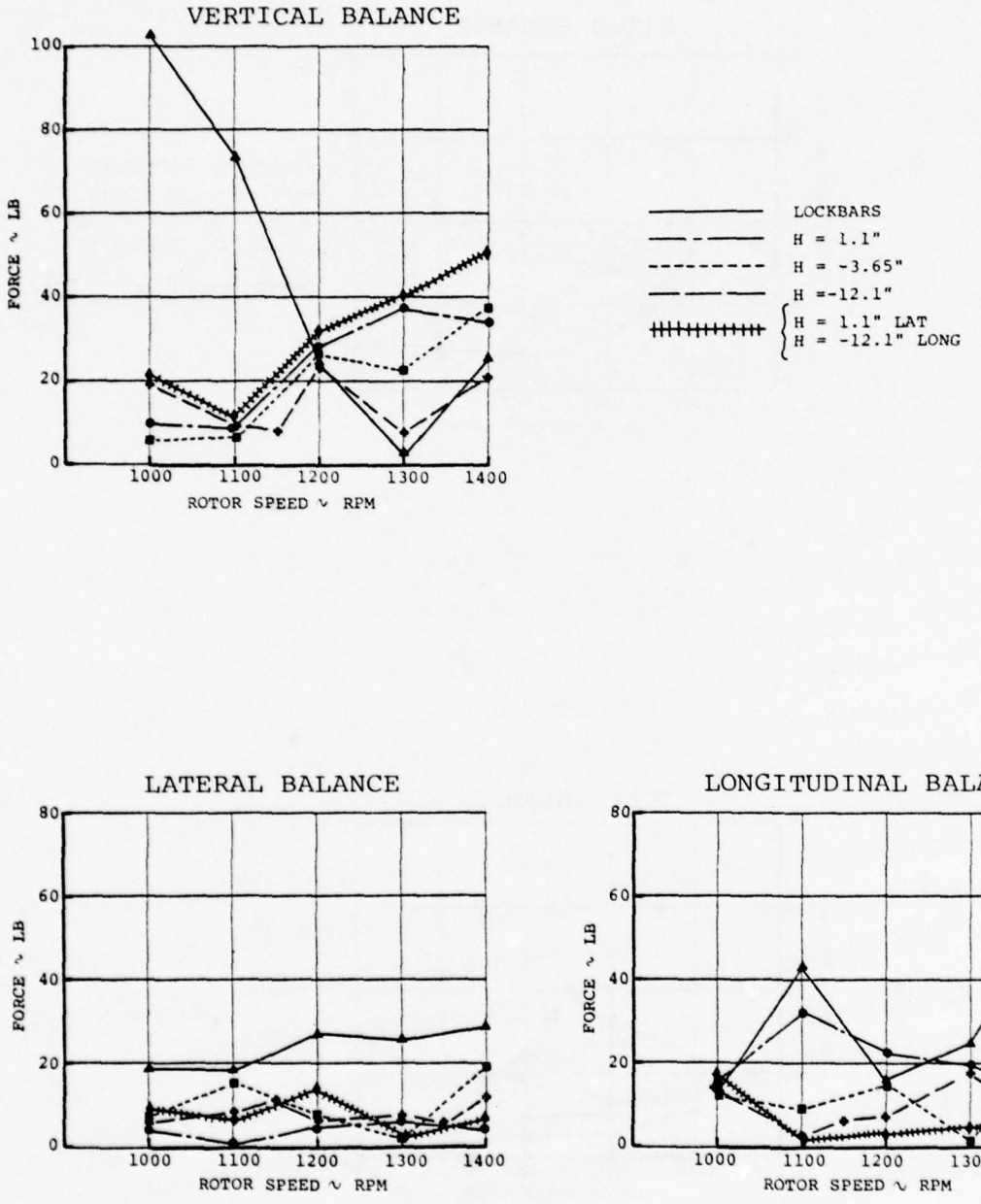

Figure 36. RPM Sweep at μ .3, 4/Rev Vertical and Inplane Balance Loads

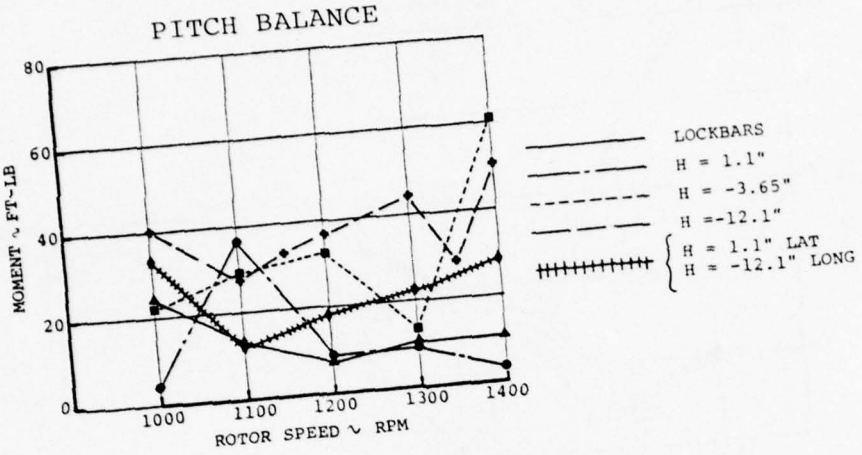

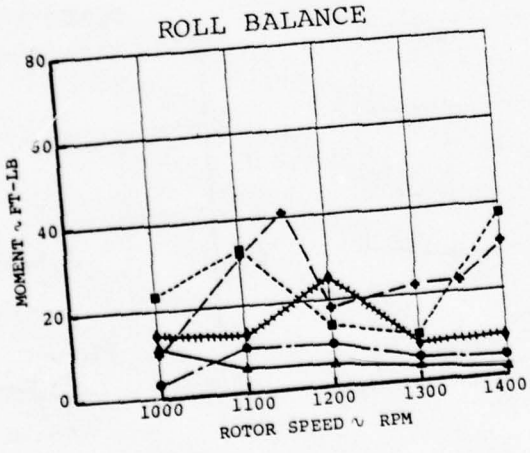

Figure 37. RPM Sweep at μ = .3, 4/Rev Moment Balance Loads

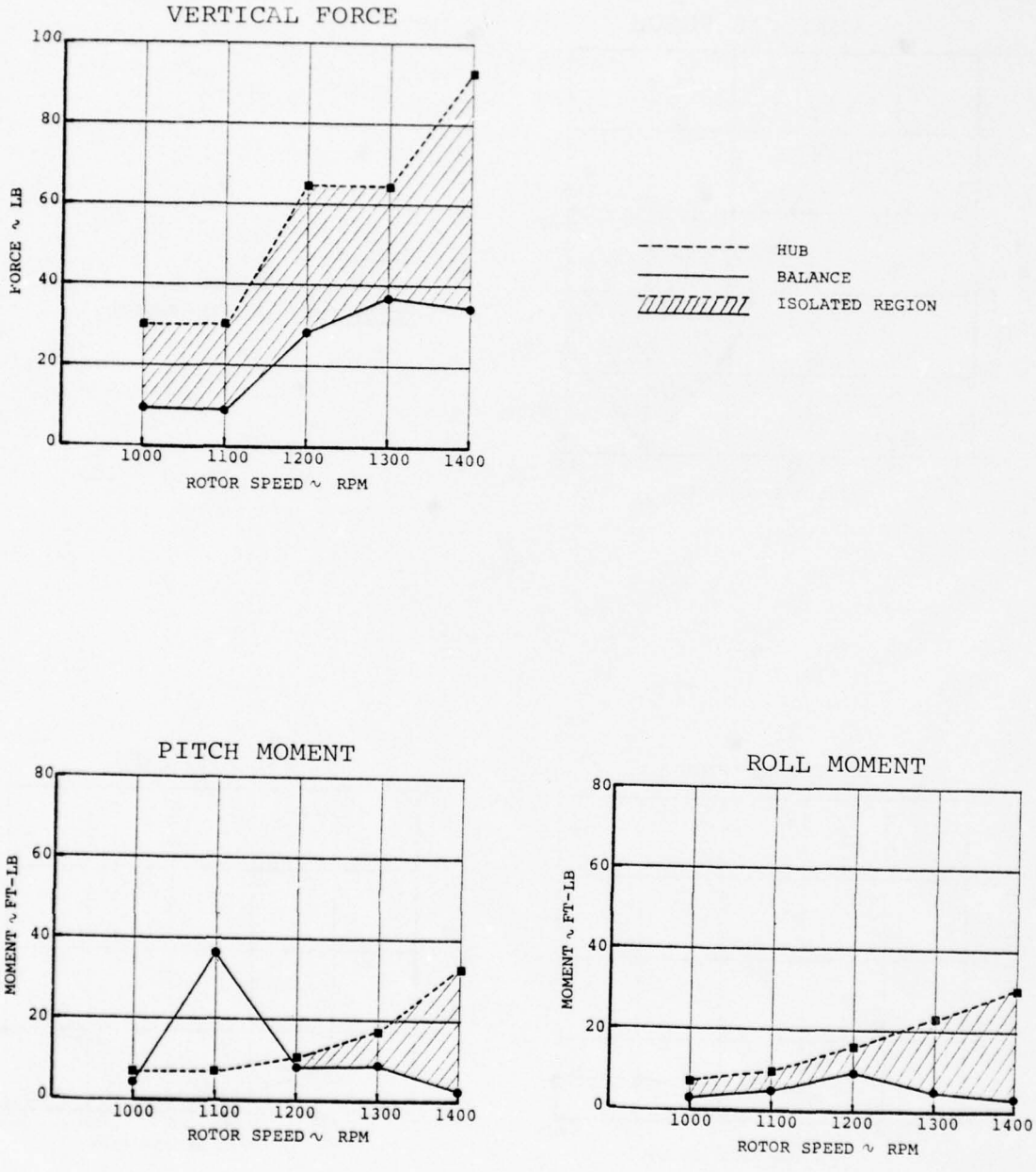

Figure 38. RPM Sweep at μ = .3, Focus H = 1.1 in., 4/Rev Balance vs Hub Loads

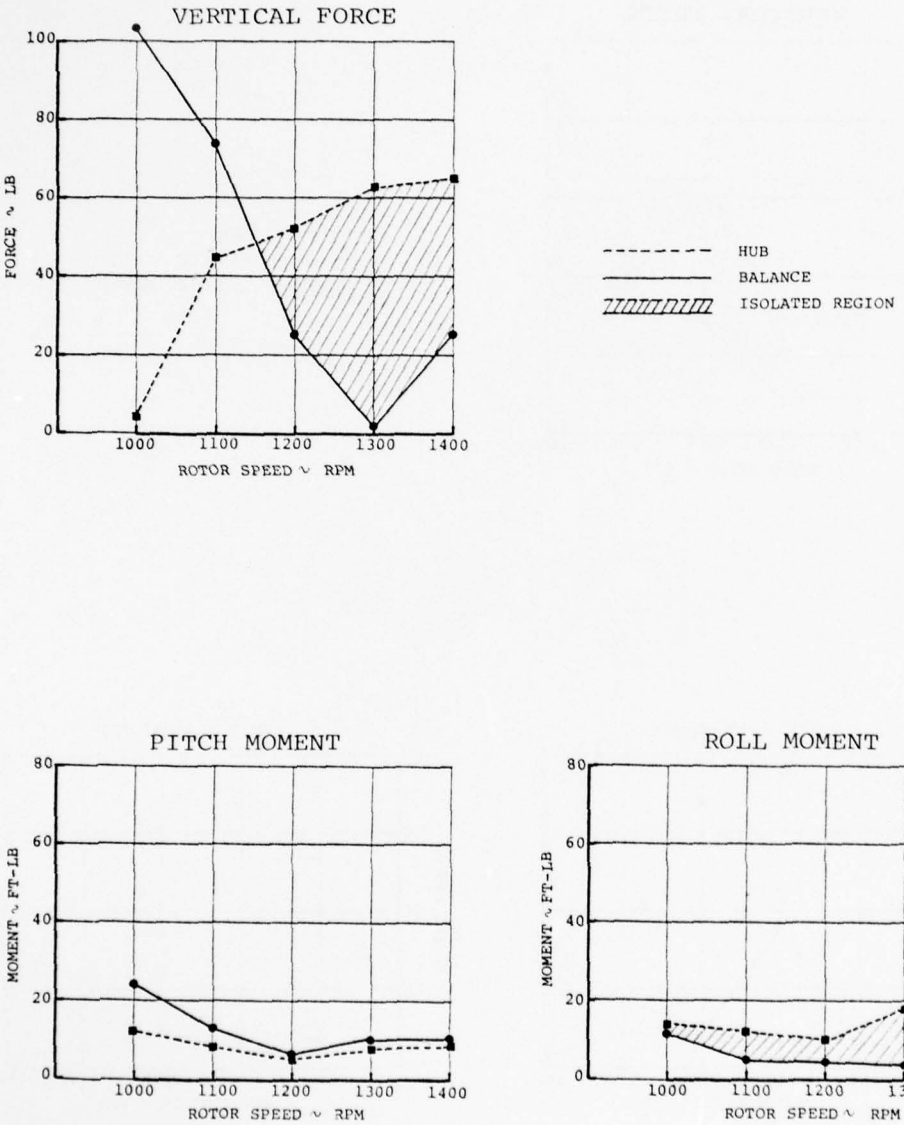

Figure 39. RPM Sweep at μ = .3, Lockbars Installed, 4/Rev Balance vs Hub Loads

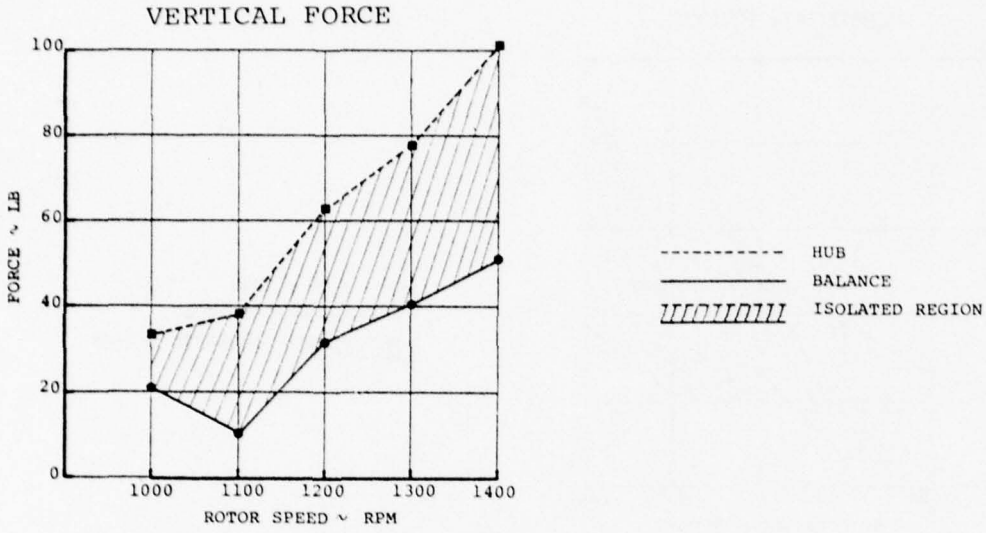

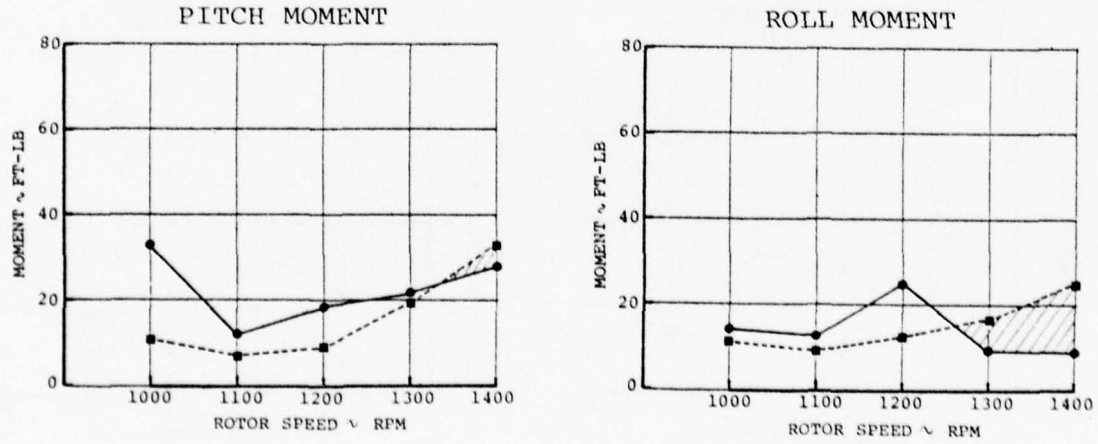

Figure 40. RPM Sweep at μ = .3, H = 1.1 in. Lateral/ H = -12.1 in. Longitudinal, 4/Rev Balance vs Hub Loads

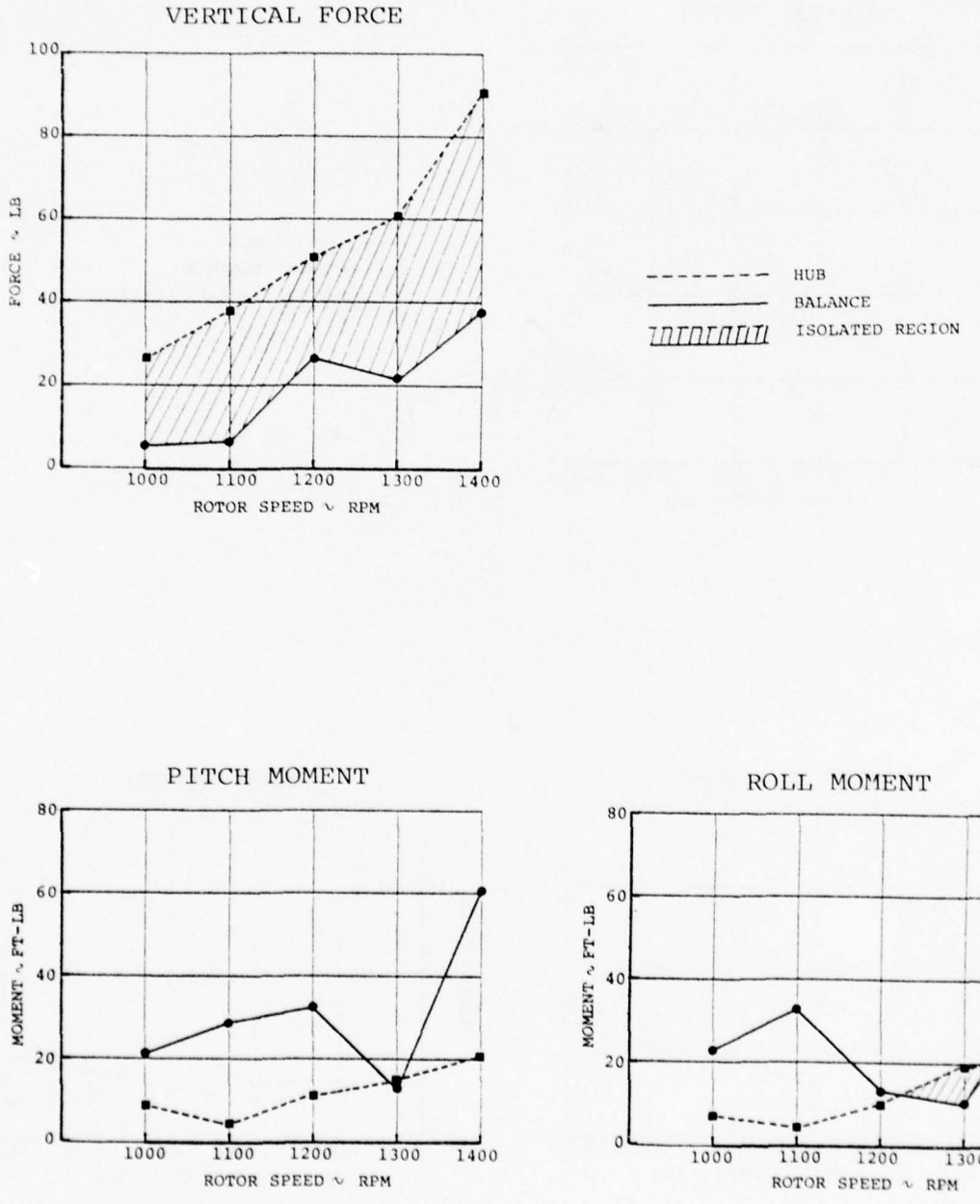

Figure 41. RPM Sweep at μ = .3, Focus H = -3.65 in., 4/Rev Balance vs Hub Loads

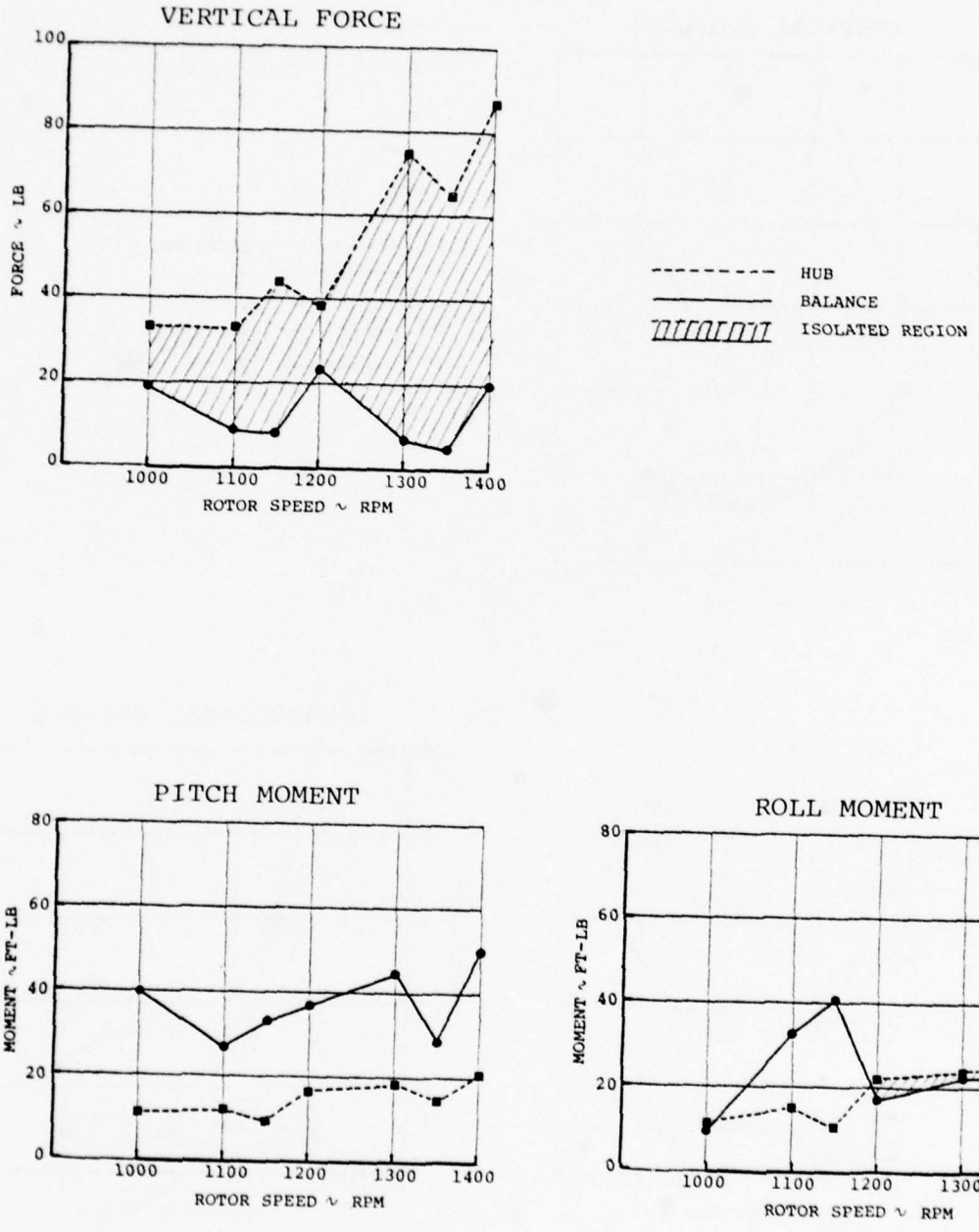

Figure 42. RPM Sweep at μ = .3, Focus H = -12.1 in., 4/Rev Balance vs Hub Loads

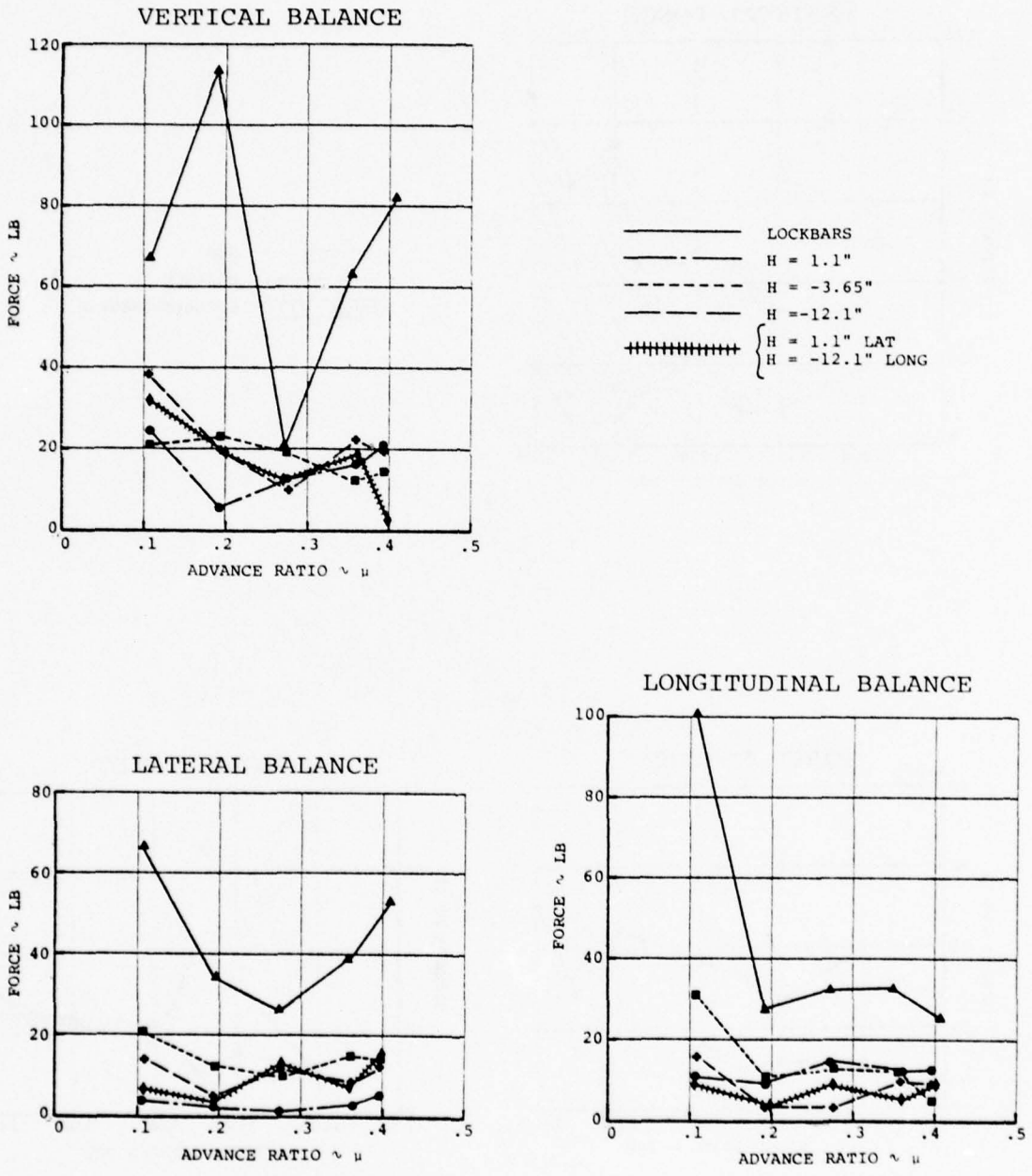

Figure 43. Airspeed Sweep at 1175 RPM, 4/Rev Vertical and Inplane Balance Loads

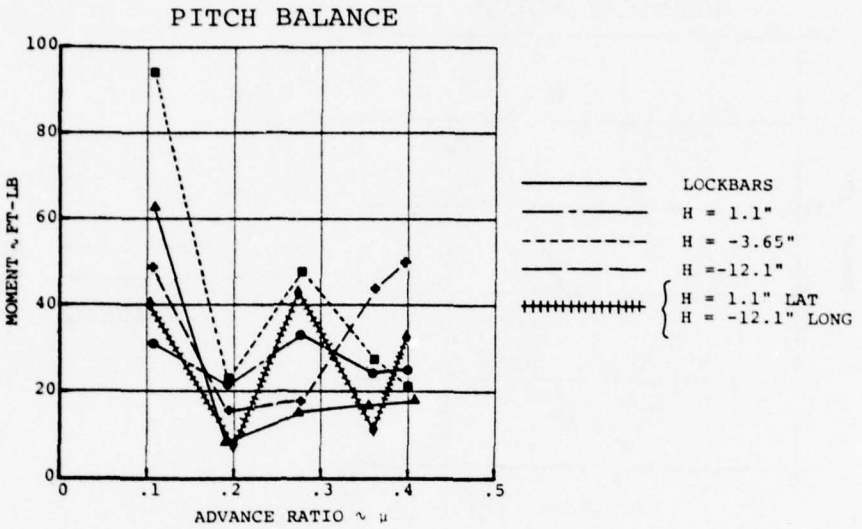

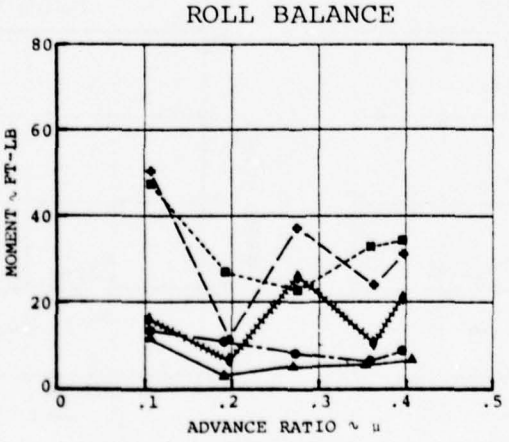

Figure 44. Airspeed Sweep at 1175 RPM, 4/Rev Moment Balance Loads

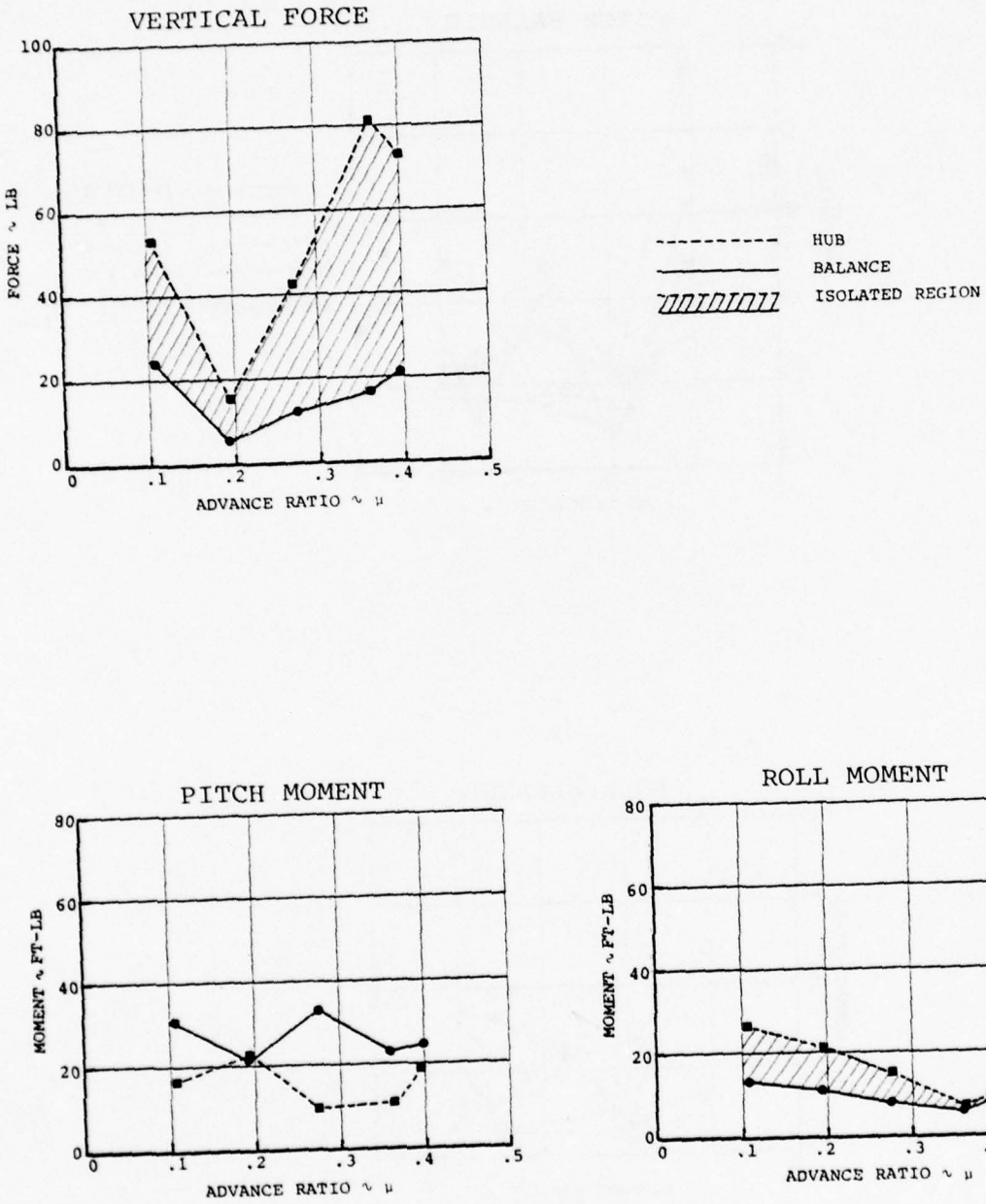

Figure 45. Airspeed Sweep at 1175 RPM, Focus H = 1.1 in., 4/Rev Balance vs Hub Loads

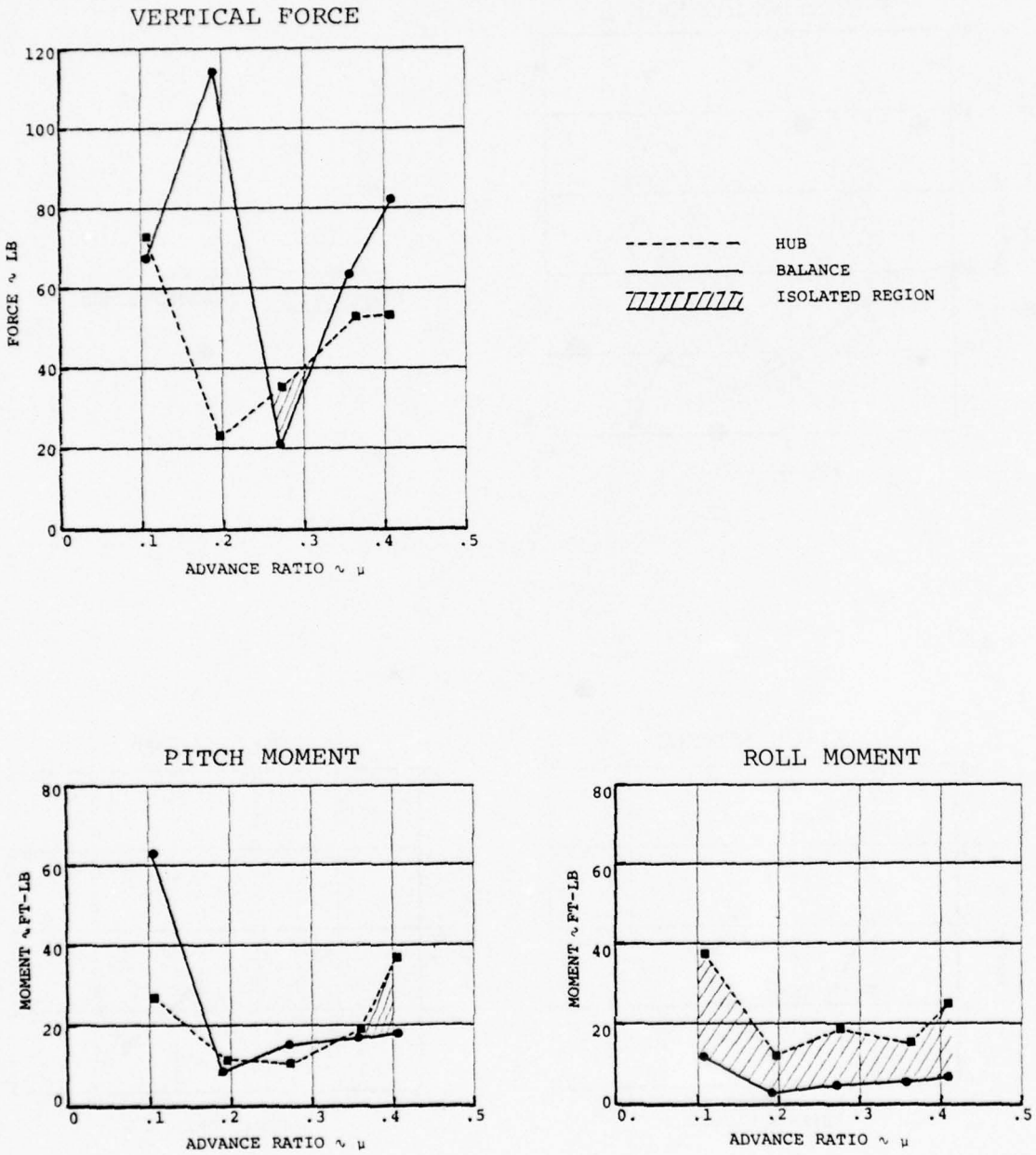

Figure 46. Airspeed Sweep at 1175 RPM, Lockbars Installed, 4/Rev Balance vs Hub Loads

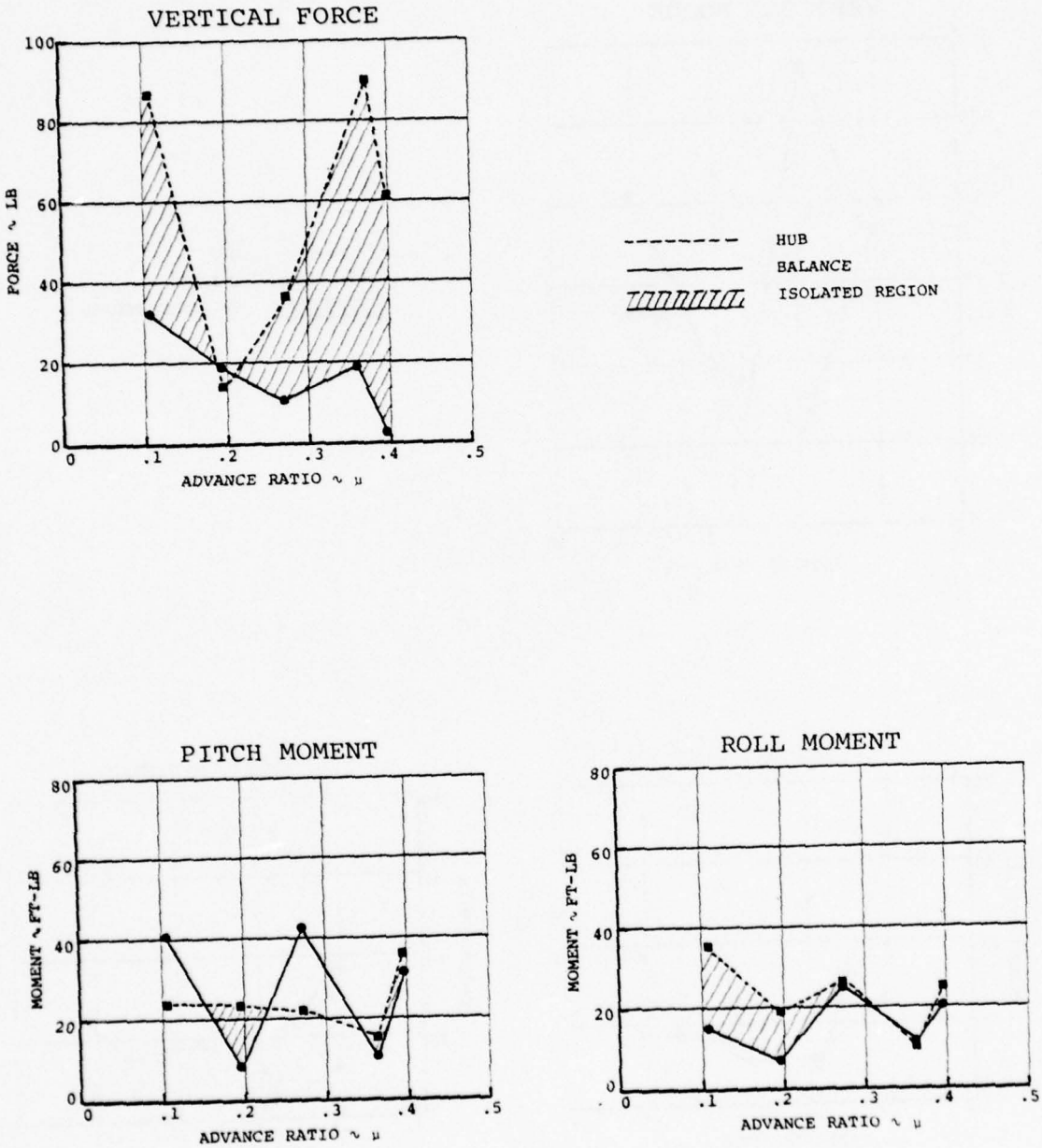

Figure 47. Airspeed Sweep at 1175 RPM, H = 1.1 in. Lateral/ H =-12.1 in. Longitudinal, 4/Rev Balance vs Hub Loads

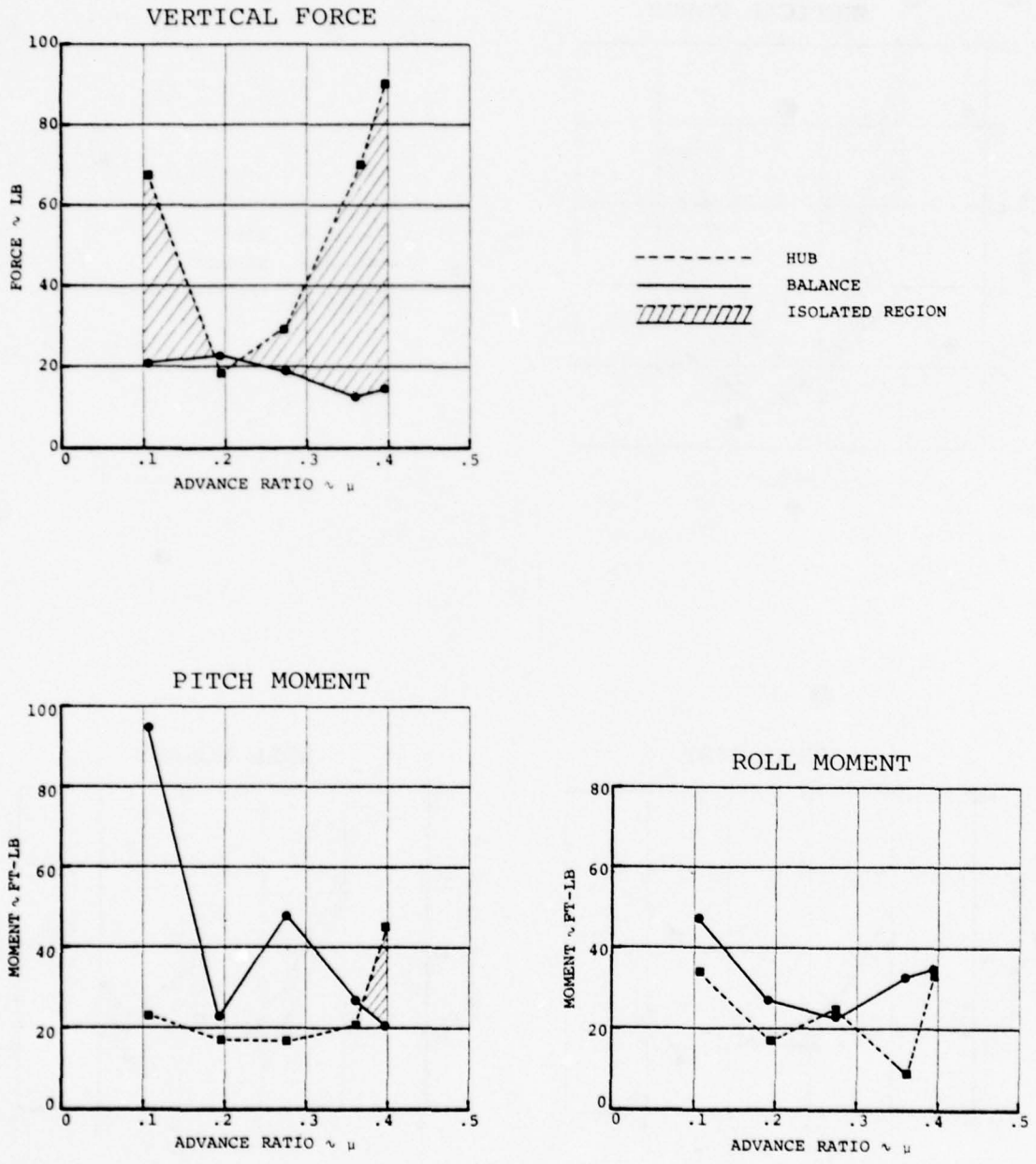

Figure 48. Airspeed Sweep at 1175 RPM, Focus H = -3.65 in., 4/Rev Balance vs Hub Loads

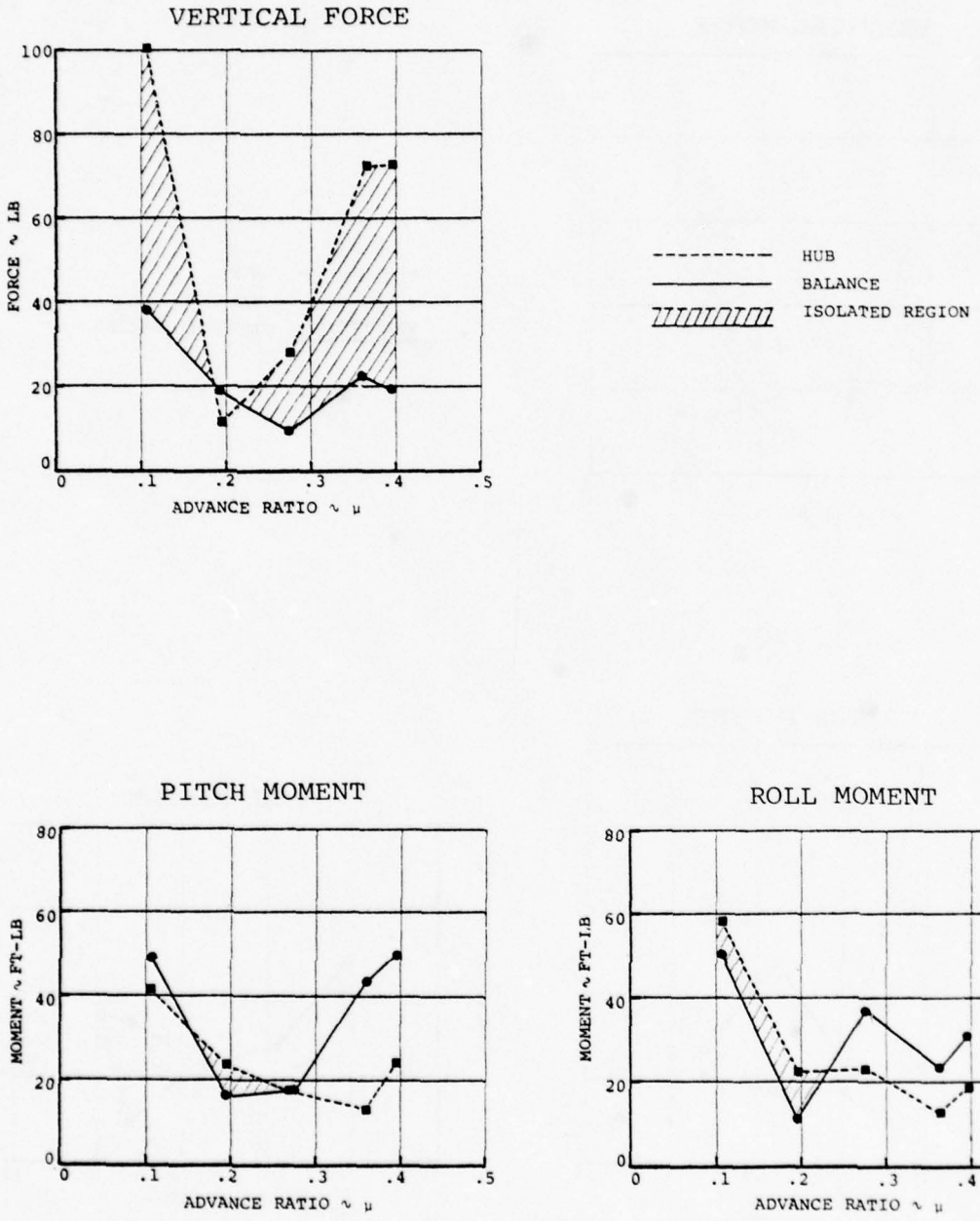

Figure 49. Airspeed Sweep at 1175 RPM, Focus H = -12.1 in., 4/Rev Balance vs Hub Loads

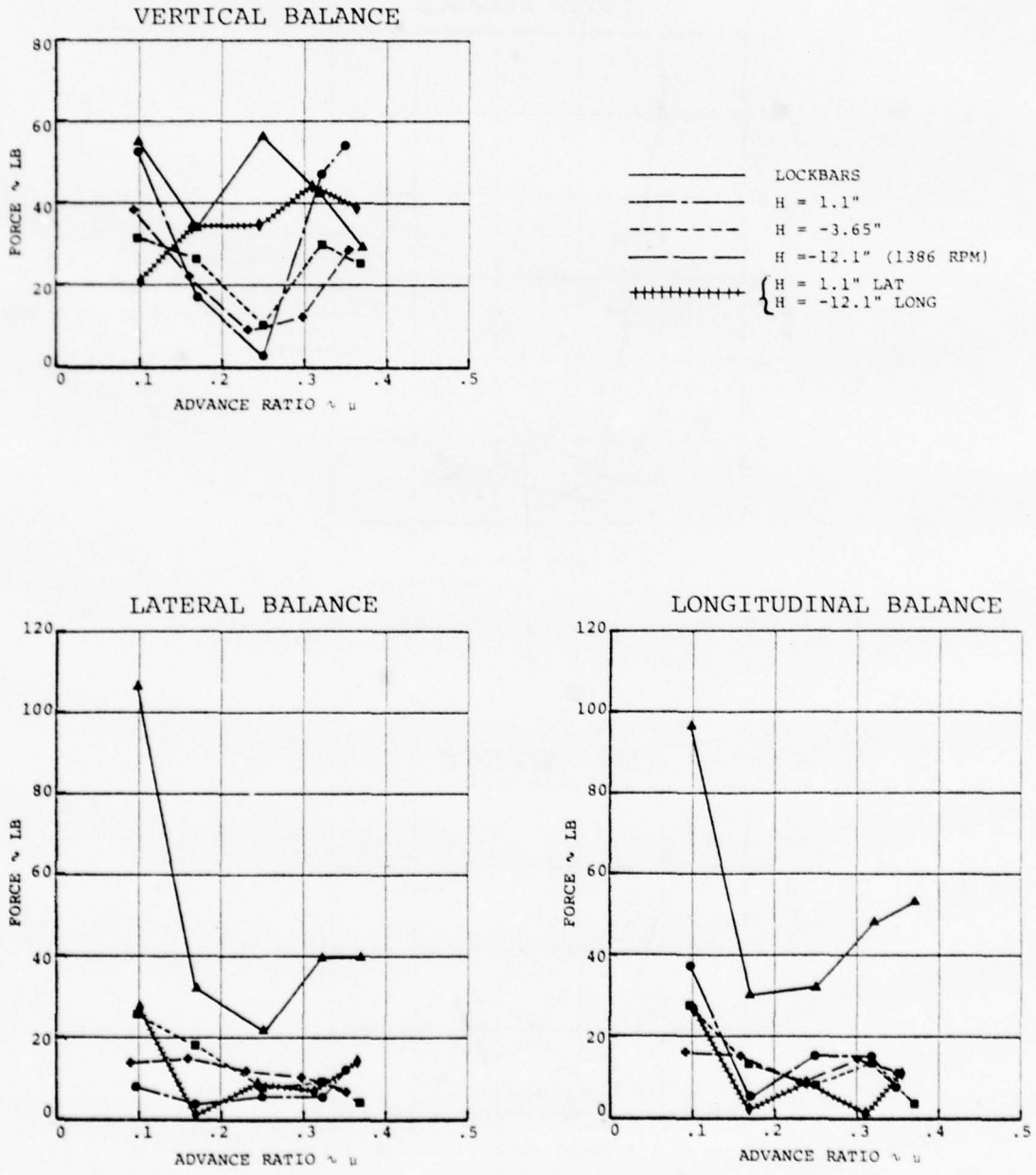

Figure 50. Airspeed Sweep at 1300 RPM, 4/Rev Vertical and Inplane Balance Loads

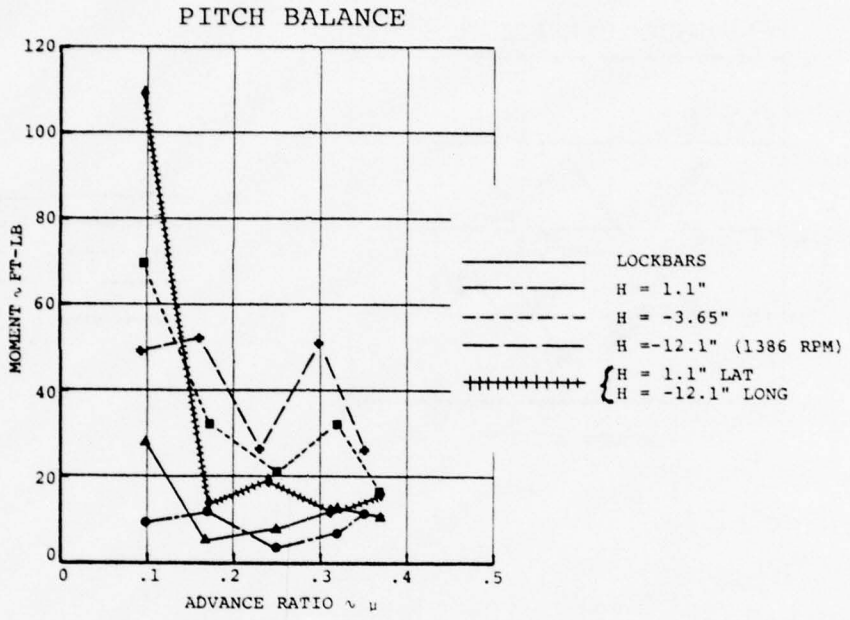

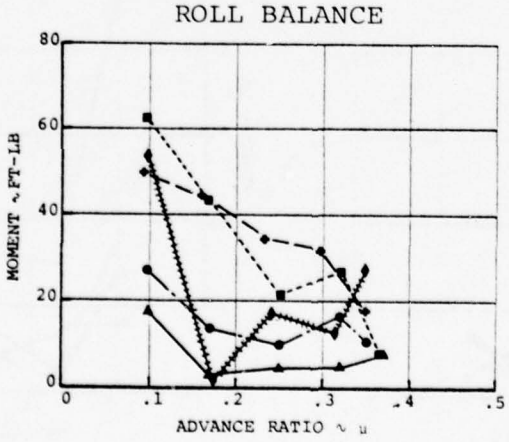

Figure 51. Airspeed Sweep at 1300 RPM, 4/Rev Moment Balance Loads

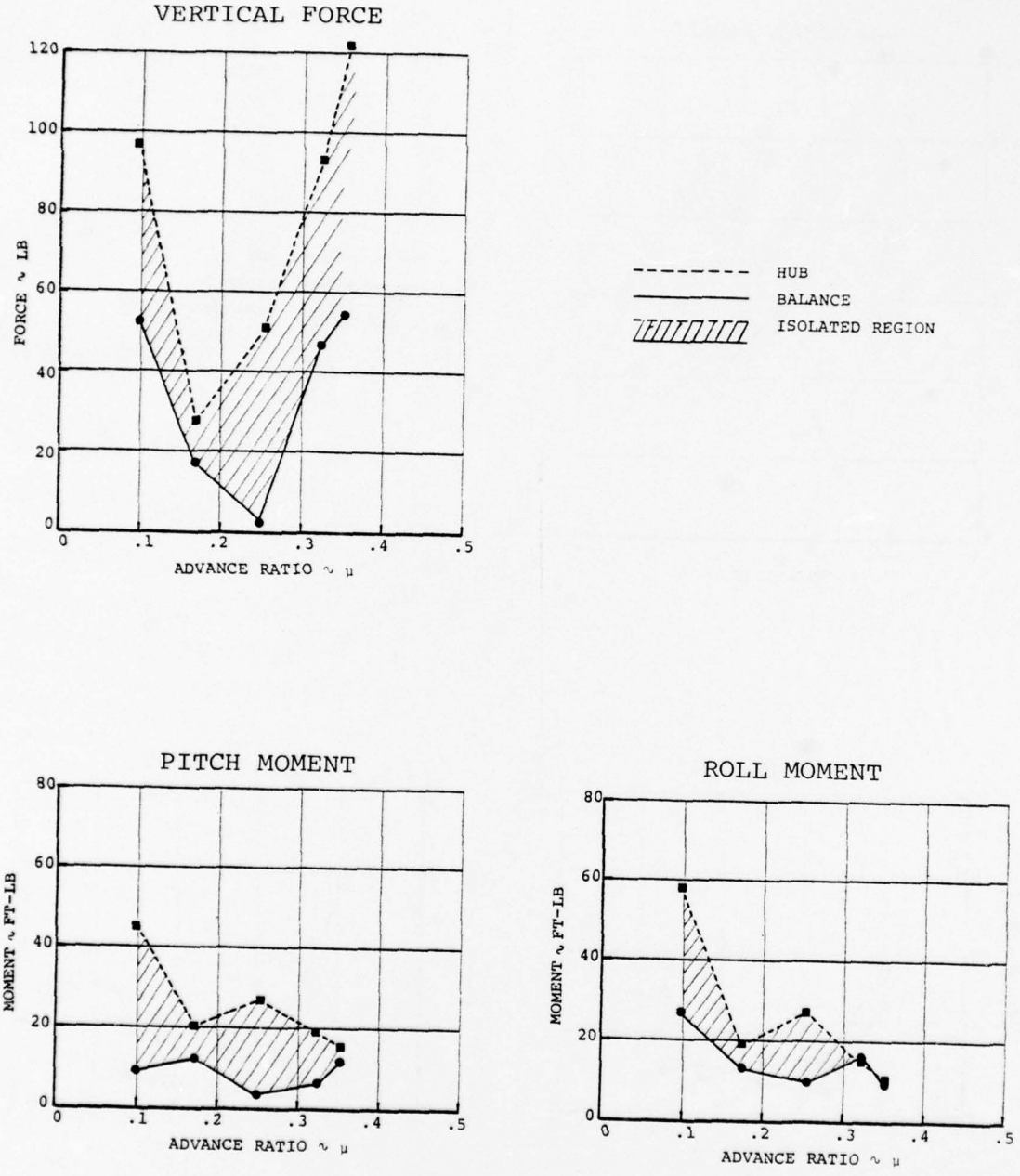

Figure 52. Airspeed Sweep at 1300 RPM, Focus H = 1.1 in., 4/Rev Balance vs Hub Loads

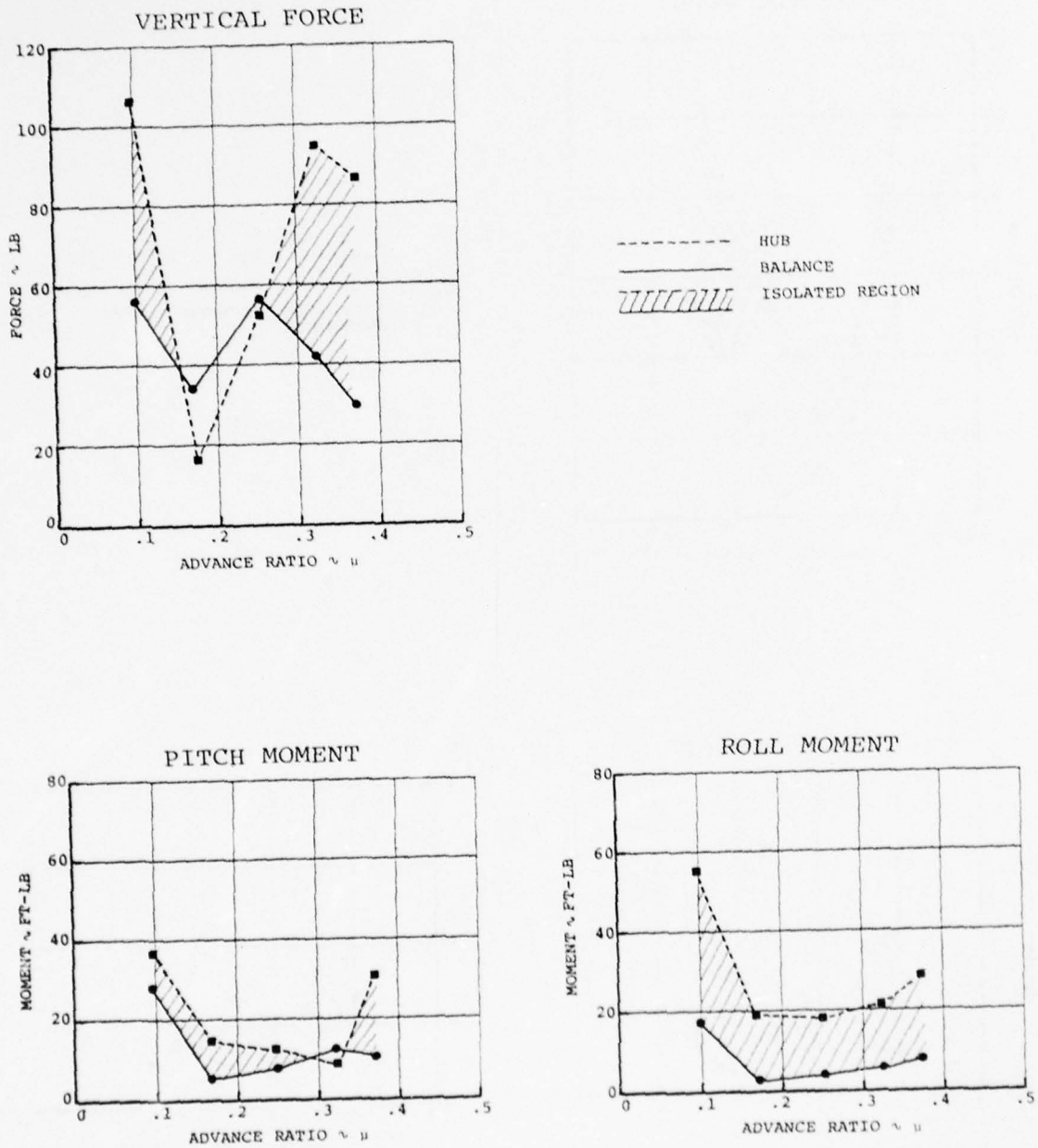

Figure 53. Airspeed Sweep at 1300 RPM, Lockbars Installed, 4/Rev Balance vs Hub Loads

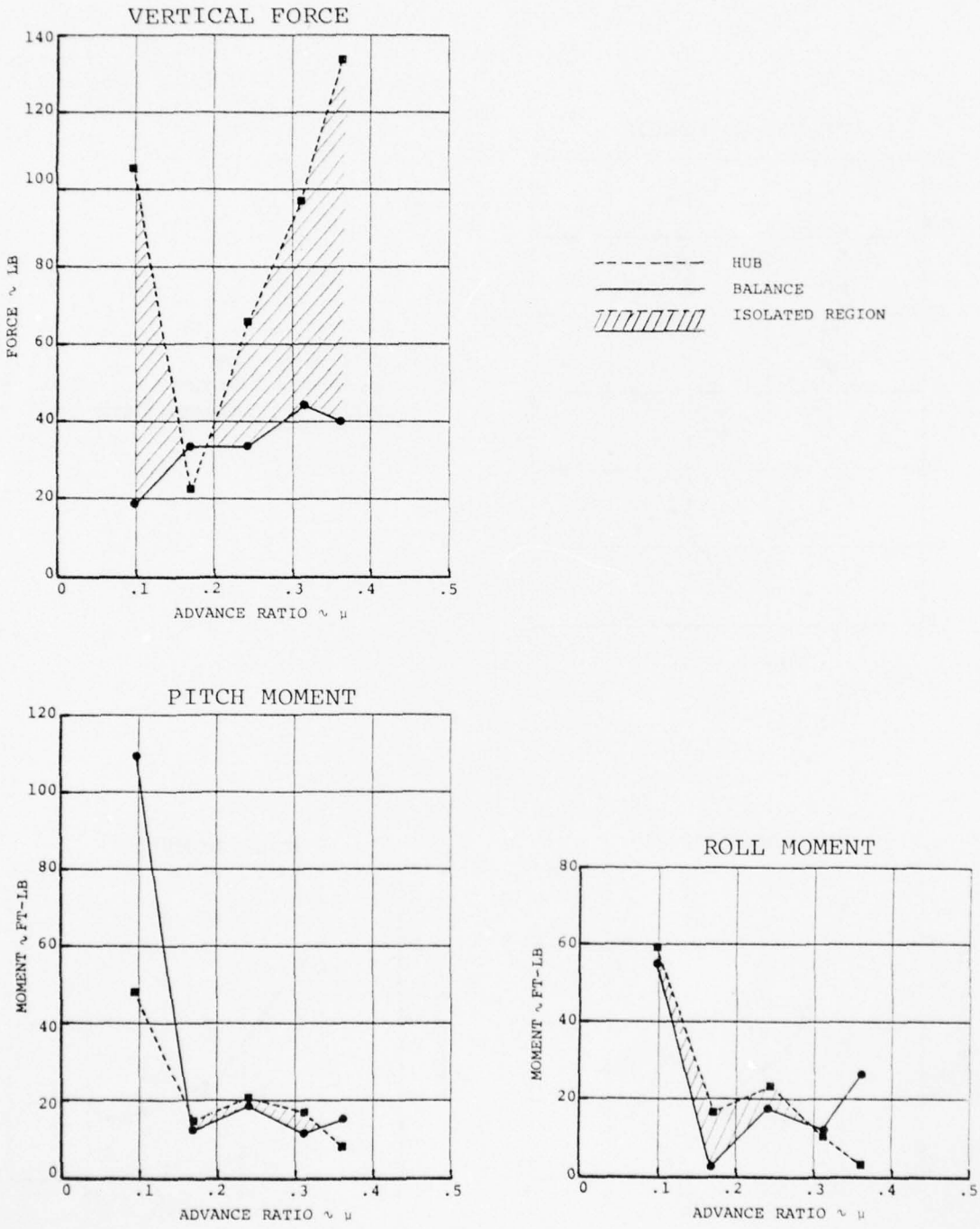

Figure 54. Airspeed Sweep at 1300 RPM, H = 1.1 in. Lateral/ H = -12.1 in. Longitudinal, 4/Rev Balance vs Hub Loads

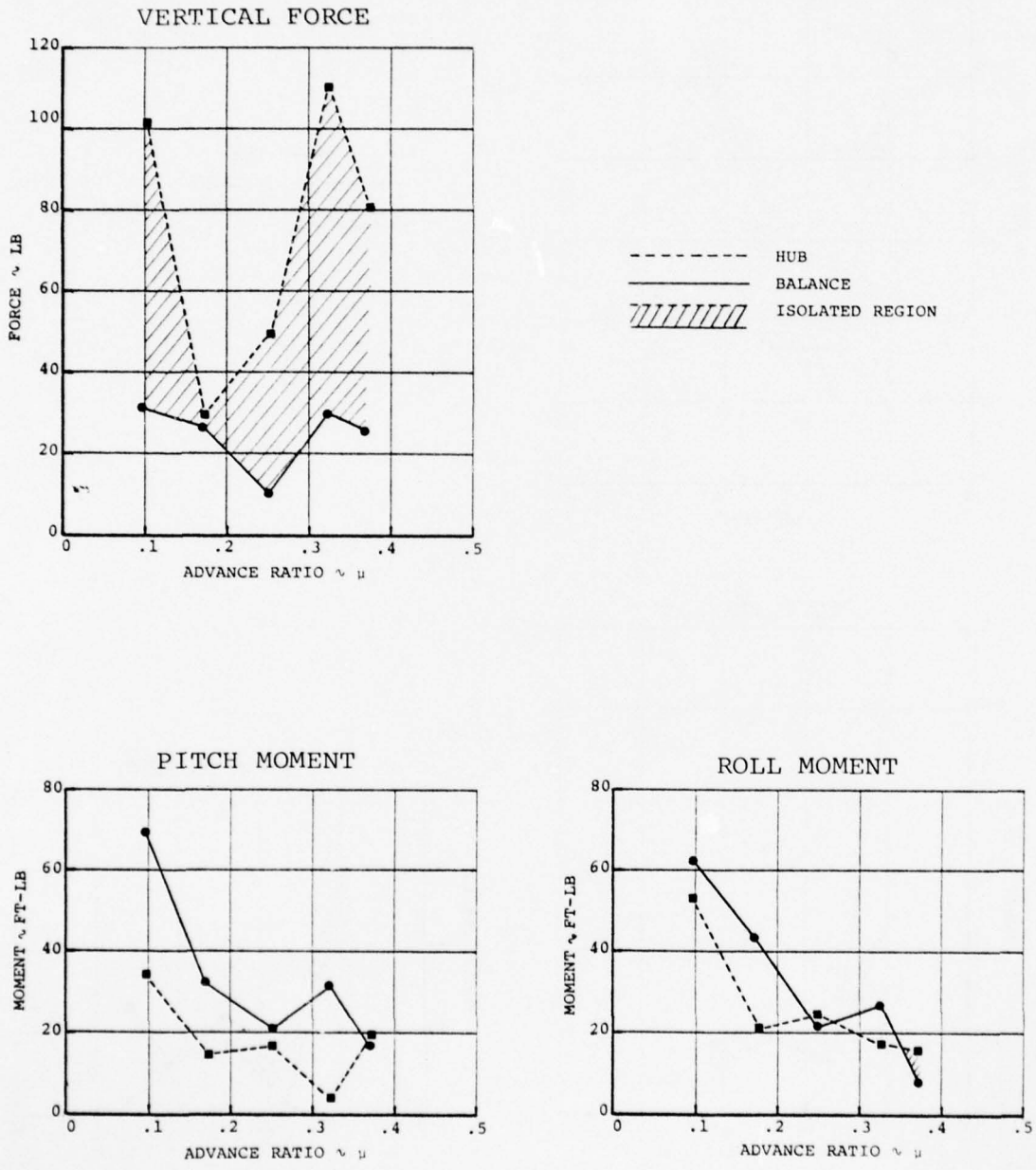

Figure 55. Airspeed Sweep at 1300 RPM, Focus H = -3.65 in., 4/Rev Balance vs Hub Loads

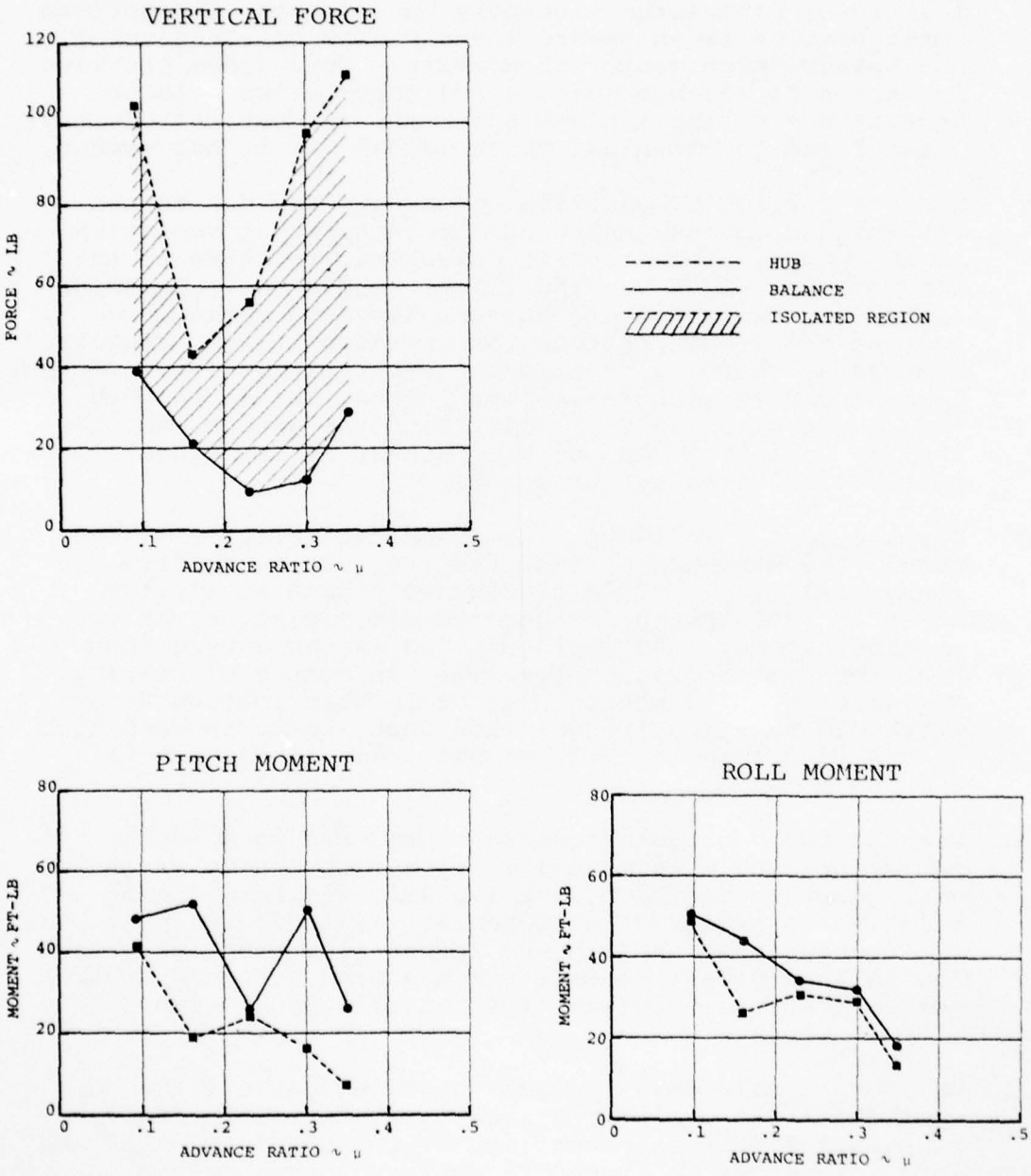

Figure 56. Airspeed Sweep at 1386 RPM, Focus H = -12.1 in., 4/Rev Balance vs Hub Loads

CONCLUSIONS

1. Based on analytical considerations, there is no single focal point that will simultaneously isolate both inplane forces and pitch/roll moments. For the four-bladed hingeless rotor with large vibratory hub moments, the optimum configuration is an upward focus at the combined rotor and transmission center of gravity. This focus provides isolation of the hub moments and reduces the balance moments due to the inplane hub loads without introducing lateral and longitudinal "kick loads" due to hub moment.

2. Since a portion of the balance moments are due to the inplane hub forces, there can be an apparent variation in the moment isolation effectiveness, relative to the hub moments, under varying flight conditions. Based on analysis, however, there appears to be no merit in varying the focal position for different flight regimes. Similarly, there is no evident justification for different lateral and longitudinal focus points, unless the hub moments in pitch and roll differ to the extent that the inplane hub force becomes predominant in one plane. This possibility seems rather remote.

3. Despite less than ideal dynamic characteristics of the model, the wind tunnel test results tend to confirm the analytical findings. Airspeed sweep data at a rotor speed of 1300 RPM showed good moment isolation for two configurations. One configuration was an upward focus near the combined rotor/transmission center of gravity. The second configuration was the lockbar configuration, which had an effective downward focus that produced high lateral and longitudinal balance "kick loads" due to the hub moments.

4. For the two configurations that produced good moment isolation, the wind tunnel results showed some variation with airspeed in the moment isolation effectiveness relative to measured hub moments. As indicated previously, however, the inplane hub forces also contribute to the balance moment so that the measured hub moments are not an absolute reference for measuring isolation effectiveness.

5. While vertical isolation was not intended, all the test configurations except the lockbar configuration showed substantial vertical isolation over most of the airspeed range. However, this can in no way be construed as a general characteristic of the focal isolation system.

6. Blade flap bending moments at the significant 3rd, 4th, and 5th harmonics and chord bending moments at the 3rd and 5th harmonics were generally similar for all the model configurations. The most significant variations occurred in the 3/rev flap moments at high advance ratios.

7. Fixed system vertical hub forces and pitch and roll moments, at the predominant 4/rev frequency, were similar for all the test configurations. Again, the greatest variations tended to occur at high forward speed.

8. The dynamic characteristics of the model differed from those of a simple system with only pitch and roll degrees of freedom. Several natural frequencies of the model were present below the 4/rev isolation frequency.

RECOMMENDATIONS

Based on the results of this program, it is recommended that the following items be considered for any similar programs in the future:

1. Any attempt to model a rotor isolation system should include a reasonably scaled transmission mass and inertia. This constitutes a difficult problem for an operating wind tunnel model. Froude scaling as opposed to Mach scaling does not change the required mass and inertia; however, it does offer considerable relief in terms of strength and stiffness.

2. Since isolation characteristics tend to be a function of both the geometry and natural frequency, a variable geometry model should also include provisions for readily modifying the isolator stiffness.

3. Inplane hub forces contribute to mounting plane moments, and under certain conditions hub moments contribute to mounting plane horizontal forces. Under these circumstances, the magnitude and phase of all the rotor loads must be measured in order to determine true isolation efficiencies.

4. A means for measuring the vibratory loads other than a conventional balance is required. The balance must be sensitive enough to measure the vibratory loads, which requires that the balance be relatively soft. This introduces balance natural modes that intrude on the intended isolator modes.

APPENDIX A

ANALYSIS OF A SINGLE DEGREE OF FREEDOM

FOCAL ISOLATION MODEL

Summing the moments about the focus and the balance in Figure A-1 leads to the following equations:

$$M_H \text{SIN}\Omega t + F_H\ (D+H)\ \text{SIN}\Omega t - m\ddot{X}\,H - I\ddot{\theta} - K_\theta\theta = 0 \qquad (1)$$

$$F_H L\ \text{SIN}\Omega t - m\ddot{X}\,L + K_\theta\theta - M_B = 0 \qquad (2)$$

Summing the forces at the balance yields a third equation

$$F_H \text{SIN}\Omega t - m\ddot{X} - F_B = 0 \qquad (3)$$

Assume simple harmonic motion so that

$$\theta = \theta\ \text{SIN}\Omega t$$

$$M_B = M_B\ \text{SIN}\Omega t$$

$$F_B = F_B\ \text{SIN}\Omega t$$

Since $X = H\theta = H\theta\ \text{SIN}\Omega t$, then $\ddot{X} = -H\Omega^2\theta\text{SIN}\Omega t$

Substituting the preceding expressions in Equations (1), (2), and (3)

$$M_H + F_H\ (D+H) + mH^2\Omega^2\theta + I\Omega^2\theta - K_\theta\theta = 0 \qquad (4)$$

$$F_H L + mLH\Omega^2\theta + K_\theta\theta - M_B = 0 \qquad (5)$$

$$F_H + mH\Omega^2\theta - F_B = 0 \qquad (6)$$

For free vibration with $F_H = M_H = 0$, the natural frequency is

$$\omega_n^2 = K_\theta/(I + mH^2)$$

If the radius of gyration is defined as

$$K^2 = I/m$$

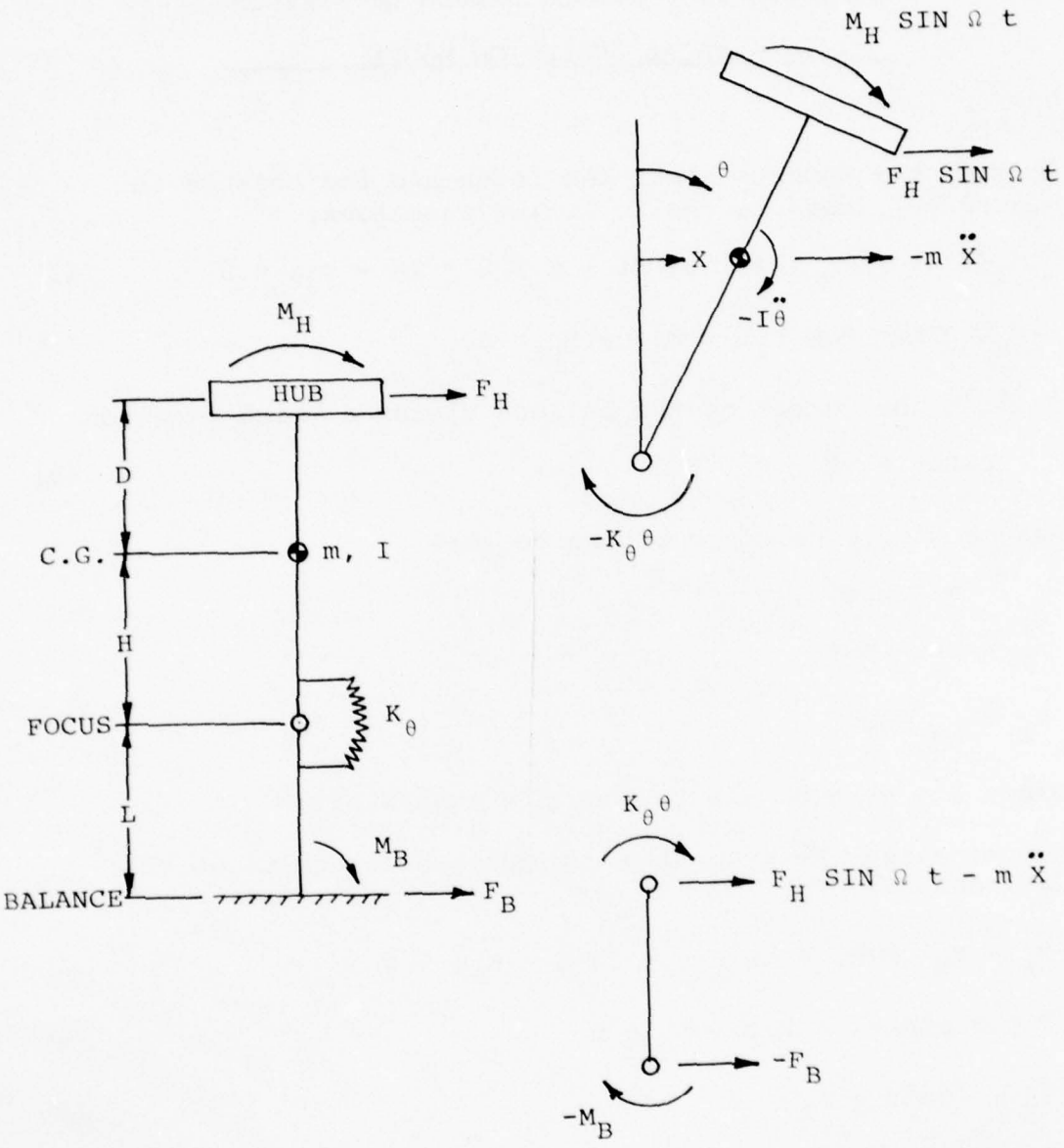

Figure A-1. Single Degree of Freedom Focal Isolation Model

then $m = 1/K^2$ and $K_\theta = \omega_n^2 I\ (1 + H^2/K^2)$

Replacing m and K_θ in Equations (4), (5), and (6)

$$M_H + F_H\ (D+H) + I\ (\Omega^2-\omega_n^2)\ (1 + H^2/K^2)\ \theta = 0 \qquad (7)$$

$$F_H L + I\Omega^2\ (L/K)\ (H/K)\ \theta + I\omega_n^2\ (1 + H^2/K^2)\ \theta - M_B = 0 \qquad (8)$$

$$F_H + I\Omega^2\ (H/K^2)\ \theta - F_B = 0 \qquad (9)$$

For $F_H = 0$, obtain the ratio M_B/M_H, which defines the balance moment due to hub moment, from Equations (7) and (8).

$$\frac{M_B}{M_H} = \frac{-\Omega^2(L/K)\ (H/K) - \omega_n^2\ (1 + H^2/K^2)}{(\Omega^2-\omega_n^2)\ (1 + H^2/K^2)}$$

$$\boxed{\frac{M_B}{M_H} = \frac{1}{(1-\beta^2)} + \frac{(L/K)\ (H/K)\ \beta^2}{(1 + H^2/K^2)\ (1-\beta^2)}} \qquad (10)$$

where $\beta^2 = \Omega^2/\omega_n^2$

For $M_H = 0$, obtain the ratio F_B/F_H, which defines the balance force due to hub force, from Equations (7) and (9).

$$\frac{F_B}{F_H} = 1 - \frac{\Omega^2(H/K^2)\ (D+H)}{(\Omega^2-\omega_n^2)\ (1 + H^2/K^2)}$$

$$\boxed{\frac{F_B}{F_H} = 1 + \frac{(H/K)\ (D/K + H/K)\ \beta^2}{(1 + H^2/K^2)\ (1-\beta^2)}} \qquad (11)$$

For $F_H = 0$, obtain the ratio $K F_B / M$, which defines the balance force due to hub moment, from Equations (7) and (9).

$$\frac{K F_B}{M_H} = \frac{K\Omega^2 (H/K^2)}{(\Omega^2-\omega_n^2)(1 + H^2/K^2)}$$

$$\boxed{\frac{K F_B}{M_H} = \frac{(H/K)\beta^2}{(1 + H^2/K^2)(1-\beta^2)}} \qquad (12)$$

For $M_H = 0$, obtain the ratio $M_B/K F_H$, which defines the balance moment due to hub forces, from Equations (7) and (8).

$$\frac{M_B}{K F_H} = \frac{L}{K} - \left[\frac{\Omega^2 (L/K)(H/K) + \omega_n^2 (1 + H^2/K^2)}{K(\Omega^2-\omega_n^2)(1-H^2/K2)}\right] (D + H)$$

$$\boxed{\frac{M_B}{K F_H} = \frac{(H/K + D/K)}{(1-\beta^2)} + \frac{L}{K} + \frac{(L/K)(H/K)(D/K + H/K)\beta^2}{(1 + H^2/K^2)(1-\beta^2)}} \qquad (13)$$

APPENDIX B

PROCEDURE FOR CALCULATING HUB LOADS

The procedure used to compute 4/rev fixed system hub loads from measured blade root flap bending moments is essentially an influence coefficient method. The method applies only to hub vertical force and hub pitch and roll moments. Using the Boeing Vertol C-60 Rotor Analysis Program, rotor forced responses are calculated for a number of airspeeds. Influence coefficients, relating the flap bending moment at the root measurement location to the rotating shear and moment at the rotor center, are obtained from the C-60 results. Coefficients are required for the sine and cosine components of the 3rd, 4th, and 5th harmonics. For any given load and harmonic, the coefficients thus obtained are generally found to be essentially constant.

Using averaged values of the coefficients, it is then possible to compute the rotating system loads at the rotor center from the measured root flap bending moments. Desired fixed system loads are then obtained by a transformation of the rotating system loads. The detailed calculations are outlined below.

Define terms as follows:

F_{4S} = 4/Rev Vertical Force Coefficient, Sine

F_{4C} = 4/Rev Vertical Force Coefficient, Cosine

M_{3S} = 3/Rev Moment Coefficient, Sine

M_{3C} = 3/Rev Moment Coefficient, Cosine

M_{5S} = 5/Rev Moment Coefficient, Sine

M_{5C} = 5/Rev Moment Coefficient, Cosine

FB_{ns} = n/Rev Flap Moment, Sine

FB_{nc} = n/Rev Flap Moment, Cosine

4/Rev Vertical Force

(Sine) $$FZ_{4S} = 4\left[(F_{4S})(FB_{4S})\right] \quad (14)$$

(Cosine) $$FZ_{4C} = 4\left[(F_{4C})(FB_{4C})\right] \quad (15)$$

4/Rev Pitch Moment

$$\text{(Sine)} \qquad MY_{4S} = -2\left[(M_{3S})(FB_{3S}) + (M_{5S})(FB_{5S})\right] \tag{16}$$

$$\text{(Cosine)} \qquad MY_{4C} = -2\left[(M_{3C})(FB_{3C}) + (M_{5C})(FB_{5C})\right] \tag{17}$$

4/Rev Roll Moment

$$\text{(Sine)} \qquad MX_{4S} = 2\left[(M_{3C})(FB_{3C}) - (M_{5C})(FB_{5C})\right] \tag{18}$$

$$\text{(Cosine)} \qquad MX_{4C} = 2\left[(M_{5S})(FB_{5S}) - (M_{3S})(FB_{3S})\right] \tag{19}$$